REPORT NO.
UCB/EERC-82/11
AUGUST 1982

EARTHQUAKE ENGINEERING RESEARCH CENTER

DYNAMIC RESPONSE ANALYSIS OF TECHI DAM

by

RAY W. CLOUGH
ROY M. STEPHEN
JAMES SHAW-HAN KUO

Report to the National Science Foundation

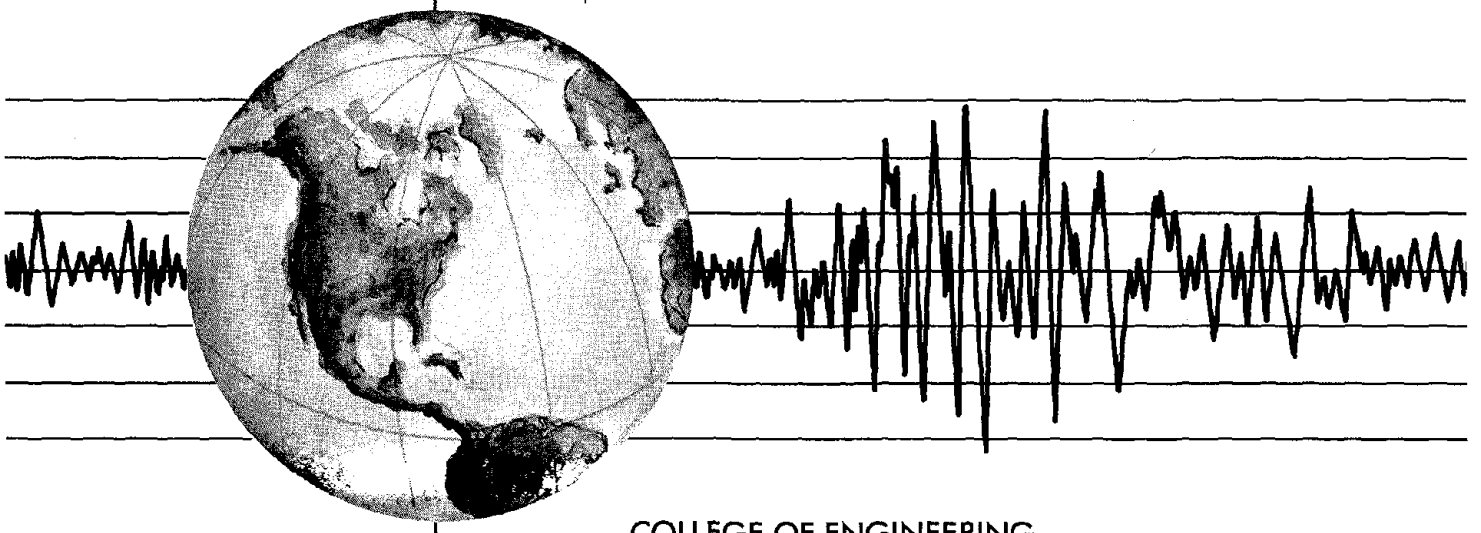

COLLEGE OF ENGINEERING

UNIVERSITY OF CALIFORNIA · Berkeley, California

For sale by the National Technical Information Service, U.S. Department of Commerce, Springfield, Virginia 22161.

See back of report for up to date listing of EERC reports.

50272-101

REPORT DOCUMENTATION PAGE	1. REPORT NO. NSF/CEE-82060	2.	3. Recipient's Accession No. PB83 147496
4. Title and Subtitle: Dynamic Response Analysis of Techi Dam			5. Report Date: August 1982 6.
7. Author(s): Ray W. Clough, Roy M. Stephen, James Shaw-Han Kuo			8. Performing Organization Rept. No. UCB/EERC-82/11
9. Performing Organization Name and Address: Earthquake Engineering Research Center University of California, Berkeley 47th Street and Hoffman Blvd. Richmond, Calif. 94804			10. Project/Task/Work Unit No. 11. Contract(C) or Grant(G) No. (C) (G) PFR-78-19333
12. Sponsoring Organization Name and Address: National Science Foundation 1800 G Street, N. W. Washington, D.C. 20550			13. Type of Report & Period Covered 14.

15. Supplementary Notes

16. Abstract (Limit: 200 words)

This report summarizes the results obtained by Earthquake Engineering Research Center personnel during a cooperative investigation with the Center for Earthquake Engineering Research (CEER) of National Taiwan University, Taipei, of the dynamic behavior of Techi Dam. Part I describes a field study of Techi Dam, a doubly curved arch dam 590 ft high located in central Taiwan, using rotating mass vibration generators. The measured vibration mode shapes, frequencies, and damping ratios are reported. Part II describes the analysis of the vibration mode shapes and frequencies using the computer program ADAP. In addition to the ADAP finite element models of the dam and foundation, this analysis also made use of a subroutine RSVOIR, which modeled the incompressible reservoir interaction effects both by an extended Westergaard procedure and also with liquid finite elements. Part III presents the stresses calculated in Techi Dam when subjected to the Design Basis Earthquake which was formulated for this site by CEER.

The principal conclusions of the investigations are that the finite element model of the reservoir is significantly better than the extended Westergaard model, and that Techi Dam can resist without damage the Design Basis Earthquake, which has a return period of 100 years.

17. Document Analysis a. Descriptors

b. Identifiers/Open-Ended Terms

c. COSATI Field/Group

18. Availability Statement: Release Unlimited	19. Security Class (This Report): UNCLASSIFIED	21. No. of Pages: 119
	20. Security Class (This Page): UNCLASSIFIED	22. Price

DYNAMIC RESPONSE ANALYSIS OF TECHI DAM

by

Ray W. Clough
Roy M. Stephen
and
James Shaw-Han Kuo

Report to the National Science Foundation

Report No. UCB/EERC-82/11
Earthquake Engineering Research Center
College of Engineering
University of California
Berkeley, California

August 1982

ABSTRACT

This report summarizes the results obtained by the Earthquake Engineering Research Center (EERC) during a cooperative investigation of the dynamic behavior of Techi Dam, conducted jointly by the EERC and the Center for Earthquake Engineering Research of National Taiwan University, Taipei. The report is presented in three parts, corresponding to three phases of the research effort. Part I describes a field study of Techi Dam, a doubly curved arch dam 590 ft. high located in central Taiwan. Rotating mass vibration generators were used, and the measured vibration mode shapes, frequencies, and damping ratios are reported. Part II describes the analysis of the vibration mode shapes and frequencies using the computer program ADAP. In addition to the ADAP finite element models of the dam and foundation, this analysis also made use of a subroutine RSVOIR, which modeled the incompressible reservoir interaction effects both by an extended Westergaard procedure and also with liquid finite elements. Part III presents the stresses calculated in Techi Dam when subjected to the Design Basis Earthquake which was formulated for this site by the CEER of National Taiwan University.

The principal conclusions of the investigations are that the finite element model of the reservoir is significantly better than the extended Westergaard model, and that Techi Dam is safe against damage during the Design Basis Earthquake, which has a return period of 100 years.

ACKNOWLEDGEMENTS

The authors of this report sincerely thank the National Science Foundation for their financial support through Grant No. PFR-78-19333 that made this very interesting research effort possible. They also acknowledge with thanks the contributions made by their colleagues at the National Taiwan University under the leadership of Professor S.-T. Mau. Of course, our study of Techi Dam was feasible only on the basis of this cooperative research effort.

Finally, the authors wish to thank Mr. Richard Parsons, Principal Laboratory Mechanician, in the Division of Structural Engineering and Structural Mechanics at the University of California, Berkeley, for the assistance he gave to Mr. R. M. Stephen in the field measurement program, to Ms. Gail Feazell for her work in preparation of the figures, and to Ms. Toni Avery for her typing of the manuscript.

TABLE OF CONTENTS

	Page
ABSTRACT	i
ACKNOWLEDGEMENTS	iii
TABLE OF CONTENTS	v
LIST OF FIGURES	vii
INTRODUCTION	1
PART I FORCED VIBRATION STUDY	3
GENERAL DESCRIPTION OF TECHI DAM	3
FORCED VIBRATION TEST EQUIPMENT	3
Vibration Generators	3
Accelerometers	5
Seismometers	5
Equipment for Measurement of Frequency	6
Recording Equipment	6
EXPERIMENTAL PROCEDURE AND DATA REDUCTION	7
Evaluation of Modal Frequencies	7
Measurement of Mode Shapes	8
Determination of Modal Damping Ratios	9
EXPERIMENTAL RESULTS	10
Modal Frequencies and Damping Ratios	10
Mode Shapes	12
Discussion of the Results	12
PART II ANALYSIS OF VIBRATION PROPERTIES	14
FORMULATION OF MATHEMATICAL MODEL	14
Type of Model Selected	14
Material Properties	16
Finite Element Mesh Arrangements	16

Page

RESULTS OF ANALYSES. 20

General Comments. 20

Correlation of Vibration Frequencies. 22

Correlation of Vibration Mode Shapes. 22

PART III ANALYSIS OF EARTHQUAKE RESPONSE 25

METHOD OF ANALYSIS 25

DESIGN BASIS EARTHQUAKE. 29

CALCULATED STRESSES IN TECHI DAM 29

Static Stresses 31

Static plus Upstream-Downstream Earthquake. 32

Static plus Cross-Canyon Earthquake 33

DISCUSSION OF STRESS RESULTS 33

CONCLUSIONS AND RECOMMENDATIONS 37

REFERENCES. 40

LIST OF FIGURES

Figure		Page
1	Location of Techi dam.	41
2	View of dam.	42
3	Plan of Techi dam showing location of vibration generators	43
4	Profile of dam looking upstream.	44
5	Forced vibration generator	45
6	Vibration force output vs. speed-non-counterbalanced (after Hudson)	46
7	Resonance curve: symmetric	47
8	Resonance curve: symmetric	48
9	Resonance curve: symmetric	49
10	Resonance curve: anti-symmetric.	50
11	Resonance curve: anti-symmetric.	51
12	Resonance curve: anti-symmetric.	52
13	Resonance curve: anti-symmetric.	53
14	Symmetric excitation-crest mode shape.	54
15	Symmetric excitation-crest mode shape.	55
16	Symmetric excitation-crest mode shape.	56
17	Anti-symmetric excitation-crest mode shape	57
18	Anti-symmetric excitation-crest mode shape	58
19	Anti-symmetric excitation-crest mode shape	59
20	Anti-symmetric excitation-crest mode shape	60
21	Symmetric excitation-mode shapes on section 7.	61
22	Anti-symmetric excitation-mode shapes on section 7	62
23	Anti-symmetric excitation-mode shapes on section 7	63
24	Symmetric excitation-mode shapes on section 11	64
25	Anti-symmetric excitation-mode shapes on section 11.	65

Figure		Page
26	Anti-symmetric excitation-mode shapes on section 11.	66
27	Symmetric excitation-mode shapes on section 4.	67
28	Anti-symmetric excitation-mode shapes on section 4	68
29	Anti-symmetric excitation-mode shapes on section 4	69
30	Finite element mesh of dam body (Techi dam) upstream face projected on xz-plane.	70
31	Section of foundation block at x-z plane (showing traces of element section lines).	71
32	Section of foundation block and dam at y-z plane (showing element mesh at the boundary).	72
33	Prismatic finite element reservoir model	73
34	Pressure distribution on rigid Techi dam face (due to 1 g acceleration upstream)	74
35	Decrease of fixed mode frequency with reservoir depth. . . .	75
36	Variation of modal frequency with reservoir depth.	76
37a	First vibration mode shape correlation	77
37b	Second vibration mode shape correlation.	78
37c	Third vibration mode shape correlation	79
37d	Fourth vibration mode shape correlation.	80
37e	Fifth vibration mode shape correlation	81
37f	Sixth vibration mode shape correlation	82
37g	Seventh vibration mode shape correlation	83
38	Response spectra for Operational Basis Earthquake and Design Basis Earthquake -- 5% damping (reference 2).	84
39	Static stress distribution, Techi dam.	85
40	Maximum compressive stresses: static plus U-D earthquake . .	89
41	Maximum tensile stresses: static plus U-D earthquake	93
42	Maximum compressive stresses: static plus C-C earthquake . .	97
43	Maximum tensile stresses: static plus C-C earthquake	101

INTRODUCTION

In 1979, a cooperative research project was initiated by the Earthquake Engineering Research Center (EERC) of the University of California, Berkeley and the Center for Earthquake Engineering Research (CEER) of National Taiwan University, Taipei. Funding for the EERC part of the investigation was provided by the National Science Foundation as part of the U.S.-Taiwan Cooperative Research Program in Earthquake Engineering, while the funding for CEER was similarly provided by the National Science Council of Taiwan. The general purpose of the project was to improve and verify analysis procedures for predicting the response behavior of concrete arch dams when subjected to severe earthquake motions.

A major component of the research program involved the study of Techi Dam, a doubly curved thin shell arch dam nearly 600 ft. high located on the Tachia River about 100 km south of Taipei. This structure, completed in 1974, is considered to represent good modern design practice for a rather large dam, and therefore is appropriate for demonstrating current capabilities for performing earthquake response analyses of arch dams. The study of Techi Dam was divided into three phases: (1) field measurement of its actual vibration mode shapes and frequencies, (2) calculation of the vibration mode shapes and frequencies, and correlation with the measured results, and (3) calculation of the dynamic response to the Design Basis Earthquake, an event having a 100 year return period at the dam site. The field measurement phase of the work included forced vibration studies using EERC vibration generators and performed by EERC personnel with the assistance of CEER researchers, as well as a series of ambient vibration measurement programs carried out by CEER personnel. Analytical studies were carried out both at EERC in Berkeley and at CEER

in Taipei. The seismic risk analysis for the dam site was conducted by the CEER personnel in Taipei; this led to the definition of the response spectrum for the Design Basis Earthquake that was used in the dynamic analysis of the dam.

The purpose of this report is to describe the work done by EERC personnel in the study of Techi Dam. It is divided into three parts, corresponding to the three phases of the investigation listed above. Part I describes the forced vibration study of the dam and presents the mode shape and frequency results from that phase of the work. Principal Development Engineer R. M. Stephen of EERC was in charge of that measurement program, and he prepared Part I of the report. Part II describes the analytical investigation of the mode shapes and frequencies performed in Berkeley. This work was done by Research Assistant James S.-H. Kuo as part of his Ph.D. dissertation research, and the details of the analytical procedures are described in his report (1); only the essential results are presented here, including correlation of the analytical predictions with the measured data. In this correlation, results from the ambient vibration study performed at the CEER, NTU (2) are discussed, as well as the EERC data presented in Part I. In Part III the dynamic response analysis of the Techi Dam is described briefly, and the expected stress state due to the Design Base Earthquake combined with the static gravity and water load effects is summarized. This analysis also was performed by Research Assistant J. S.-H. Kuo as part of his doctoral dissertation. The combined report integrating these various components was written by the senior author.

PART I FORCED VIBRATION STUDY

GENERAL DESCRIPTION OF TECHI DAM

The Techi Dam is located on the upper reaches of the Tachia River approximately 50 km east of Taichung and 100 km south of Taipei (Fig. 1). The objective of the forced vibration study was to determine the resonant frequencies and mode shapes of the dam.

The dam is a 180 m (590 ft.) high double-curvature, thin-arch concrete structure, as shown in Fig. 2. It has a crest length of 290 m (951 ft.) with the radius at the crest varying from approximately 115 m (377 ft.) to 235 m (772 ft.). The thickness is 4.5 m (14.8 ft.) at the crest and 20 m (65.6 ft.) at the base. The overflow spillway located near the center of the dam is 55 m (180.4 ft.) long and is depressed 7.75 m (25.4 ft.) below the normal crest elevation. Fig. 3 is a plan view of the dam showing locations of the shaking machines and of the measurement stations. Fig. 4 is an elevation view of the structure looking upstream. The dam construction was completed in September 1974. The forced vibration study was carried out and completed in June 1979.

FORCED VIBRATION TEST EQUIPMENT

Vibration Generators: Forced vibrations were produced by two rotating-mass vibration generators or shaking machines, one of which is shown in Fig. 5 located adjacent to station 10. These machines were developed at the California Institute of Technology under the supervision of the Earthquake Engineering Research Institute for the Office of Architecture and Construction, State of California (3). Each machine consists of an electric motor driving two pie-shaped baskets or rotors, each of which produces a centrifugal force as a result of the rotation. The two rotors are mounted on a common vertical shaft and rotate in opposite directions so that the

resultant of their centrifugal forces is a sinusoidal rectilinear force. When the baskets are lined up, a peak value of the sinusoidal force will be exerted. The structural design of the machines limits the peak value of force to 5,000 lbs. This maximum force may be attained at a number of combinations of eccentric mass and rotational speed, since the output force is proportional to the square of the rotational speed as well as the mass of the baskets and the lead plates inserted in the baskets. The maximum force of 5,000 lbs. can be reached for a minimum rotational speed of 2.5 cps when all the lead plates are placed in the baskets. At higher speeds the eccentric mass must be reduced in order not to surpass the maximum force of 5,000 lbs. The maximum operating speed is 10 cps, and the minimum practical speed is approximately 0.5 cps. At 0.5 cps with all lead plates in the baskets, a force of 200 lbs. can be generated. The relationship between output force and frequency of rotation of the baskets for different basket loads is shown in Fig. 6.

The speed of rotation of each motor driving the baskets is controlled by an electronic amplidyne housed in a control unit. The control unit allows the machines to be synchronized or operated 180^{0} out-of-phase. This makes it convenient, in structures with a line of symmetry, to excite either symmetric or anti-symmetric vibrations without changing the position of either machine.

The vibration generators are located on the dam crest approximately 200 ft. apart. One vibration generator was bolted to the dam crest adjacent to station 10. This was the master generator during the test program; the other generator or "slave" was bolted to the crest of the dam adjacent to station 7. The location of this equipment on the crest of the dam oriented to apply radial exciting forces, is shown in Fig. 3.

Accelerometers: Generally the transducers used to detect horizontal accelerations produced by these shakers are Statham Model A4 linear accelerometers, with a maximum rating of ± 0.25 g and a natural frequency of approximately 15 Hz. However, in this experiment it was noted that a large amount of noise was recorded when these accelerometers were used. It was later found that the intake system on the dam generated a vibrational frequency at between 16 and 20 Hz and because this was very close to the natural frequency of the accelerometers, they were not operable. A single ± 0.5 g Statham accelerometer was available with a natural frequency of approximately 21 Hz and this was used in some cases to verify the frequency response curves determined using the Ranger Seismometers.

Seismometers: When it was found that the ± 0.25 g Statham accelerometers would not respond properly, it was decided to use the Kinemetrics Ranger Seismometers Model SS-1 as the vibration pickups because six of these were available at the dam site. The Model SS-1 seismometer has a strong, permanent magnet as the seismic inertial mass moving within a stationary coil attached to the seismometer case. Small rod magnets at the periphery of the coil produce a reversed field which provides a destabilizing force to extend the natural period of the mass and its suspension. The resulting seismometer frequency is 1 Hz, and damping is set at 0.7 critical. The output for a given velocity is a constant voltage at all frequencies greater than 1 Hz and falls off at 12 dB/octave for frequencies less than 1 Hz.

The Kinemetrics Signal Conditioner, Model SC-1, was used to amplify and control simultaneously four seismometer signals. The four input channels have isolated circuitry to integrate and differentiate the amplified input signal. All outputs are simultaneously or independently available for recording. A modification to the signal conditioner allows

for outputing each channel separately or for taking the sum or difference on two channels and outputing the average of those channels. Each channel provides a nominal maximum gain of 100,000. An 18 dB/octave low pass filter is available with a cut-off frequency continuously selectable between 1 Hz and 100 Hz for each channel. During these tests the filter was set at approximately 8 Hz. A second signal conditioner supplied by the National Taiwan University was used to amplify and control the additional two seismometers.

In general for this study the amplifiers were set on the integrated mode so that the output was proportional to the measured displacements.

Equipment for Measurement of Frequency: The vibration excitation frequencies provided by the shaking machines were determined by measurement of the speed of rotation of the electric motor driving the baskets. A tachometer, attached to a rotating shaft driven by a transmission belt from the motor, generated a sinusoidal signal of frequency 300 times the frequency of rotation of the baskets. Hence, the maximum accuracy of frequency measurements was $\pm$ 1 count in the total number of counts in a period of 1 second (the gating period), i.e., $\pm$ 1/3 of 1% at 1 cps and $\pm$ 1/9 of 1% at 3 cps.

Recording Equipment: A Rockland FFT 512/S Real-Time Spectrum Analyzer was used to facilitate the rapid determination of the modal frequencies. This unit is a single channel analyzer that calculates 512 spectral values from any given analog signal but displays only 400 to reduce aliasing errors. Twelve analysis ranges are provided from 0-2 Hz to 0-10 KHz. This equipment was used to obtain a preliminary estimate of the dam frequencies, using ambient vibration signals from two seismometers as described in the following section.

During the forced vibration tests, the electrical signals from the signal conditioners were fed to a Honeywell Model 1858 Graphic Data Acquisition System with 8-in. wide chart. In frequency-response tests, the digital counter reading was observed and recorded manually on the chart alongside the associated traces.

EXPERIMENTAL PROCEDURE AND DATA REDUCTION

Evaluation of Modal Frequencies: To measure the vibration frequencies of the dam, two seismometers were mounted on the crest near stations 7 and 10. First a preliminary estimate of the frequencies was determined using the ambient vibratory motion of the dam. For this purpose, the output from the two seismometers was first summed and fed to the spectrum analyzer to get the symmetric modal frequencies, and secondly the output was differenced to get the anti-symmetric modal frequencies. With the ambient modal frequencies known, the forced vibration generators were used to determine the resonant frequencies by sweeping the frequency ranges noted from the ambient study.

The sweeping technique involves increasing the exciting frequency slowly until traces on the recording chart are large enough for measurement. Above this level, the frequency is increased in steps until the upper speed limit of the machine is reached. Near resonance, where the slope of the freqeuncy-response curve is changing rapidly, the frequency-interval steps are as small as the speed control permits; however, in frequency ranges away from resonance these steps are relatively large. Each time the frequency is set to a particular value, the vibration response is given sufficient time to become steady-state before the traces are recorded. At the same time, the frequency of vibration, as recorded on a digital counter, is observed and written on

the chart with its corresponding traces. Plotting the vibration response at each frequency step results in the frequency-response curve.

In the case where the accelerometer was used, frequency-response curves in the form of acceleration amplitude versus existing frequency could have been plotted directly from the data on the recording chart. However, such curves represent response to a force which increases with the square of the exciting frequency; to obtain the so-called normalized curves for constant force, each acceleration amplitude should be divided by the square of its corresponding exciting frequency (assuming linear stiffness and damping for the structural system). If the original acceleration amplitudes are divided by the fourth power of the frequency, the displacement frequency-response curve for constant exciting force is obtained.

Measurement of Mode Shapes: Once the resonant frequencies of the structure were found, the mode shapes at each of these frequencies were determined. Because there were insufficient transducers to measure the vibration amplitude of all the required points simultaneously, it was necessary, after recording the amplitudes of a number of points, to stop the vibration, shift the instruments to new positions, and then vibrate the structure at resonance once more. This procedure was repeated until the vibration amplitude of all required points had been recorded.

Because the structure may not vibrate at exactly the same amplitude in each test run, it was necessary to maintain one reference instrument (near a point of maximum displacement) during all the mode shape measurements for a particular mode. Subsequently, all measured modal vibration amplitudes were adjusted to a constant value of the reference amplitude.

It was necessary to make corrections to the recorded amplitudes to compensate for differences between calibration factors for each

seismometer. However, absolute calibration was not required to determine the mode shapes; cross-calibration was sufficient. The seismometers and all equipment associated with them in their respective recording channels were cross-calibrated simply by placing them all together and measuring the vibration amplitude of all of the seismometers when the structure was vibrated at each of the resonant frequencies.

Determination of Modal Damping Ratios: Damping ratios were found from the normalized frequency-response curves by the formula:

$$\xi = \frac{\Delta f}{2f}$$

where

ξ = damping ratio for a selected mode

f = resonant frequency for that mode

Δf = difference in frequency of the two points on the resonance curve for that mode with amplitudes of $1/\sqrt{2}$ times the resonant (peak) amplitude.

Strictly, the expression for ξ is only applicable to the displacement resonance curve of a linear, single degree-of-freedom system with a small amount of viscous damping. However, it has been used widely for systems differing appreciably from that for which the formula was derived, and it has become accepted as a reasonable measure of damping. In this respect, it should be remembered that in the case of typical civil engineering structures, generally it is not necessary to measure damping precisely in a percentage sense; it is sufficient to know the range in which an equivalent viscous damping coefficient lies. Meaningful ranges for an arch dam might be defined as: under 1%, 1-2%, 2-5%, 5-10%, over 10%.

EXPERIMENTAL RESULTS

Modal Frequencies and Damping Ratios: In searching for the resonant frequencies, the seismometer or accelerometer (as the case may have been) was located at either station 7 or 10; in most cases station 7 was used. The initial frequency search was started on June 7, 1979, but it was not until June 8 that data actually used in the frequency response curves was taken. The water elevation on this day was 1393.4 m (4570.4 ft.), some 17.6 m (57.7 ft.) below the crest elevation of the dam.

The frequency response curves determined in the regions of the ambient frequency measurements are plotted in Figs. 7 through 13. Symmetric or antisymmetric excitation was used for each case, as noted on the figure. The curves in each case are plotted in the form of normalized displacement amplitude versus exciting frequency. For convenience, the actual peak exciting force (F_r) and maximum displacement amplitude (U_r) for each of the excited resonant frequencies are shown on the plot along with the date the data was taken and the water elevation on that date.

It is interesting to note that the frequency response curves plotted in Figs. 7 and 11 both represent essentially the same mode (f = 3.24 to 3.26 Hz), even though the first was produced by symmetric excitation and the other by antisymmetric excitation. As may be seen from the mode shape plots presented in the following section, significant energy is put into the structure when vibrating with this mode shape if either symmetric or antisymmetric excitation is applied.

The resonant frequencies and damping factors evaluated from the response curves are listed in Tables 1 and 2, respectively. The

exciting force generated by each shaking machine and the corresponding peak displacement amplitude induced at each resonant frequency are given in Tables 3 and 4, respectively.

TABLE 1 MODAL FREQUENCIES (Hz)

Excitation	Mode					
	1	2	3	4	5	6
Symmetric		3.24	4.80		5.55	
Anti-Symmetric	2.65	3.26		5.04		6.84

TABLE 2 DAMPING RATIOS (%) FROM RESONANCE CURVES

Excitation	Mode					
	1	2	3	4	5	6
Symmetric		6.0	6.9-9.7		4.1-5.5	
Anti-Symmetric	2.4-4.3	4.6		4.1-5.1		2.9

TABLE 3 APPLIED EXCITING FORCE (lb) (Each Machine)

Excitation	Mode					
	1	2	3	4	5	6
Symmetric		8088	8464		7120	
Anti-Symmetric	7246	6972		8464		4964

TABLE 4 PEAK DISPLACEMENT AMPLITUDES ($\times 10^{-3}$ in).

Excitation	Mode					
	1	2	3	4	5	6
Symmetric		0.268	0.233		0.180	
Anti-Symmetric	0.449	0.351		0.230		0.051

Mode Shapes: Once the resonant frequencies were determined, the modal displacements of the crest and of vertical sections at stations 4, 7, and 11 were found. Both radial and tangential readings were taken. The seismometer readings were normalized and then corrected with the appropriate calibration factors. For both the crest and the vertical sections, the readings were normalized relative to the readings at station 7.

The crest mode shapes are plotted in Figs. 14 through 20 and the vertical section mode shapes are shown in Figs. 21 through 29. As was noted above, the mode shape produced by symmetric excitation (Fig. 14) is essentially the same as that produced by antisymmetric excitation (Fig. 18). Also it may be seen that the positions of the shakers are such that significant energy is supplied whether the two machines are operating in-phase or out-of-phase.

Discussion of the Results: During the initial stages of the test program the water elevation was rather constant. However, starting the week of June 11 steady heavy rains fell in the watershed for the reservoir, and the water level rose from 1395.45 m (4577.1 ft.) on June 11 to 1401.1 m (4595.6 ft.) on June 15, a rise of some 5.65 m (18.5 ft.). The large rise in water level took place after most of the resonant frequencies had been determined, but before the mode shapes were measured. Time did not permit redoing the frequency response curves, so the mode shapes were determined using the resonant frequencies which had already been determined. It was noted during the mode shape runs that the peak or maximum response on the seismometers were at a somewhat lower frequency than had previously been determined during the response curve determinations. However, these differences

were not very large, and it is felt that the measured mode shapes are a good reflection of the true mode shapes.

PART II ANALYSIS OF VIBRATION PROPERTIES

FORMULATION OF MATHEMATICAL MODEL

Type of Model Selected: Because an arch dam is a complex three-dimensional system of arbitrary geometric form, the finite element method is the only analytical procedure suitable for implementation into a general purpose arch dam analysis program. Such a general purpose program, called ADAP (4), was developed in 1972-73 by the EERC under a research grant from the U.S. Bureau of Reclamation; it was considered to be the best program available for use in this project, and therefore, was selected for the analysis of Techi Dam.

ADAP provides a variety of 3D solid elements for modeling the body of a concrete arch dam. These include thickshell elements (THKSHL), based on an isoparameteric formulation which provides for quadratic geometric form and displacements in the two faces that represent the dam extrados and intrados, but only linear configurations and displacement patterns through the thickness of the dam. These elements use reduced integration to improve their ability to model the bending mechanism of the shell. Also included in ADAP are transition elements that facilitate the attachment of the dam to the foundation rock; such elements are needed because the foundation rock is modeled by 8-node brick elements. In addition, a three dimensional shell element (3DSHEL) is provided that is similar in character to THKSHL, but expresses the nodal displacements in rectangular coordinates rather than reducing them to mid-surface translations and rotations.

Because the ADAP development project was not extended to include the reservoir interaction mechanism (as originally planned), the program described in Reference 4 takes no account of reservoir interaction in

the dynamic response analysis. Therefore, an important part of the present cooperative research program was the development of pre-processor subroutines for representing the reservoir effect. Two such subroutines were prepared, both contained in a program with the name RSVOIR. A detailed description of this program is contained in the report by J. S.-H. Kuo (1) so only a brief general description will be provided here.

In both of the RSVOIR subroutines, it is assumed that the reservoir water is incompressible, so its effect on the dynamic response of the dam can be represented by an "added mass" matrix; in each subroutine the added mass matrix is evaluated in a form suitable to be combined with the mass matrix of the concrete dam elements evaluated by ADAP. The simpler subroutine is merely an extension of the Westergaard procedure originally developed for gravity dams (5). The mass associated with each node of the dam face is based on the Westergaard pressure distribution formula, but is modified by pre- and post-multiplying by the direction cosine vector to account for the orientation of the dam face relative to the rectangular coordinate axes.

In the second subroutine, the reservoir is discretized as an assemblage of fluid elements in which the nodal quantity is the hydrodynamic pressure. Because the interaction mechanism is represented by the liquid pressure at the dam face, all other nodes in the reservoir model can be eliminated and the interface pressures can then be converted into the added mass matrix. The liquid elements used to model the reservoir are of the same type as the 3DSHEL elements available for modeling the concrete. The major difference between the added mass matrices produced by the two subroutines is that the finite element result is fully coupled while the Westergaard matrix has no nodal coupling.

In other words, when using the finite element matrix, an acceleration at any dam face node will induce a change of pressure at all other face nodes; with the Westergaard model the change of pressure is indicated only at the node that is accelerated.

Material Properties: The mechanical properties used in formulating the finite element models of dam and foundation were as follows:

Property	Dam Concrete	Foundation Rock	Units
Youngs Modulus, E	5.677×10^6	8.516×10^6	psi
Poisson's Ratio, ν	0.21	0.21	---
Unit Weight, ρ	150	162	pcf
Compressive Strength, σ_c	5365	21,000	psi
Tensile Strength, σ_t	500	930	psi

No data was available for determination of temperature changes in the dam, therefore thermal stresses were ignored. This is equivalent to assuming that all stresses induced by temperature changes have been eliminated by creep effects.

The only property of the reservoir water that need be considered in evaluating the reservoir added mass matrix is its unit weight; this was taken as 62.3 pcf.

Finite Element Mesh Arrangements: In defining the finite element model for analysis of Techi Dam, the element mesh arrangements must be established for the concrete dam body, for the foundation rock in contact with the concrete, and for the reservoir water if the finite element reservoir model is used. The meshes used for each of these components are described in the following sub-sections.

(1) Dam Body: The ADAP program includes a mesh generator subroutine intended to simplify the development of the mesh of 3-dimensional elements representing the dam body. The basic concept of this generator is that all nodes are arranged in horizontal sections of the dam and in vertical lines projected up from the intersection of these horizontal lines with the canyon wall. In the case of Techi Dam, however, a pulvino block forms the contact with the abutment rock, and a perimetral joint surface is provided between this block and the dam body, as shown in Fig. 4. Also, the contraction joints between the blocks of the dam body are inclined rather than vertical. Consequently, the standard mesh generator was not appropriate to model this dam, and it was necessary to use the option of defining directly the nodal point coordinates for the dam body mesh.

For this purpose, it was decided to use horizontal node lines as in the mesh generator approach, but to provide joints at the dam-pulvino block interface, and to use inclined (rather than vertical) node lines to obtain more favorable element shapes. A preliminary arrangement was based on four horizontal section lines and defined the pulvino block by appropriately positioned nodes along these sections (plus additional block nodes in the canyon base). However, preliminary studies demonstrated that the resulting highly skewed pulvino block elements did not perform well, so the inner block nodes were shifted upwards to make the sides of the block elements normal to the abutment. The final mesh arrangement for the dam concrete is shown in Fig. 30; it contains 26 elements in the dam body and 10 elements in the pulvino block. Both THKSHL and 3DSHEL elements were considered in the dam body for preliminary studies, but the mesh finally selected employed only 3DSHEL elements in the body and pulvino block.

(2) Foundation Rock: ADAP also includes a mesh generation option to model the foundation rock, and provides for three different degrees of refinement. The foundation mesh is constructed on planes cut into the rock normal to the dam-rock contact surface at the interface node locations. Figure 31 shows the trace of these normal planes as they intersect the X-Z plane of the dam coordinate axes in the Techi Dam model. On each of these normal section planes, a semi-circle is drawn from the concrete-rock interface with radius equal to the dam height. Six nodes equally spaced around this semi-circle then define the boundary of the foundation rock. Figure 32 shows these boundary nodes for the six sections associated with the negative "X" portion of the foundation rock.

Three different degrees of refinement of the foundation element mesh are available in the ADAP subroutine. In the coarsest mesh, nodes are located only in a local three element system at the dam interface, and at the outer boundary of the rock, while in the intermediate level of refinement additional nodes are interposed between the local elements and the boundary positions. Preliminary analyses indicated that the intermediate mesh provided adequately for the foundation flexibility, so it was adopted for all analyses. Thus, the foundation model consisted of 130 eight node brick elements. The rock beyond this foundation zone was assumed to be rigid, so the boundary nodes (shown in Fig. 32) were all fixed in position.

In carrying out dynamic analyses, the foundation rock could be considered to have mass, and thus contribute to the inertial forces acting in the structural system; or it can be treated as massless and thus introduce only a flexibility effect to the system behavior as it does in static analyses. Because the seismic input applied to the dam represents a free-field surface effect (not the motion at the foundation

block boundary) it is more consistent to assume the rock is massless and thus avoid wave propagation effects in the foundation block. This approach also is more efficient computationally because the interior nodes in the foundation rock can be eliminated by static condensation, and thus do not increase the number of system degrees of freedom. For these reasons, the foundation elements were assumed to be massless in these analyses.

(3) Reservoir Water: As was mentioned earlier, added mass matrices representing the reservoir interaction effects were evaluated using both a modified Westergaard model and a finite element model. The Westergaard mass coefficients depend on the water pressure expressed by the Westergaard parabolic formula multiplied by the dam surface area tributary to each dam interface nodal point; these values are then modified to account for the orientation of the dam face. Obviously, no finite element mesh is required for the reservoir water in this approach; it depends only on the mesh arrangement for the dam face.

Where the reservoir hydrodynamic pressures are expressed by the finite element method, however, it is necessary to model an adequate portion of the reservoir as an assemblage of liquid elements. In preliminary studies it was determined that a reservoir model extending upstream for a distance three times the dam height showed little effect from the assumed upstream boundary, so this size reservoir was adopted in this investigation. As was noted earlier, the reservoir elements were of the same form as the 3DSHEL elements in the dam body. They have two quadratically curved surfaces each defined by eight nodes (corner nodes and mid-side nodes). The other surfaces are defined by straight lines interconnecting corresponding pairs of nodes on the curved surfaces. The

reservoir mesh was formed by projecting these straight node lines upstream from the nodes at the dam interface; five layers of water elements were defined, with the upstream dimension increased gradually from layer to layer, as shown in Fig. 33. Boundary nodes at the rock interface on the sides of the reservoir and at the upstream end of the model were assumed fixed (immovable), and the pressure was assumed zero at the top surface nodes (waves neglected).

If the reservoir level happens to coincide with the horizontal level of a line of concrete dam nodes, the evaluation of the reservoir added mass coefficients is straightforward. However, when dealing with practical vibration analyses, the reservoir may be at any arbitrary level, and it is necessary to define the vertical dimension of the top layer of reservoir elements to represent the actual water depth. Thus the upper nodes of these elements are not consistent with the elevation of the corresponding concrete interface nodes, and the integration procedures used to evaluate the added mass coefficients must be modified. The technique used in RSVOIR (1) involves merely defining the concrete interface accelerations at the locations of the standard fluid element integration points, using the concrete element interpolation functions.

RESULTS OF ANALYSES

General Comments: The basic purpose of the vibration analyses of Techi Dam was to obtain a reliable set of modal coordinates to be used in the mode-superposition earthquake response analysis of the structure. The purpose of the vibration measurement program was to provide comparative data for use in refining the mathematical model to be used in the vibration analysis, and ultimately to give confidence in the earthquake response analysis results. The principal assumptions made in formulating

the mathematical model that needed verification or refinement were the type of reservoir model to be used (finite element or Westergaard), the Young's Moduli of the dam concrete and foundation rock, and the mesh arrangement.

To decide on the optimum mesh arrangement for the dam body and foundation rock, a series of eigenproblem analyses were performed, using the subspace iteration method incorporated in ADAP. Analyses of the system without foundation or reservoir led to the choice of the dam body mesh (Fig. 30), and analyses of this dam model with two levels of foundation refinement led to the choice of the foundation model discussed above.

Both the Westergaard and the finite element reservoir model were used for most vibration analyses so that both could be used for correlation with the measured vibration results. However, it soon became apparent that the Westergaard model tended to exaggerate the reservoir interaction effect and that the finite element results were more reliable. Consequently, the Young's Modulus used for the dam and foundation rock was verified by satisfactory agreement between the measured vibration frequencies and the analytical results using the finite element model, as will be demonstrated later.

Another comparison between the Westergaard and the finite element reservoir models was made by assuming that the dam was rigid and subjecting it to a unit acceleration in the upstream direction. The pressure distribution indicated by the two forms of added mass matrix are depicted in Fig. 34. This figure clearly shows that the Westergaard model indicates excessive reservoir interaction; this conclusion will be verified later by comparison of analytical results with the measured vibration frequencies.

Correlation of Vibration Frequencies: Because the level of water in the reservoir has a major effect on the vibration frequencies and because the water level changed considerably during the vibration measurement program, it was necessary to carry out the vibration analysis of the dam for a suitable range of water levels. In Fig. 35 is shown the variations of first mode frequency with the water level, expressed as the percentage of the empty reservoir frequency. Analytical results for both the Westergaard and the finite element model are shown, and the excessive reservoir influence shown by the Westergaard model is apparent. Also shown is the corresponding result from a study of a typical gravity dam(6). The fact that the influence of the upper part of the reservoir is similar for the arch and gravity dams is interesting, but probably the curve for an arch dam in a wider valley would have a steeper slope.

The changes of frequency as a function of water level are presented in different form in Fig. 36, which shows analytical and experimental results for the first four vibration modes. Agreement between analysis and experiment is quite good for the 90% reservoir level, but it is evident that the finite element model tends to exaggerate the reservoir interaction for the full reservoir. Also, the results shown for the Westergaard model clearly overestimate the reservoir interaction for all water levels. The complete set of analytical and measured frequencies for all modes, based on the 90% water level, is presented in Table 5.

Correlation of Vibration Mode Shapes: Although the mode shapes do not provide a quantitative correlation between analytical and experimental results, it is important to compare the shapes for each mode in order to ensure that the same mode actually is being compared. Plots of the measured and calculated radial displacement components along the crest of the dam for modes 1 through 7 are presented in Fig. 37 a through g,

TABLE 5 CORRELATION OF VIBRATION FREQUENCIES (Hz)
Reservoir at 90% Depth (538 ft.)

Mode No.	Type	Experimental		Analytical	
		Forced	Ambient	FEM	Westergaard**
1	AS	2.65	2.64	2.76	2.27
2	S	3.26	3.27	3.10	2.71
3	S	4.56*	4.60	4.75	4.06
4	AS	5.03	4.87	5.06	4.57
5	AS	5.53	5.74	5.43	4.65
6	S	(Missed)	5.96	5.79	4.79
7	S	6.82	6.85	6.52	5.47

*Mode shape not found.

**By interpolation for 90% depth.

respectively. Also shown on the same sheets are the radial displacement patterns at vertical sections through stations 4, 7, and 11. It will be noted that the experimental mode shapes were not obtained for modes 3 and 6, although a frequency response curve was established indicating a modal frequency of 4.56 Hz for mode 3.

It is apparent from these figures that several modes have rather similar shapes and that it is necessary to examine both the crest displacements and the vertical section displacements to establish the appropriate model number. Also it must be realized that the vibration generators do not excite any single pure mode shape, but actually provide input to all modes having finite radial displacements at the shaker locations. Of course, the modes with frequencies close to the excitation frequency are amplified significantly, and if the structure has very low damping the vibration mode generally will be apparent from this test procedure. But with damping ratios in the 5 to 10% range, significant interaction will be excited between modes with closely spaced frequencies, and such mode shapes will not be well defined by this test procedure.

PART III ANALYSIS OF EARTHQUAKE RESPONSE

METHOD OF ANALYSIS

Although it is recognized that significant nonlinear mechanisms may participate in the earthquake response of an arch dam, it is customary to neglect such mechanisms in a seismic safety evaluation and to assume that the dynamic behavior is linearly elastic. The magnitude and distribution of stresses resulting from the linear response analysis then provide a basis for judgement concerning the possibility of significant nonlinear behavior and of the consequences of such inelastic deformations. Because the mathematical model of an arch dam-foundation-reservoir system generally includes hundreds of degrees of freedom, it is desirable to take advantage of the assumed linearity of the system to evaluate the dynamic response in terms of its vibration mode coordinates. Assuming that the system has proportional viscous damping, the modal coordinate response is completely uncoupled, i.e., the response in each mode is independent of all other modes, and the total response is obtained by superposing the single degree of freedom modal responses. This is the mode-superposition method of analysis, and is the procedure incorporated in the ADAP program.

The equation of motion of the dam-foundation-reservoir system, represented by the finite element method, may be written

$$[\underline{m} + \underline{m}_a]\ddot{\underline{v}} + \underline{c}\,\dot{\underline{v}} + \underline{k}\,\underline{v} = -[\underline{m} + \underline{m}_a]\underline{r}\,\ddot{v}_g(t) \qquad (1)$$

where

$\underline{v}$ = vector of nodal displacements of finite element mesh expressed in rectangular cartesian coordinates

$\underline{m}$ = consistent mass matrix for the concrete dam elements

$\underline{m}_a$ = added mass matrix from reservoir (non-zero at interface nodes only)

$\underline{c}$ = viscous damping matrix (assumed proportional)

$\underline{k}$ = stiffness matrix for dam and foundation rock

$\underline{r} = \langle r_x \; r_y \; r_z \rangle$

$\underline{r}_x$ = vector with ones corresponding to the "x" displacement components in $\underline{v}$ and zeros otherwise

$\underline{\ddot{v}}_g(t) = \langle \ddot{v}_{gx} \; \ddot{v}_{gy} \; \ddot{v}_{gz} \rangle^T$ = input earthquake accelerations in x, y, z.

Solving the undamped eigenproblem

$$[\underline{k} - \omega^2 [\underline{m} + \underline{m}_a]]\underline{v} = \underline{0} \tag{2}$$

for the mode shapes $\underline{\Phi} = \langle \underline{\phi}_1 \; \underline{\phi}_2 \; \underline{\phi}_3 \; \ldots \rangle$

and frequencies $= \langle \omega_1^2 \; \omega_2^2 \; \omega_3^2 \; \ldots \rangle^T$

and introducing the modal coordinate transformation

$$\underline{v} = \underline{\Phi} \, \underline{Y} \tag{3}$$

where

$$\underline{Y} = \langle Y_1 \; Y_2 \; Y_3 \; \ldots \rangle^T$$

leads to an uncoupled set of modal coordinate response equations of the form

$$\ddot{Y}_n + 2 \, \xi_n \, \omega_n \, \dot{Y}_n + \omega_n^2 \, Y_n = - \frac{\mathfrak{L}_n}{M_n} \, \underline{\ddot{v}}_g(t) \tag{4}$$

in which

$M_n = \underline{\phi}_1^T [\underline{m} + \underline{m}_a] \, \underline{\phi}_n$ = modal mass

ξ_n = modal damping ratio

$\underline{\mathfrak{L}}_n = \underline{\phi}_n^T [\underline{m} + \underline{m}_a] \, \underline{r}$

It should be noted that Eq. 4 represents the modal coordinate response due to earthquake accelerations applied in the three coordinate axes, $\underline{\ddot{v}}_g$, and $\underline{\ell}_n$ defines the corresponding three component effective earthquake input vector (due to unit accelerations).

If the modal coordinate response history $Y_n(t)$ is evaluated by Eq. 4 for all modes from any given earthquake history, then Eq. 3 provides the corresponding history in terms of the finite element coordinates $\underline{v}(t)$. The solution of Eq. 4 may be expressed by means of the Duhamel integral as follows

$$Y_n(t) = - \frac{\ell_n}{M_n \omega_n} V_n(t) \tag{5}$$

where

$$V_n(t) = \int_0^t \ddot{v}_g(\tau)\, e^{-\xi_n \omega_n (t-\tau)} \sin \omega_n (t-\tau)\, d\tau \tag{6}$$

is one form of the Duhamel integral. For design analyses or seismic safety studies, however, only the maximum modal response need be determined, and this may be evaluated conveniently from the earthquake response spectrum. For this purpose Eq. 6 will be rewritten in terms of the three earthquake components as follows:

$$Y_n(t) = Y_{nx}(t) + Y_{ny}(t) + Y_{nz}(t)$$

$$= - \frac{1}{M_n \omega_n} [\ell_{nx} V_{nx}(t) + \ell_{ny} V_{ny}(t) + \ell_{nz} V_{nz}(t)]$$

Then considering the maximum response from the x component earthquake (with similar expressions for the other components)

$$Y_{nx_{max}} = \frac{\ell_n}{M_n \omega_n} S_{vx_n} \tag{7}$$

where S_{vx_n} is called the pseudo-velocity response spectrum of the x component earthquake $\ddot{v}_{gx}(t)$ and is given by the maximum value of the Duhamel integral (Eq. 6) achieved at any time during the earthquake.

The earthquake response spectrum defined for the Techi dam site is discussed in the following section. It represents a single coordinate component of the earthquake motion, and may be applied as a separate effect in any direction. The corresponding maximum value of the modal coordinate then is given by Eq. 7. However, because the modal coordinates do not achieve their maxima at the same instant of time, the maximum displacement in finite element coordinates cannot be obtained by introducing the modal coordinate maxima into Eq. 3. Instead, the maximum modal values of the desired response quantities must be evaluated separately and then superposed by a procedure taking account of the probability of maximum combination. The most commonly used combination procedure is the square root of the sum of the squares method (SRSS), as follows:

$$\left.\begin{aligned} \underline{v}_{max} &\doteq \sqrt{(\underline{\phi}_1 Y_{1_{max}})^2 + (\underline{\phi}_2 Y_{2_{max}})^2 + \ldots} \\ \underline{\sigma}_{x_{max}} &\doteq \sqrt{(\sigma_{x1_{max}})^2 + (\sigma_{x2_{max}})^2 + \ldots} \end{aligned}\right\} \qquad (8)$$

It should be noted that the maximum values given by Eq. 8 are associated with the response spectrum of a single earthquake component. If the combined effect of more than one earthquake component is to be determined, then the separate results from each earthquake component may be combined by the SRSS method.

DESIGN BASIS EARTHQUAKE

As a part of this cooperative research effort on Techi Dam the CEER of National Taiwan University made a seismic risk analysis of the dam site (2). Assuming a 50 year life span (or exposure period) for Techi Dam, and earthquake return periods of 25 years and 100 years, respectively, both an "Operational Basis Earthquake" (OBE) and a "Design Basis Earthquake" (DBE) were defined. The design criteria associated with these intensities of earthquake motion are that the dam should remain functional after the OBE (hence no inelastic deformations or damage should occur), whereas some damage and concrete cracking are permitted during the DBE, but there must be no possibility of collapse or release of the reservoir.

The OBE and DBE elastic response spectra for a 5% damping ratio, specified in Reference 2, are presented here in Fig. 38. From these curves it may be noted that the first mode spectral velocity for Techi Dam (using the calculated first mode frequency $f_1 = 2.75$ Hz) are about 23 and 34 cm/sec, respectively. Of course, the values for the higher modes are smaller, according to the shapes of these curves.

CALCULATED STRESSES IN TECHI DAM

Dynamic stresses in Techi Dam were calculated by the ADAP program using the analysis procedure outlined above. Pseudo-velocity response spectrum values were taken from the Design Basis Earthquake spectrum of Fig. 38 and applied in Eq. 7 to obtain the maximum response in each mode. Then the maximum modal stress values were calculated at the upstream and downstream faces of the dam (extrados and intrados), making use of the finite element stress coefficients. The modal stresses were evaluated at the element integration points in terms of vertical and horizontal

components so that they could be superposed by the SRSS method. Then contour plots were made of the superposed stress values, showing lines of constant stress value on the upstream and downstream faces.

One of the advantages of the mode superposition method of earthquake response analysis is that relatively few modes need be considered. Especially in a SRSS response spectrum analysis, it is found that the higher modes have little effect on the calculated maximum stresses. To determine the number of modes required in the stress analysis of Techi Dam, a sequence of analyses was carried out including 3, 6, 9, 12, and 15 modes; i.e., the contributions of groups of these additional modes were included sequentially in Eq. 8. Based on this study, it was concluded that modes above number 8 did not make any significant contribution, and the results presented here are from the SRSS combination of the first eight modes.

Because an earthquake applied in the upstream-downstream (U-D) direction tends to excite the essentially symmetric vibration modes while a cross-canyon (C-C) excitation excites mainly the antisymmetric modes, it was decided to study the effect of the DBE applied separately in the x and in the y global coordinate directions. It must be noted that the results of the SRSS combination (Eq. 8) are always positive, so there is no indication of antisymmetry in the dynamic response to a cross-canyon input even though the response motion may be essentially antisymmetric.

Of course the dynamic earthquake loading is only a part of the load acting on Techi Dam. In addition it is subjected to static water pressure from the reservoir and to static gravity loads due to its own weight. In general, the dam is also subjected to stress changes resulting from temperature variation and creep; however, no information was available on these mechanisms so such stresses were neglected in this investigation.

The ADAP program has the capability of calculating directly the static stresses due to water load and dead weight. The hydrostatic pressure distribution is evaluated and converted into nodal loads acting normal to the dam face, and the gravitational body force is similarly converted into consistent element nodal loads. The program then solves the assembled static equation of equilibrium to determine the static nodal displacements, $\underline{v}$, and applies the element stress coefficients to obtain the stress components at the integration points on the dam face.

Results presented in the following sections include σ_{xx} and σ_{yy} stress contours on the upstream and downstream faces due to the static load alone, and then for the SRSS earthquake stresses combined with the static stresses. The earthquake effects are presented first for the upstream-downstream earthquake, and then for the cross-canyon earthquake. The static stresses do have their appropriate sign (+ = tension, - = compression) so in combining the SRSS earthquake stresses with the static stresses, the maximum (tensile) combination was obtained by adding the SRSS values to the static values, while the minimum (maximum compression) combination was obtained by subtracting the SRSS values from the static. It must be noted here that the stress components are identified in local element coordinates rather than global, so σ_{xx} represents the horizontal stress component in the dam face (arch stress) while σ_{yy} represents the vertical stress component (cantilever stress).

Static Stresses: The static stress contours for the upstream face are presented in Figs. 39 a and b for σ_{xx} and σ_{yy}, respectively, while the corresponding results for the downstream face are presented in Figs. 39 c and d. These figures clearly show that the dam is well designed for static loads and that the symmetric loading produces essentially

symmetric stress patterns. The peak compressive stress of about 800 psi is well within the strength of the concrete. The arch stresses (σ_{xx}) show almost no tensile values, while in the cantilever direction the maximum tensile stresses are only 50 and 75 psi on the upstream and downstream faces respectively, again well within the concrete strength in tension. The contours indicate a symmetric downstream arch displacement that reaches maximum curvature at about two-thirds dam height.

Static plus Upstream-Downstream Earthquake: The maximum compressive stress contours (minimum σ_{xx} and σ_{yy}) due to static loads plus upstream-downstream (U-D) earthquake are presented in Fig. 40 a, b, c, and d, in the same sequence. Comparison with Fig. 39 shows that compression due to the earthquake in this direction merely amplifies the static compressive stresses, increasing them by about 50 percent. Clearly, these results show no risk of compressive failure of the concrete.

The maximum tensile stress contours (maximum σ_{xx} and σ_{yy}) due to static loads plus the U-D earthquake are shown in Fig. 41, a-d, again in the same sequence. The general pattern of these arch stress components is similar to the static arch stress results, but with a very large added tensile component. The arch tensile stresses near the crest of the dam have very high values with an indicated maximum of over 1600 psi right at the crest in the center of the upstream face. However, arch stresses in excess of 600 psi are limited to about the top 10 meters upstream and are localized in a top-center zone of about 20 meter radius on the downstream face. In the cantilever direction, the maximum tensile stresses are about 250 psi on the upstream face and about 400 psi downstream. There are within the expected tensile capacity of the concrete, so there should be no cantilever cracking due to this earthquake.

Static plus Cross-Canyon Earthquake: Figures 42 a-d presents the maximum compressive stress contours due to the static load plus cross-canyon (C-C) earthquake. Comparison with Fig. 40 a-d shows that the two earthquake orientations have similar effects on the maximum compressive stress contours. Both produce amplifications of the static stress values, but the amplification effect due to the U-D earthquake is greater in the central section of the dam, while it is greater near the quarter span sections for the C-C earthquake. The peak compressive stress is less than 1200 psi, so there is no danger of compressive failure due to this earthquake.

The maximum tensile stress contours due to static loads plus C-C earthquake are shown in Fig. 43 a-d. Comparison of these with the U-D earthquake effect in Fig. 41 shows that the C-C direction produces less critical tensile stresses. The arch stress patterns are generally of similar form, but are significantly less tensile in Fig. 43. The same type of conclusion can also be drawn from the cantilever tensile stress patterns; i.e., the stresses due to the C-C earthquake are less critical.

DISCUSSION OF STRESS RESULTS

From the results presented above, it is clear that Techi Dam is easily able to resist the static stresses due to gravity and water pressure loads; compressive stresses reach only a small fraction of the compressive strength of the concrete, and any potential static failure of a well designed arch dam must result from concrete crushing (assuming that the geological structure of the abutment rock is adequate). The intensity of the cantilever tensile stresses is well within the expected static tensile strength of the concrete, which may be taken as about 7.5 percent of the compressive cylinder strength. Using the specified value,

σ_c = 5365 psi, the allowable static tensile strength would be about 400 psi.

On the other hand, the U-D earthquake input induces dynamic tensile stresses at the crest region in excess of 1600 psi. Assuming that the dynamic tensile strength is 12.5 percent of the static compressive strength, the tensile capacity of this material would be about 670 psi, hence it is apparent that some type of tensile separation would be anticipated in the crest region of the dam during the Design Basis Earthquake. In fact, even the Operational Basis Earthquake which has a first mode spectral velocity about 2/3 that of the DBE would induce tensile crest stresses of about 1100 psi, again well in excess of the tensile strength.

However, the tensile stress patterns induced by the U-D earthquake plus static loads (Fig. 41) must be examined in greater detail before any conclusion may be drawn about possible cracking or failure. First, it must be emphasized that the tensile stresses are excessive only in the arch direction; there is no indication of possible cantilever cracking. Second, the really severe tensile stresses are localized in the top 10 meters of the upstream face, and from the stress contour configuration on the upstream and downstream faces it may be concluded that the critical deformation pattern involves upstream "bowing" of the central half of the dam crest. Thus the peak tensile stresses at the upstream face combine the effects of tensile arch action with the upstream bending mechanism. From the view of the dam shown in Fig. 4, it is evident that these arch tensile stresses cannot be developed. The contraction joints between the vertical blocks of the dam cannot resist tension; the joints near the crest of the dam would be expected merely to open up, with the greater tendency for opening at the upstream face.

Of course, the contraction joint opening is a nonlinear behavior mechanism and is not accounted for in the linear mode-superposition response spectrum analysis. Hence, the results presented here merely demonstrate that nonlinear behavior is to be expected, but do not indicate the true magnitudes of the resulting stresses. However, because the indicated joint opening is quite localized in this structure, it may be concluded that the vibration properties would not be affected greatly, and thus that the maximum response displacements would be only slightly modified. Accordingly, it may be concluded that the indicated elastic cantilever stresses as well as the compressive arch stresses, are a reasonable approximation of the actual nonlinear result.

The tensile arch stresses are fictitious, because the contraction joints would open as soon as tensile deformations were indicated. When intense stresses are indicated at the upstream face, it is probable that the contraction joint opens through the entire thickness of the crest structure, due to the combined tensile arch and bending effects.

On the other hand, the peak tensile stresses on the downstream face are probably associated with downstream bowing of the arch; thus it involves a bending effect that exceeds the arch compression mechanism. In this case, the contraction joint will open only part way through the dam thickness, and the compressive stresses at the upstream face will be accentuated by the opening mechanism. However, the peak compressive arch stresses on the upstream face indicated by the linear response analysis are only about 1600 psi, so it is apparent that there is adequate reserve capacity to avoid a dynamic crushing failure in this region resulting from stress concentration effects associated with the contraction joint opening on the downstream face.

Based on this evaluation of the dynamic response behavior, it may be concluded that Techi Dam can resist the Design Basis Earthquake without damage. Some "working" (movement) of the contraction joints can be expected in the central half of the dam, for ten meters below the crest, but this working will be mainly at the upstream face, and therefore only partly available for inspection. Some contraction joint opening may also occur in the upper central area of the downstream face, but this is not likely to leave any visible effects because the joint movement will be very small and will extend only a small distance through the dam thickness.

CONCLUSIONS AND RECOMMENDATIONS

Based on this comprehensive cooperative investigation of Techi Dam the following conclusions are drawn and recommendations made concerning the experimental and analytical procedures, and regarding the earthquake safety of Techi Dam:

(1) The rotating mass shaker study of Techi Dam provided information on the vibration properties that was essential to the refinement and verification of the mathematical model used in the seismic safety evaluation. However, it is evident that parallel ambient and analytical studies are needed to interpret the forced vibration data reliably.

(2) Ambient vibration studies can provide good experimental data much more conveniently than can a forced vibration experiment, but it is not as reliable in estimating the damping properties and ideally is used as a supplement to a shaking machine investigation.

(3) The ADAP program provides finite element models of both dam and foundation that effectively represent the prototype structure. Also, the analytical procedures for evaluating vibration properties and dynamic earthquake response are quite efficient.

(4) The finite element reservoir model included in the RSVOIR subroutine is much more reliable for analyses of arch dams than is the extended Westergaard model. The cost of evaluation of the added mass matrix from the finite element reservoir is significantly greater than by the Westergaard approach, but it does not represent an excessive part of the entire earthquake response analysis. Plans have been made to incorporate this subroutine into a revised version of ADAP.

(5) Techi Dam is well designed for both static and earthquake loads. It will exhibit some movement of the contraction joints in its upper central region during the very unlikely event of a Design Basis Earthquake, but the body of the dam will not be damaged even by this extreme event. It should be noted that no study was made here of the earthquake response of the gate structures or other appurtenances, and it is recommended that these be made the subject of further investigation.

(6) It is stated in the report by CEER (2) that strong motion seismograph recorders have been and are being installed in Techi Dam. If the dam is subjected to any significant earthquake motions in the future, with peak accelerations in excess of 0.10 g, the data provided by these seismographs will be most valuable in future development and verification of procedures for seismic safety evaluation. Such a full-scale experiment is the best basis for assessing present analytical techniques, and it is strongly recommended that a special research project be funded for this purpose when the major earthquake occurs.

(7) Although the linear response analysis procedures were adequate to assess the safety of Techi Dam, significant nonlinear response mechanisms can be expected in many arch dams if they are subjected to maximum credible earthquake motions. For this reason, it is recommended that the nonlinear response behavior of arch dams be made the subject of further intensive research.

Three principal nonlinear dynamic response mechanisms can be identified in arch dams: (1) contraction joint opening in response to tensile arch deformation, (2) cantilever cracking due to tensile stresses in the vertical dam monoliths, and (3) cavitation at the dam face when the negative hydrodynamic pressures exceed the hydrostatic pressures at any point on the dam face.

A second report by J. S.-H. Kuo (7) presents an exploratory study of the nonlinear response of an arch ring made up of monolith blocks. It provides analytical correlation with an experimental shaking table study done as part of this cooperative research effort (8). Considerable further work is needed to extend this procedure to the case of a three-dimensional arch dam. A preliminary shaking table study of a gravity dam monolith also is reported in Reference 8. This gave quantitative data on the cantilever cracking behavior of a vertical monolith, and also demonstrated the feasibility of performing a shaking table study of a complete arch dam model with reservoir. It is strongly recommended that further development of this type of research be done in the future. Only then will it be possible to study the resistance to collapse of a thin shell arch dam subjected to earthquake.

Reference 8 also gives some experimental evidence on the cavitation phenomenon in concrete dams subjected to earthquake motions. Preliminary analytical studies of this problem (9) have shown that this form of nonlinearity may not have a very significant effect on stresses caused by earthquake. However, further study is needed to substantiate this conclusion.

REFERENCES

1. Kuo, James Shaw-Han, "Fluid Structure Interaction: Added Mass Computations for Incompressible Fluid," Earthquake Engineering Research Center, Report No. UCB/EERC-82/09, University of California, Berkeley, August 1982.

2. Mau, Sheng-Taur, "A Preliminary Study of the Dynamic Characteristics of Techi Dam," Center for Earthquake Engineering Research, National Taiwan University, Taipei, June 1981.

3. Hudson, D. E., "Synchronized Vibration Generators for Dynamic Tests of Full Scale Structures," Earthquake Engineering Research Laboratory Report, California Institute of Technology, Pasadena, 1962.

4. Clough, R. W., Raphael, J. M., Mojtahedi, S., "ADAP - A Computer Program for Static and Dynamic Analysis of Arch Dams," Earthquake Engineering Research Center, Report No. EERC-73/14, University of California, Berkeley, June 1973.

5. Westergaard, H. M., "Water Pressure on Dams During Earthquakes," Transactions, ASCE, Vol. 98, 1933.

6. Chakrabarti, P. and Chopra, A. K., "Earthquake Response of Gravity Dams including Reservoir Interaction Effects," Earthquake Engineering Research Center, Report No. UCB/EERC-72/6, University of California, Berkeley, 1972.

7. Kuo, James Shaw-Han, "Joint Opening Nonlinear Mechanism: Interface Smeared Crack Model," Earthquake Engineering Research Center, Report No. UCB/EERC-82/10, University of California, Berkeley, August 1982.

8. Niwa, A. and Clough, R. W., "Shaking Table Research on Arch Dam Models," Earthquake Engineering Research Center, Report No. UCB/EERC-80/05, University of California, Berkeley, September 1980.

9. Clough, R. W. and Chang, C.-H., "Seismic Cavitation of Gravity Dam Reservoirs," Proceedings, International Conference on Numerical Methods for Coupled Problems, Swansea, United Kingdom, September 1981.

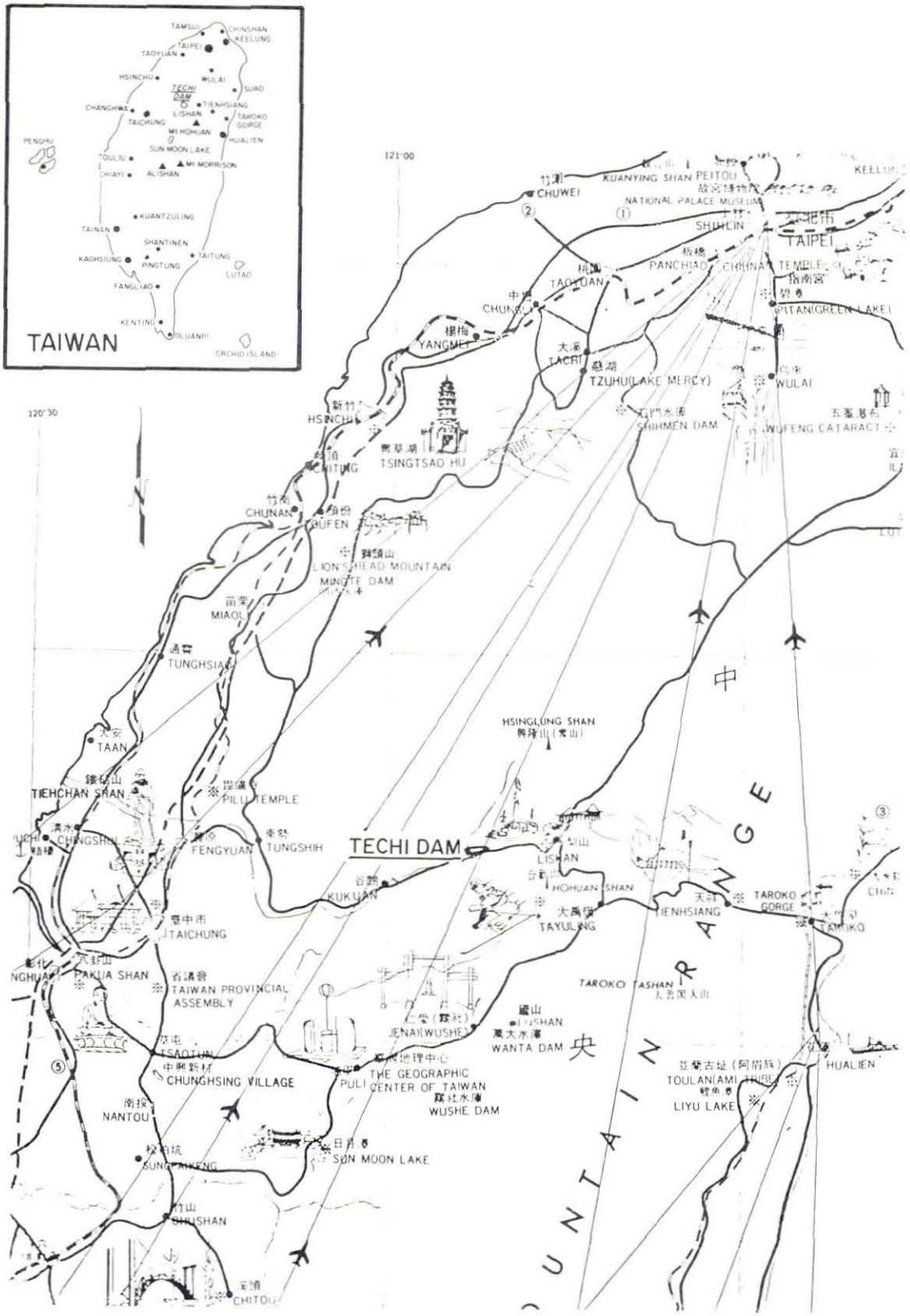

FIG.1 LOCATION OF TECHI DAM

UPSTREAM FACE

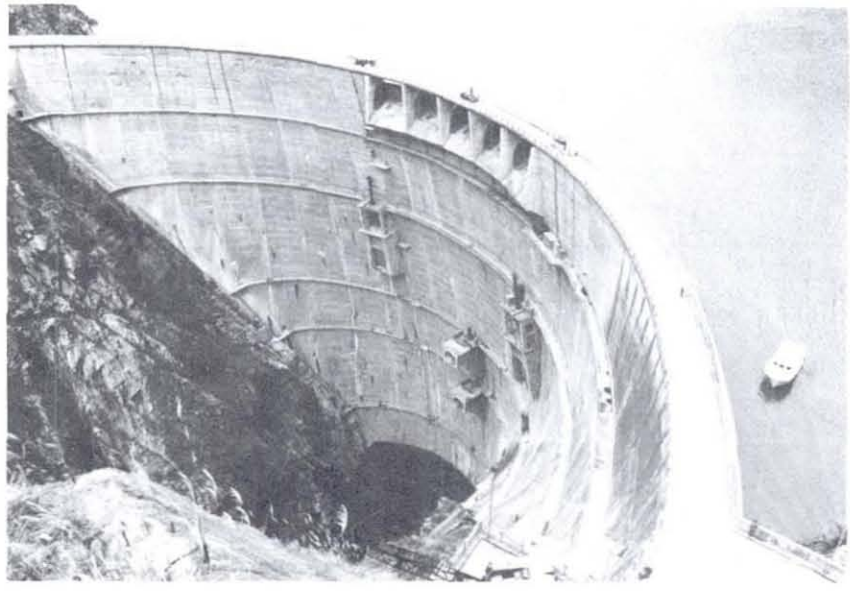

DOWNSTREAM FACE

FIG. 2 VIEW OF DAM

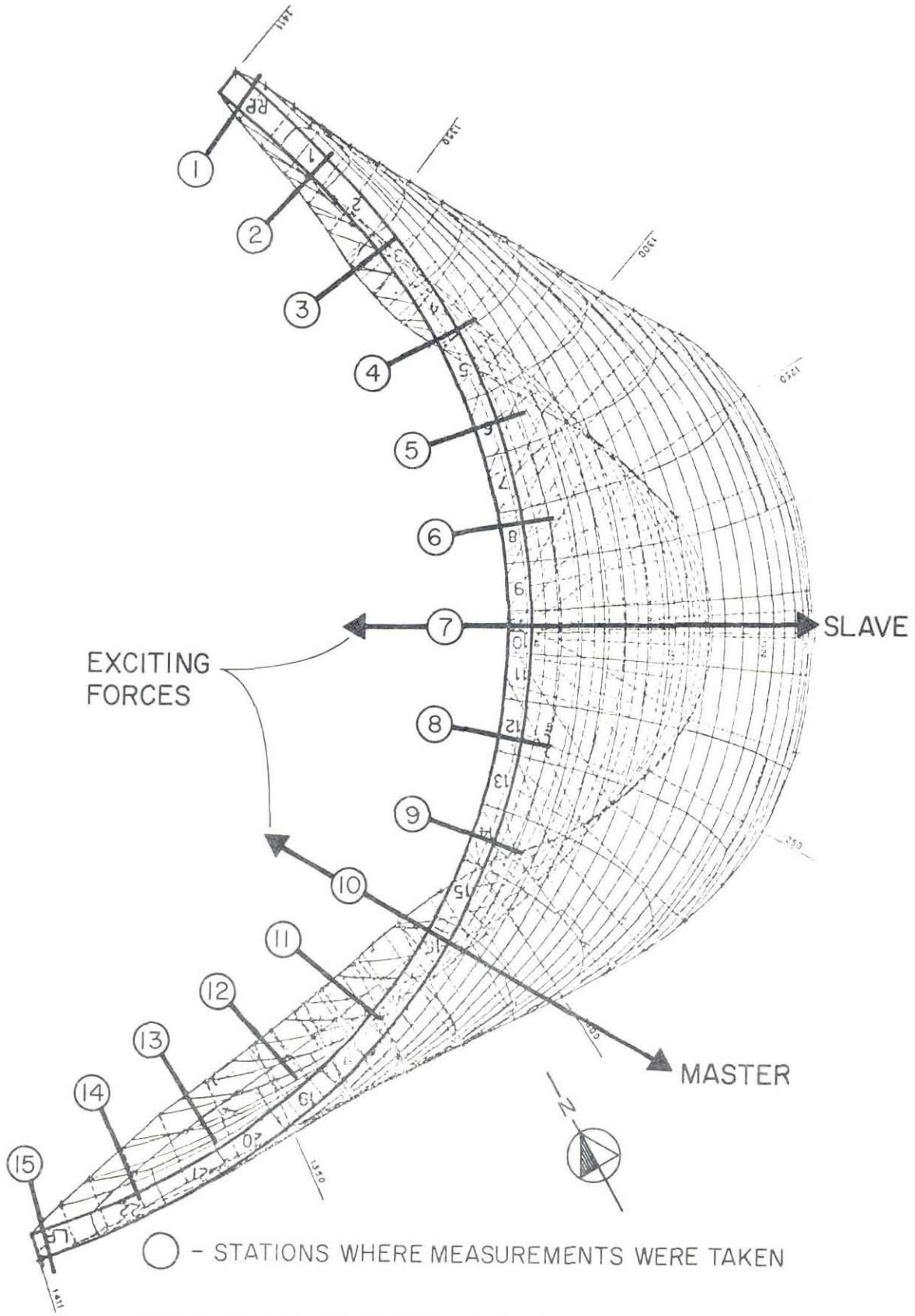

FIG. 3 PLAN OF TECHI DAM SHOWING LOCATION OF VIBRATION GENERATORS

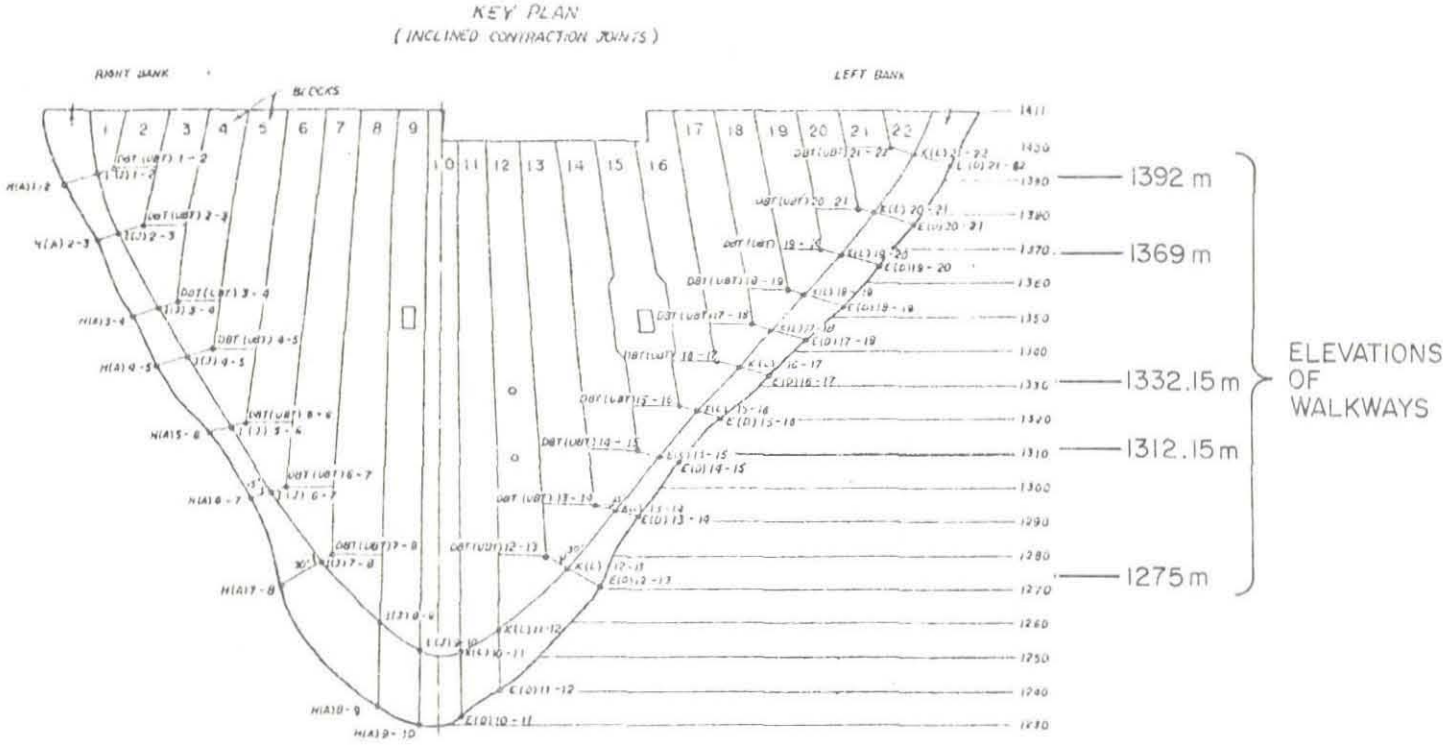

FIG. 4 PROFILE OF DAM LOOKING UPSTREAM

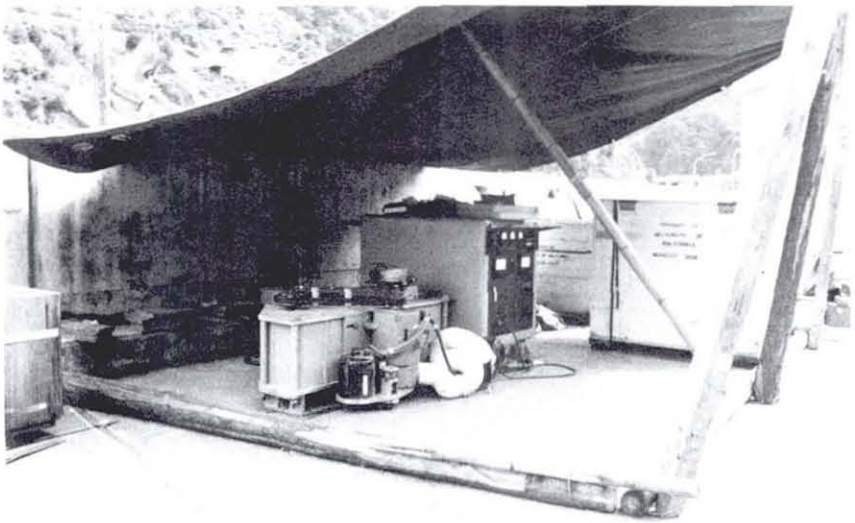

ADJACENT TO STATION 10

FIG. 5 FORCED VIBRATION GENERATOR

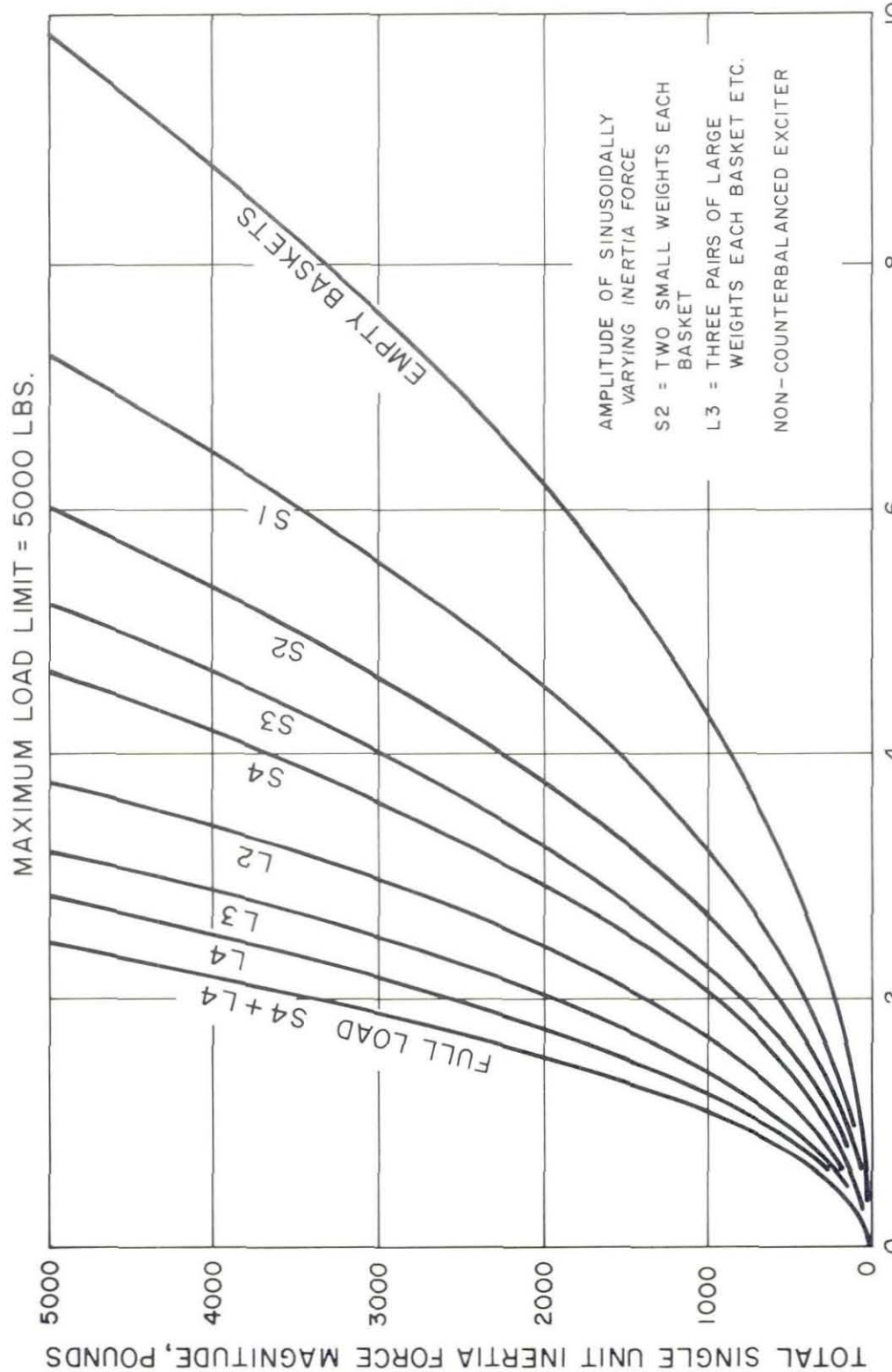

FIG.6 VIBRATION FORCE OUTPUT VS. SPEED - NON-COUNTERBALANCED (AFTER HUDSON)

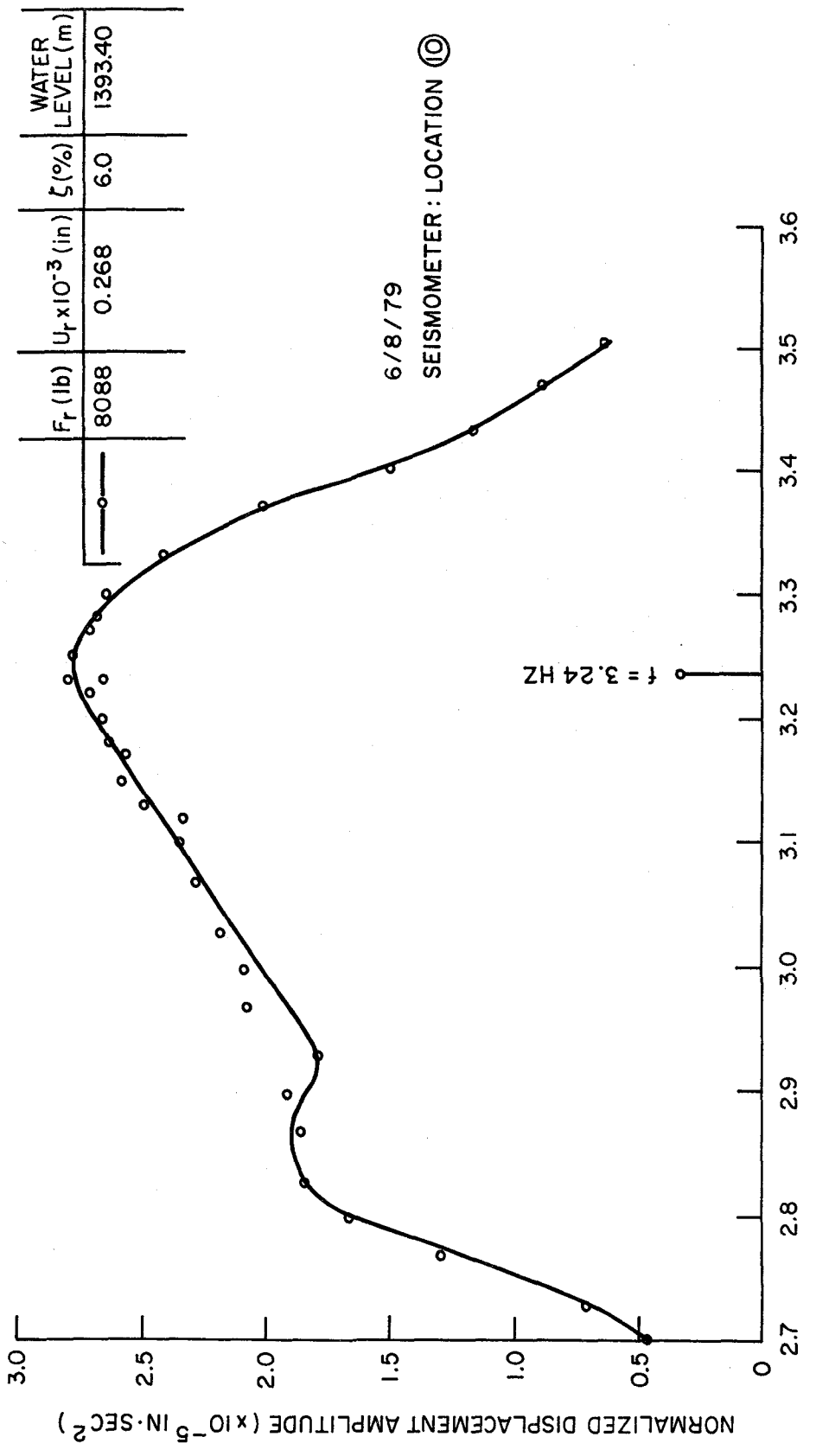

FIG. 7 RESONANCE CURVE : SYMMETRIC

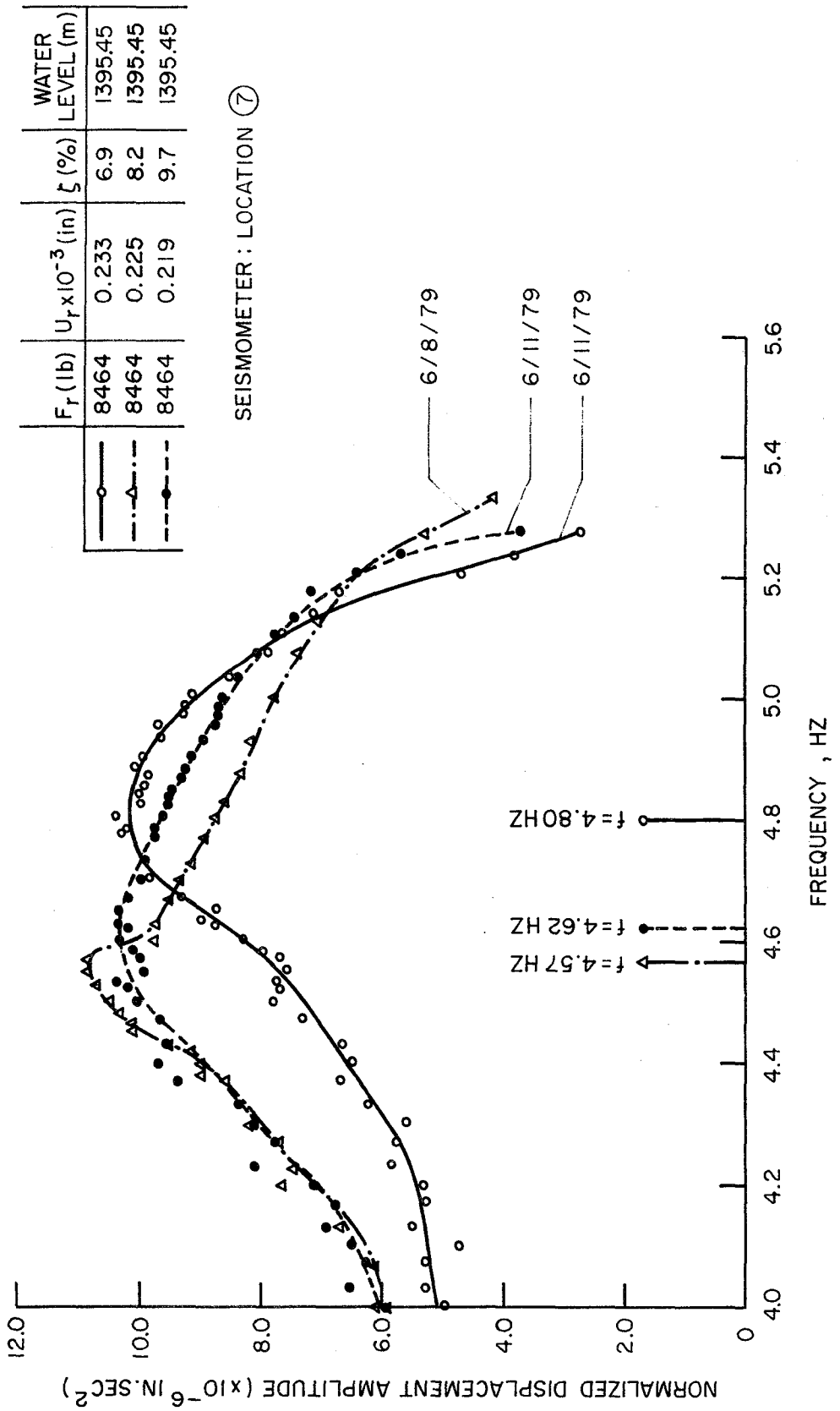

FIG. 8 RESONANCE CURVE : SYMMETRIC

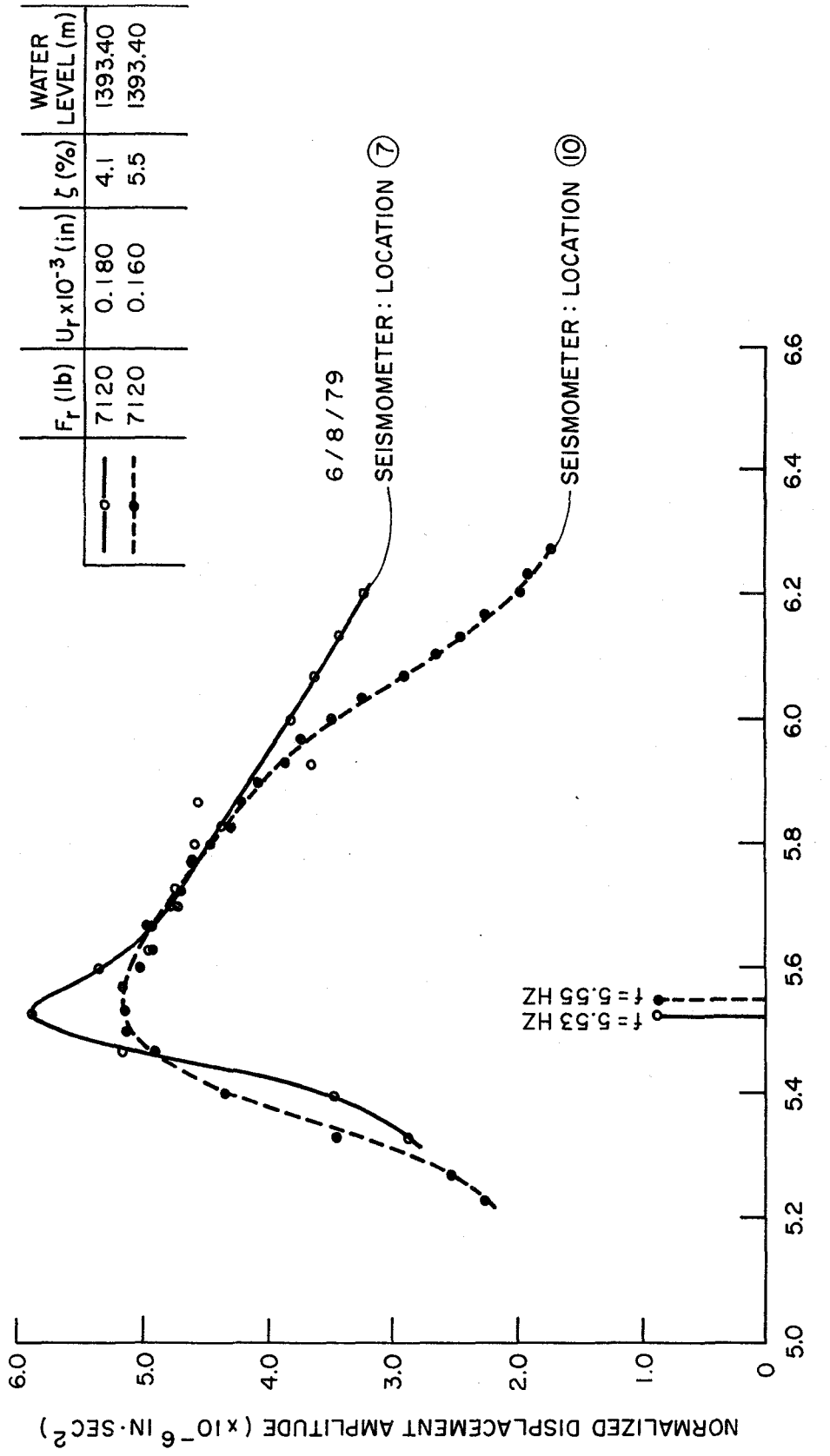

FIG. 9 RESONANCE CURVE : SYMMETRIC

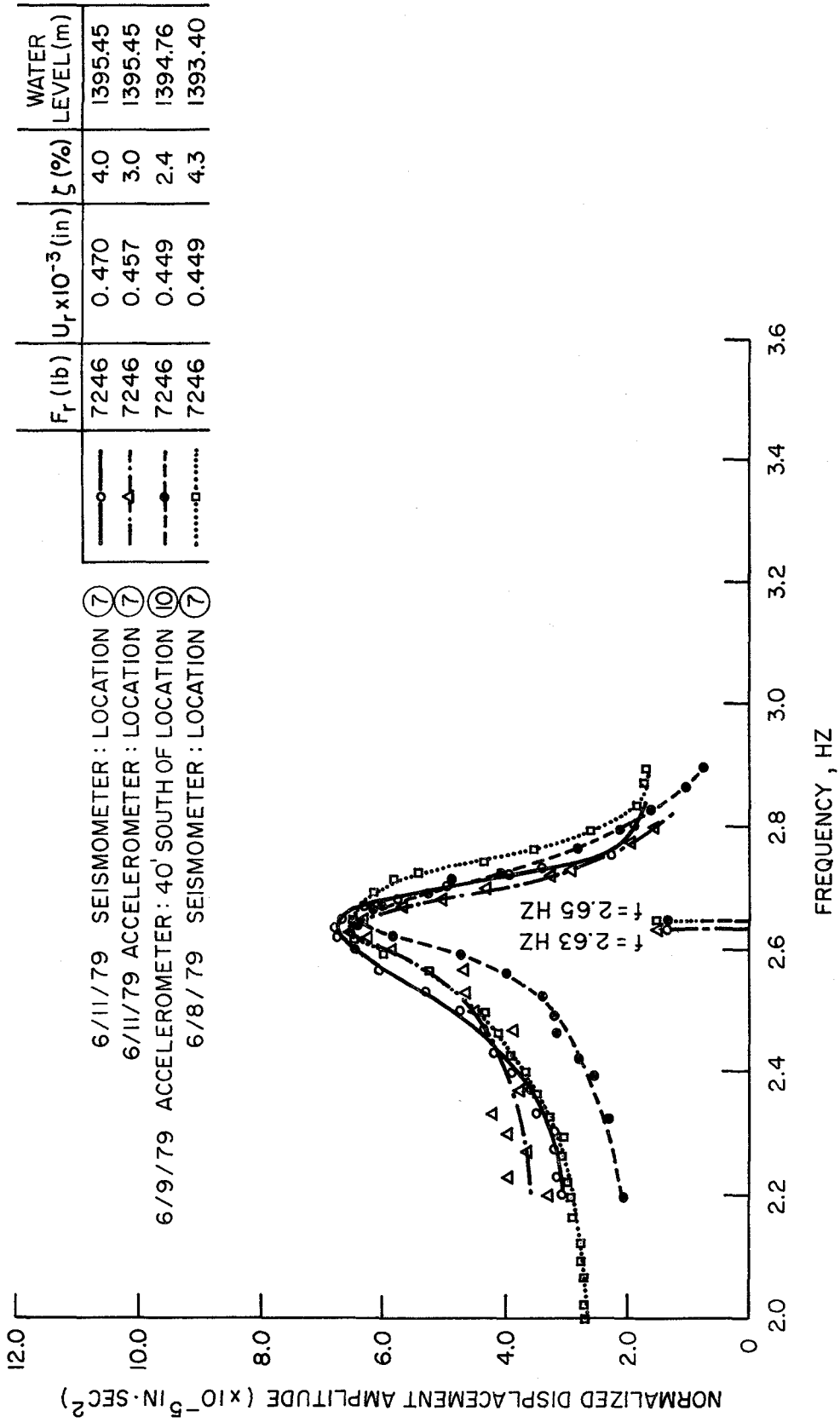

	F_r (lb)	$U_r \times 10^{-3}$ (in)	ζ (%)	WATER LEVEL(m)
6/11/79 SEISMOMETER : LOCATION ⑦	7246	0.470	4.0	1395.45
6/11/79 ACCELEROMETER : LOCATION ⑦	7246	0.457	3.0	1395.45
6/9/79 ACCELEROMETER : 40' SOUTH OF LOCATION ⑩	7246	0.449	2.4	1394.76
6/8/79 SEISMOMETER : LOCATION ⑦	7246	0.449	4.3	1393.40

FIG. 10 RESONANCE CURVE : ANTI-SYMMETRIC

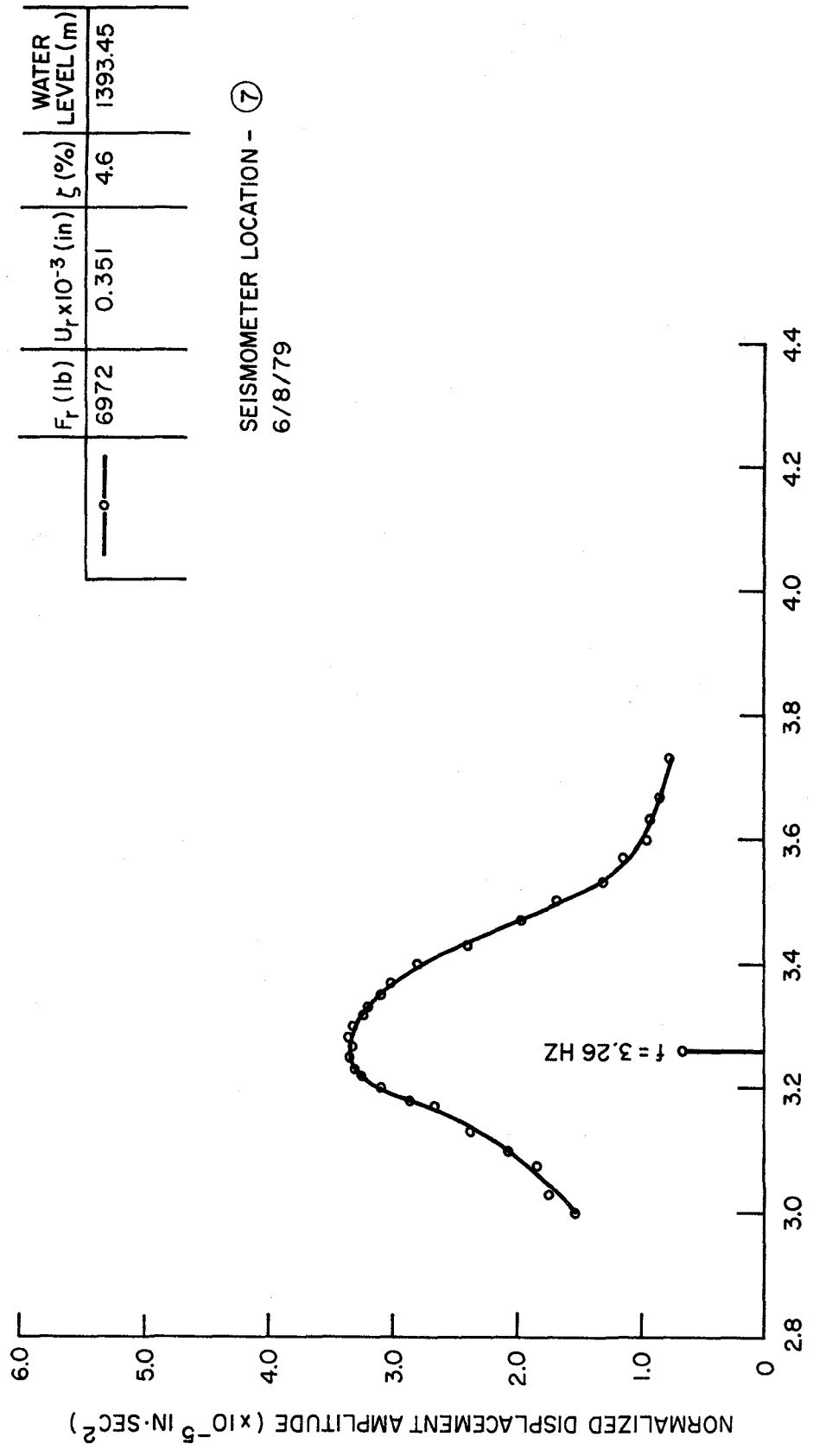

FIG. 11 RESONANCE CURVE : ANTI-SYMMETRIC

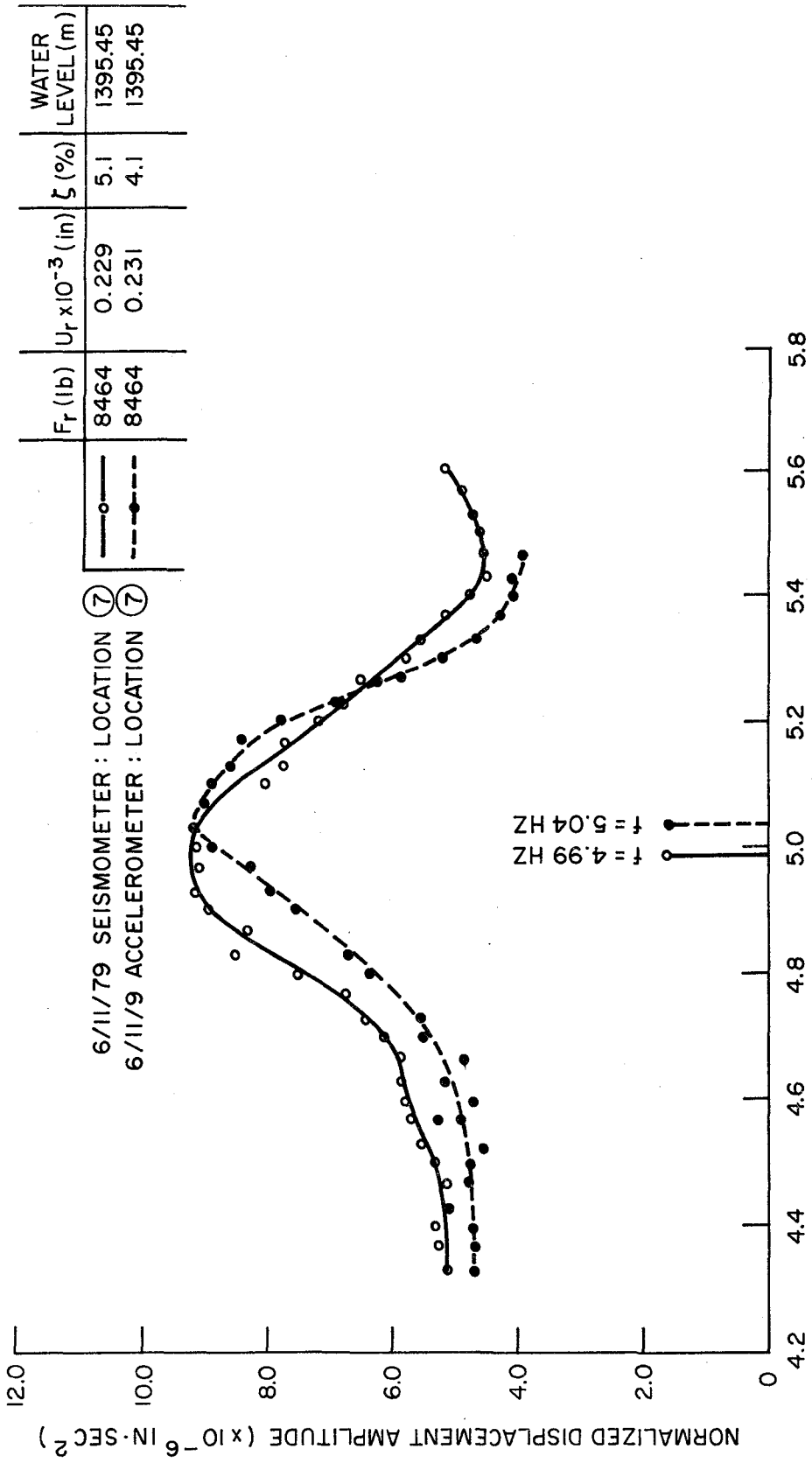

	F_r (lb)	$U_r \times 10^{-3}$ (in)	ζ (%)	WATER LEVEL (m)
—○—	8464	0.229	5.1	1395.45
- - ●- -	8464	0.231	4.1	1395.45

FIG. 12 RESONANCE CURVE : ANTI-SYMMETRIC

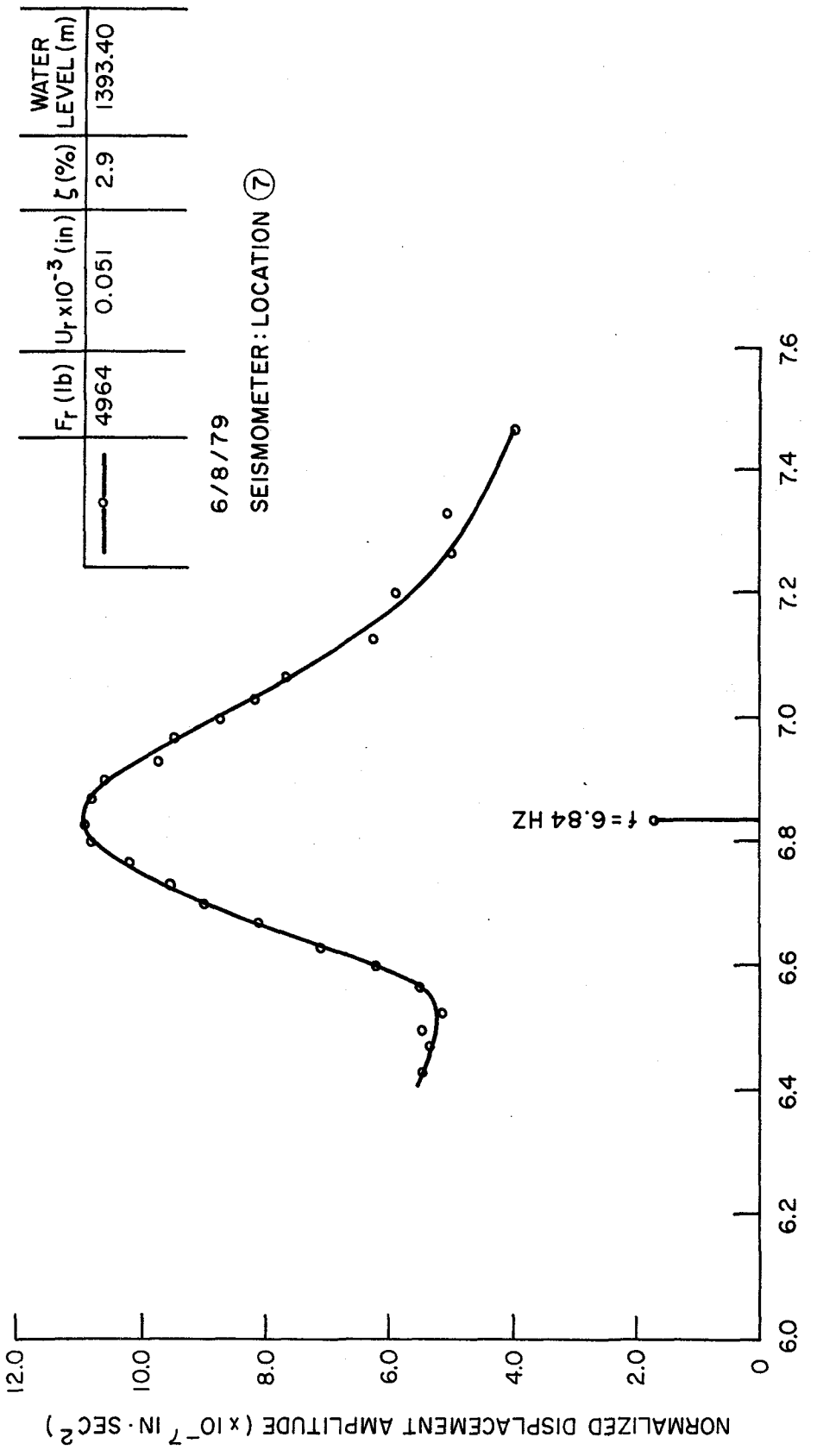

FIG. 13 RESONANCE CURVE : ANTI - SYMMETRIC

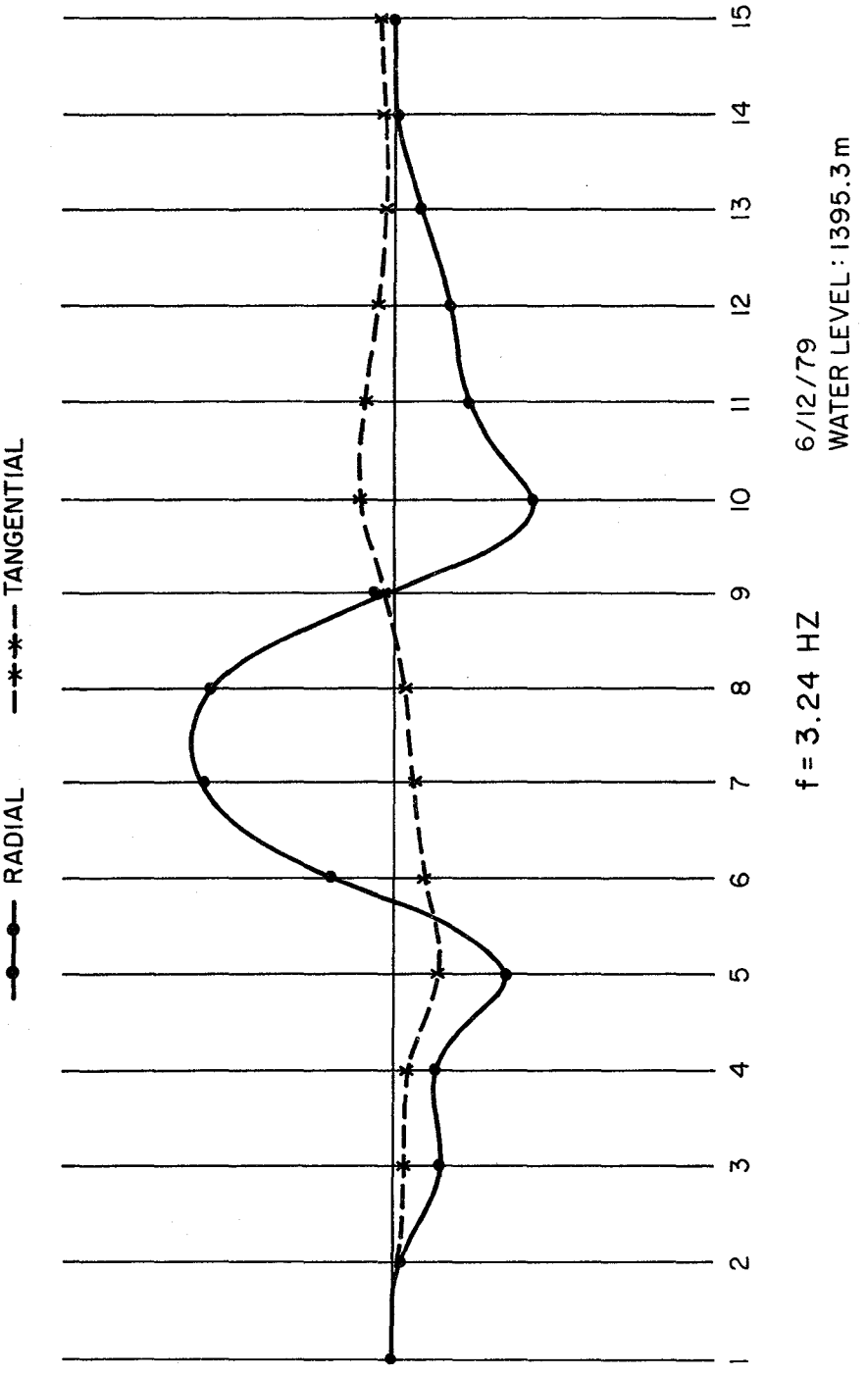

FIG.14 SYMMETRIC EXCITATION - CREST MODE SHAPE

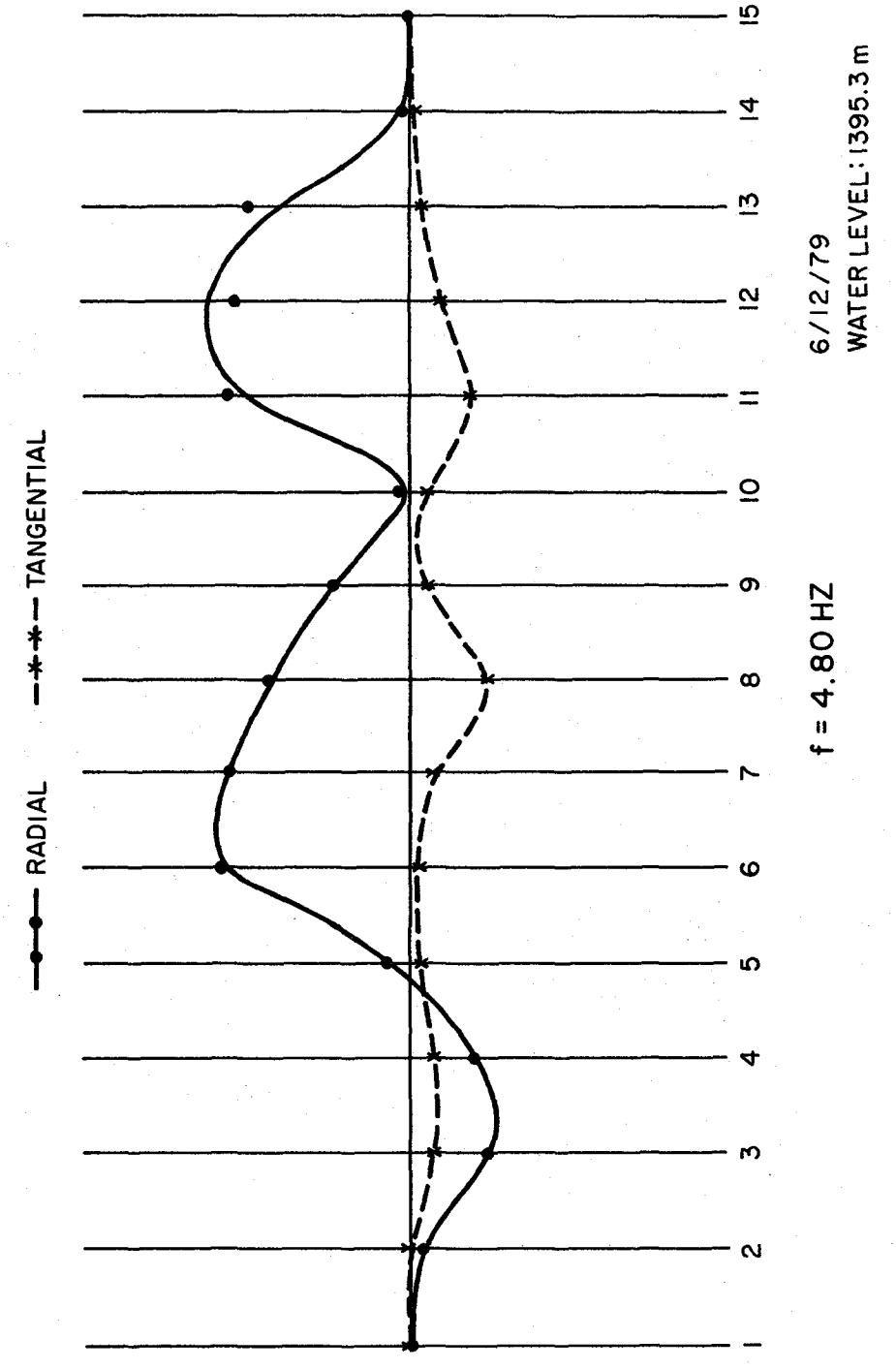

FIG.15 SYMMETRIC EXCITATION - CREST MODE SHAPE

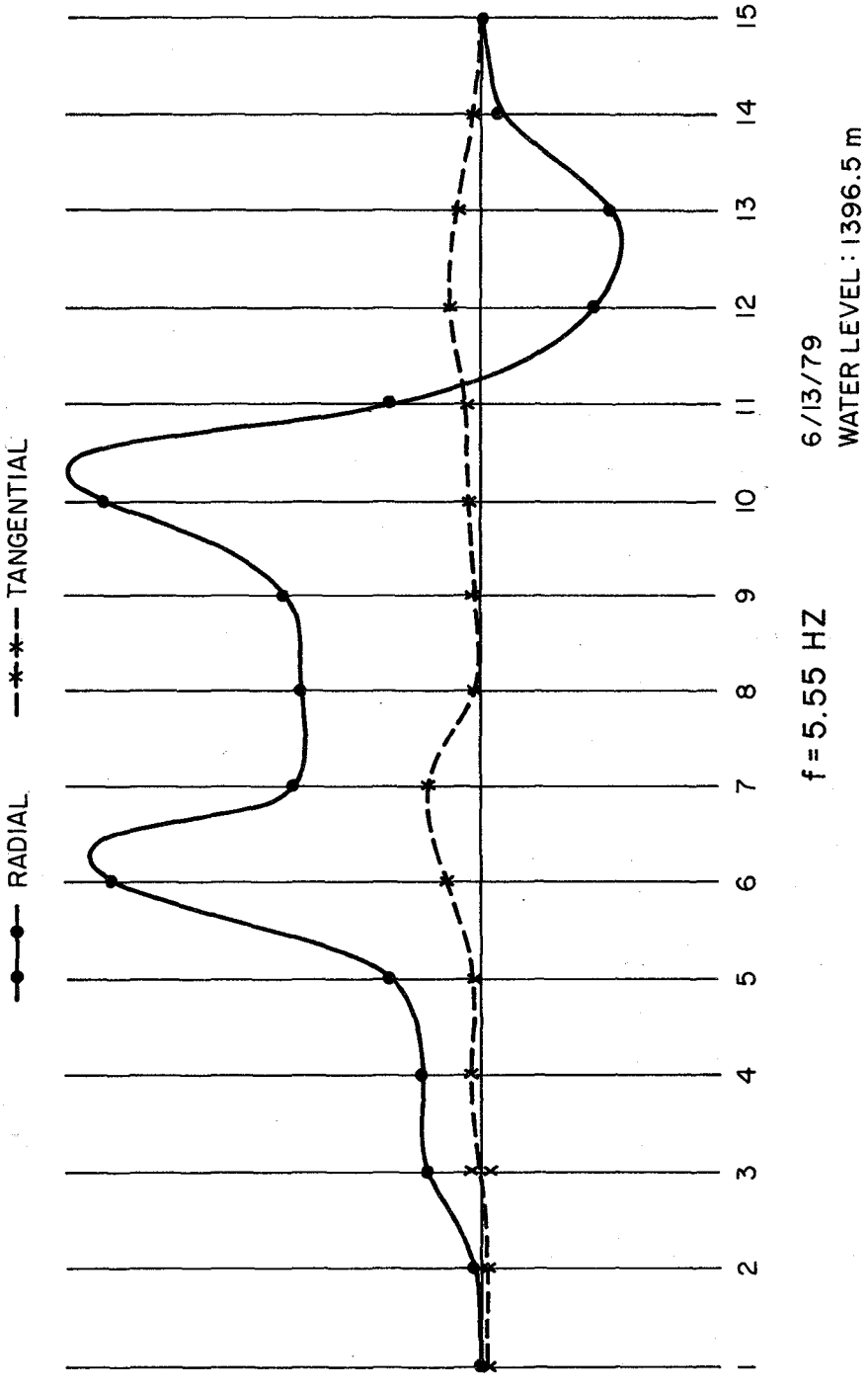

FIG.16 SYMMETRIC EXCITATION - CREST MODE SHAPE

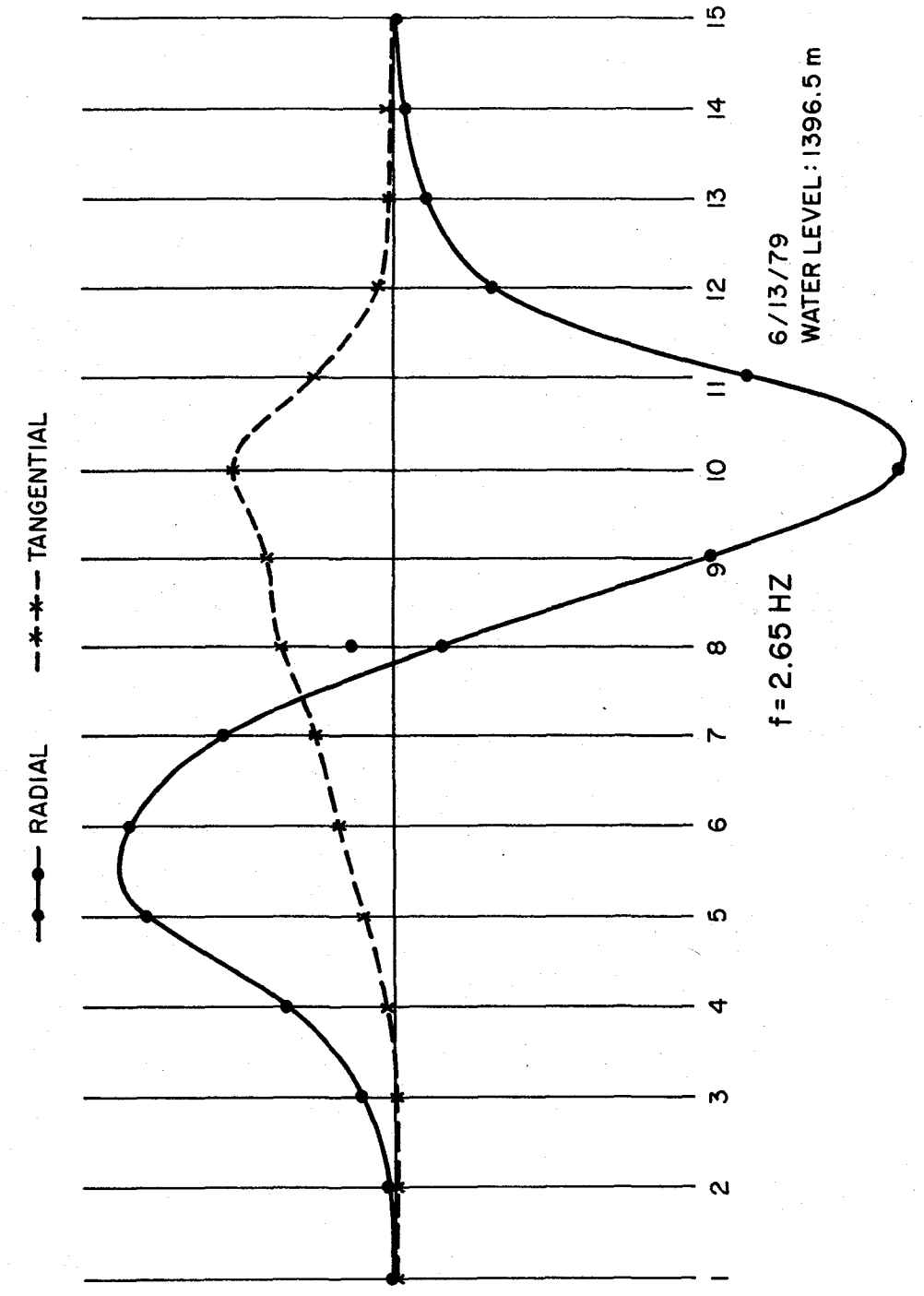

FIG.17 ANTI-SYMMETRIC EXCITATION - CREST MODE SHAPE

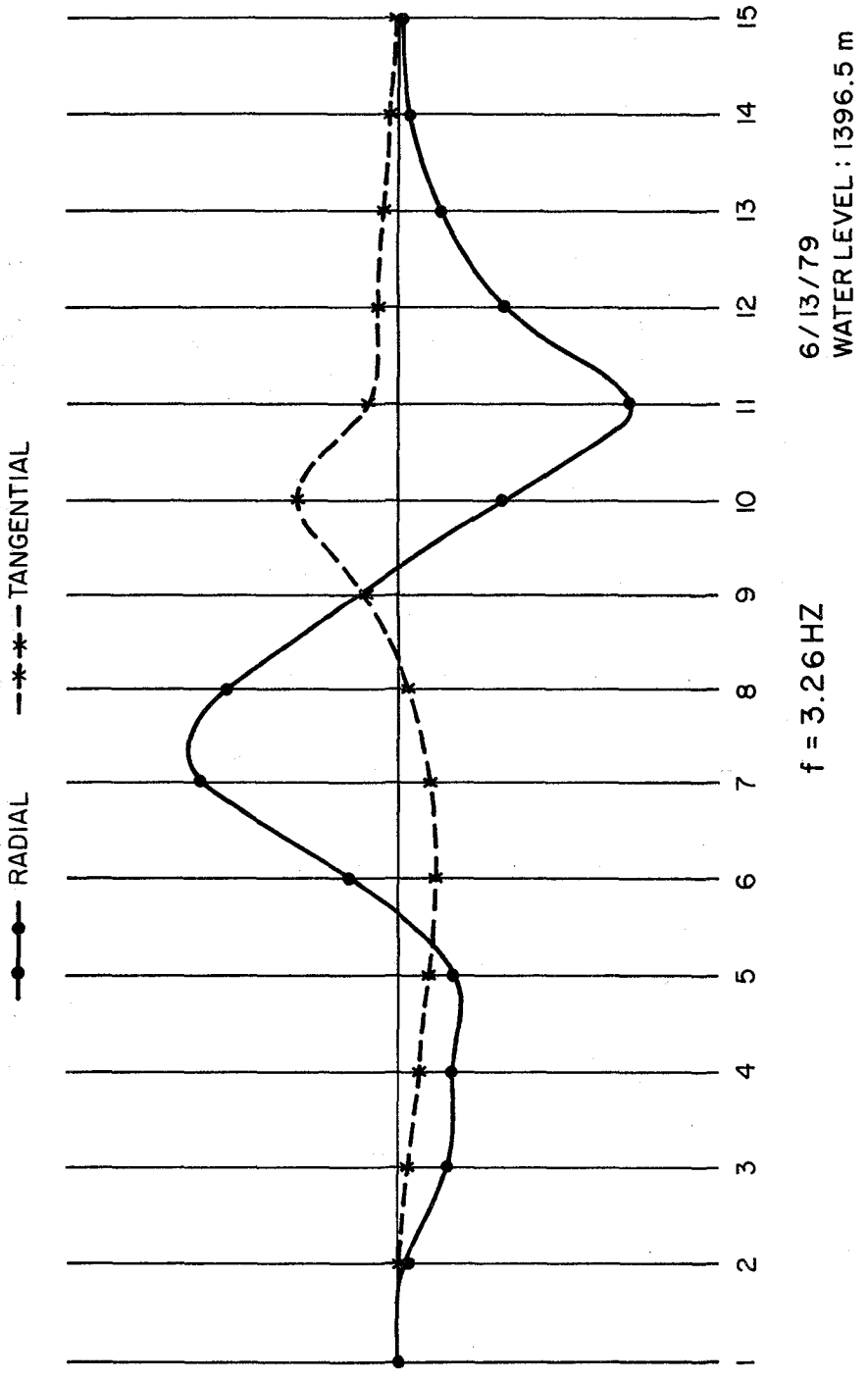

FIG.18 ANTI-SYMMETRIC EXCITATION - CREST MODE SHAPE

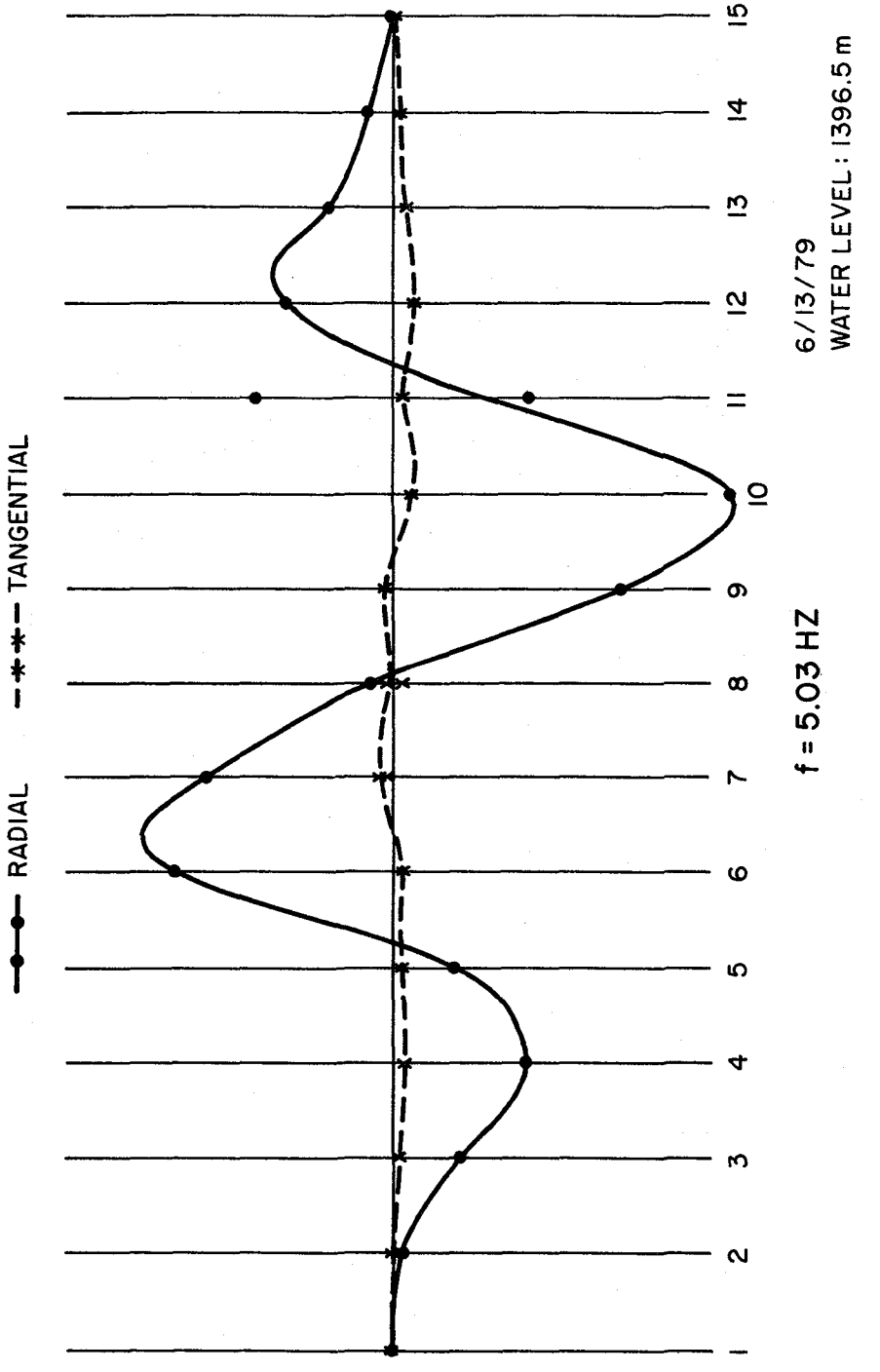

FIG.19 ANTI-SYMMETRIC EXCITATION - CREST MODE SHAPE

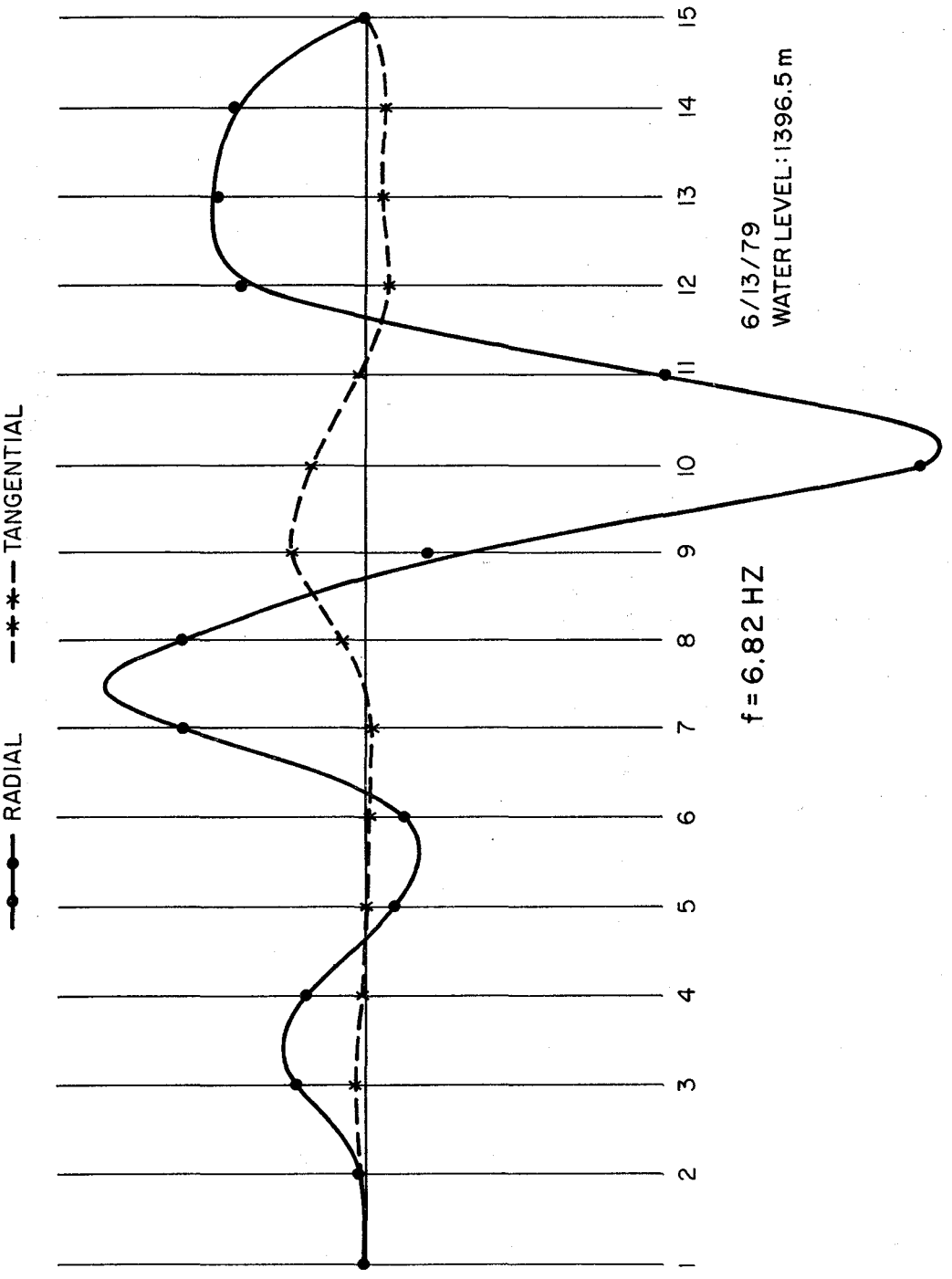

FIG. 20 ANTI-SYMMETRIC EXCITATION-CREST MODE SHAPE

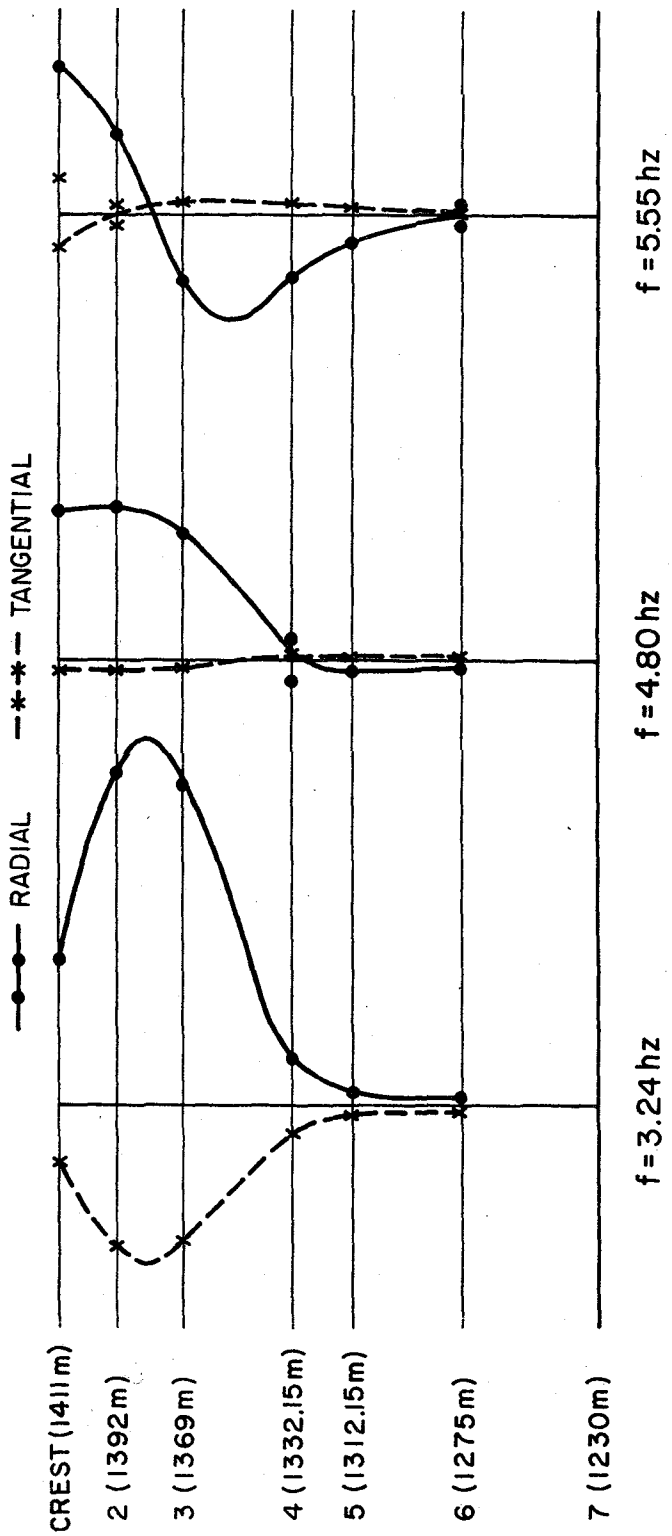

FIG.21 SYMMETRIC EXCITATION - MODE SHAPES ON SECTION 7

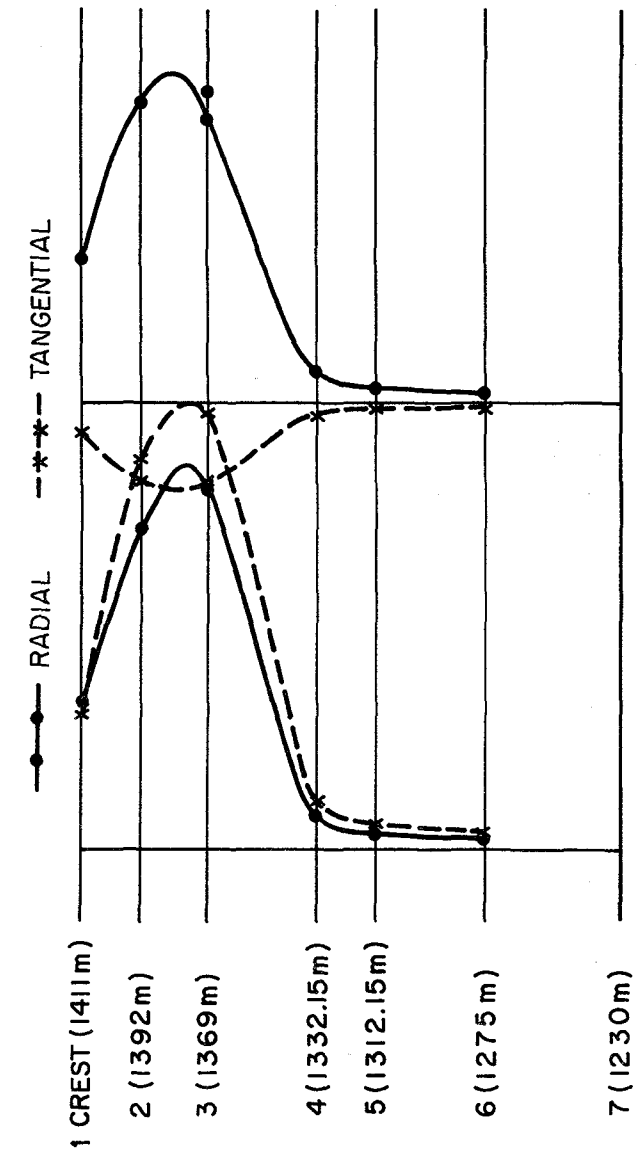

FIG. 22 ANTI-SYMMETRIC EXCITATION - MODE SHAPES ON SECTION 7

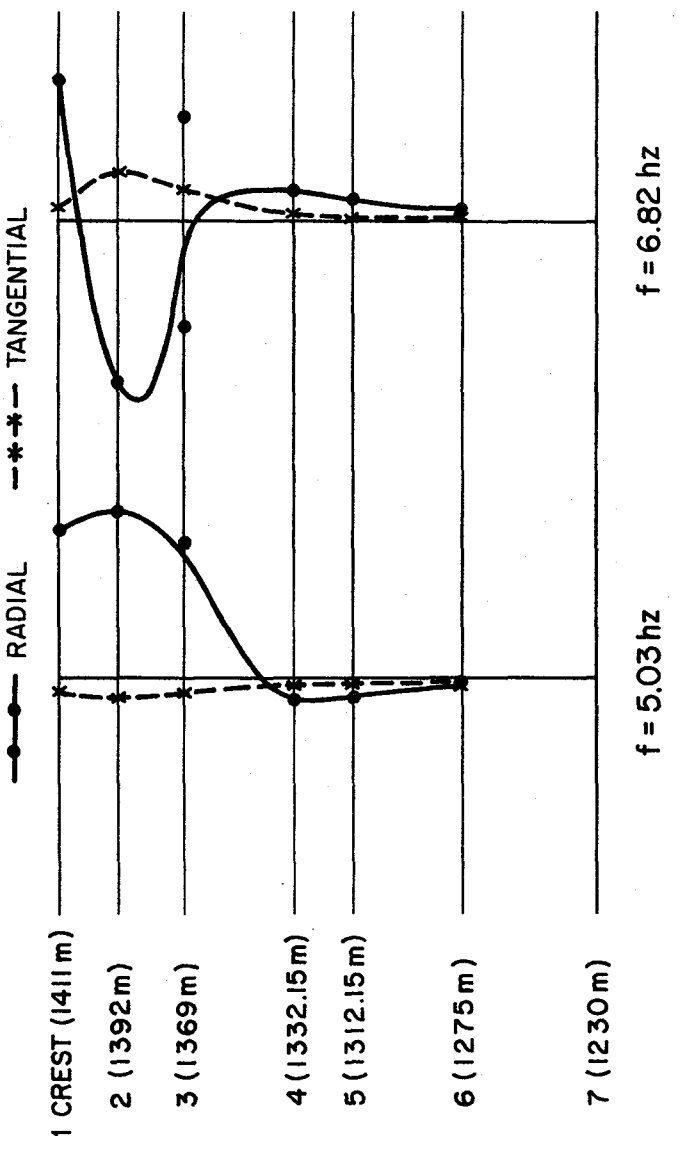

FIG.23 ANTI-SYMMETRIC EXCITATION-MODE SHAPES ON SECTION 7

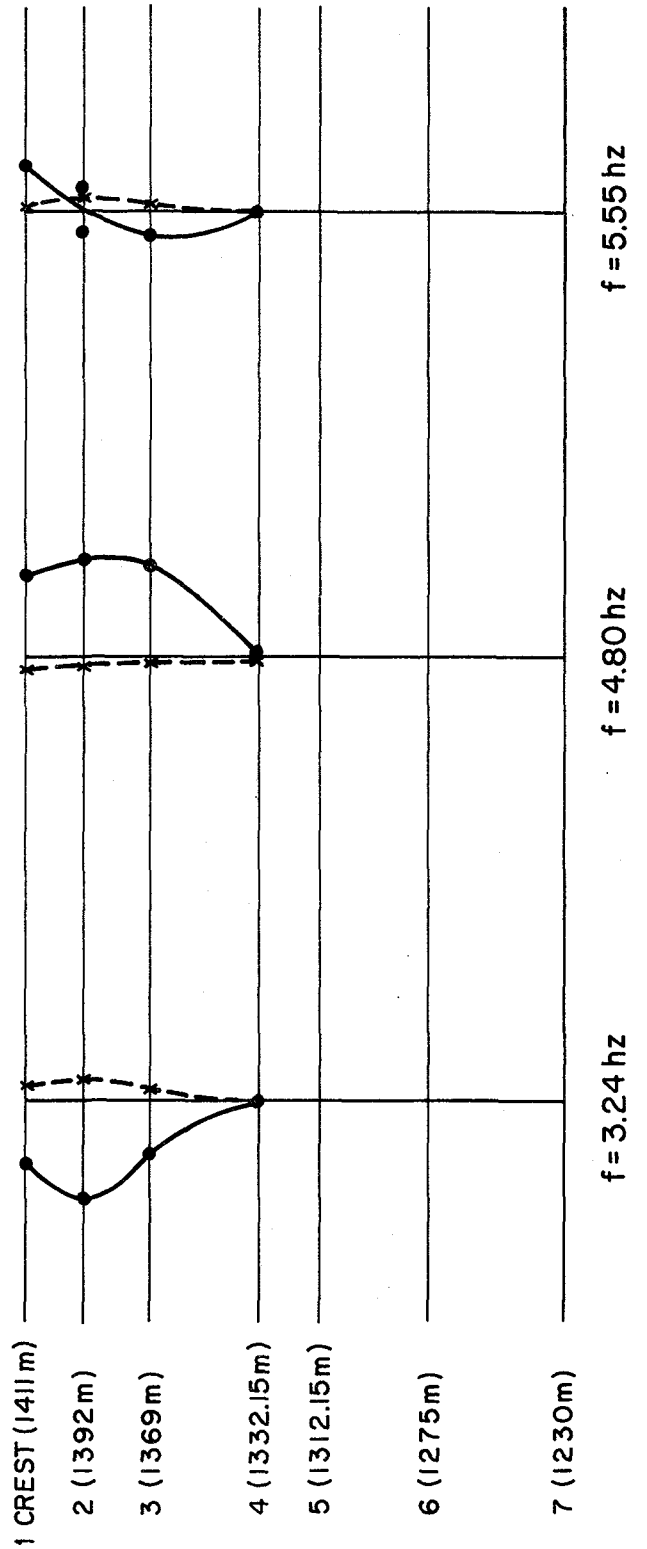

FIG.24 SYMMETRIC EXCITATION - MODE SHAPES ON SECTION II

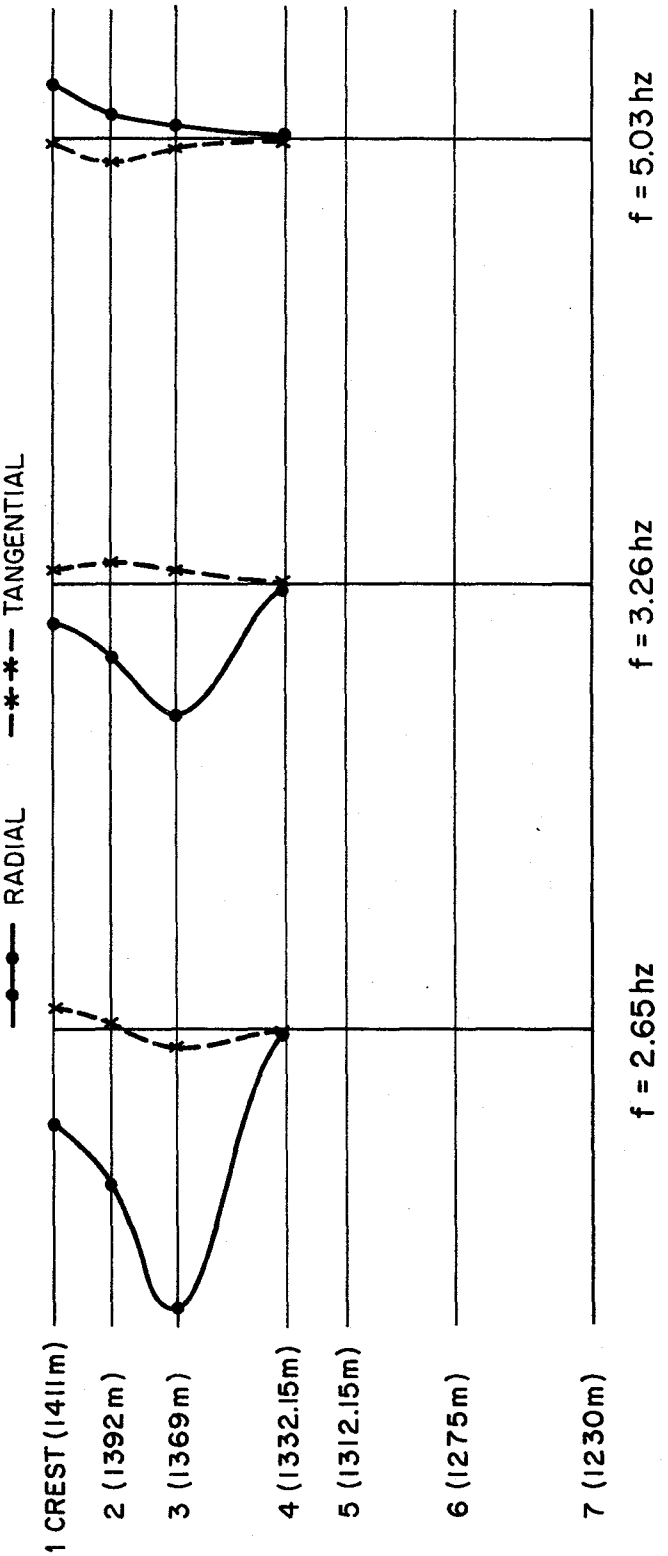

FIG. 25 ANTI-SYMMETRIC EXCITATION-MODE SHAPES ON SECTION II

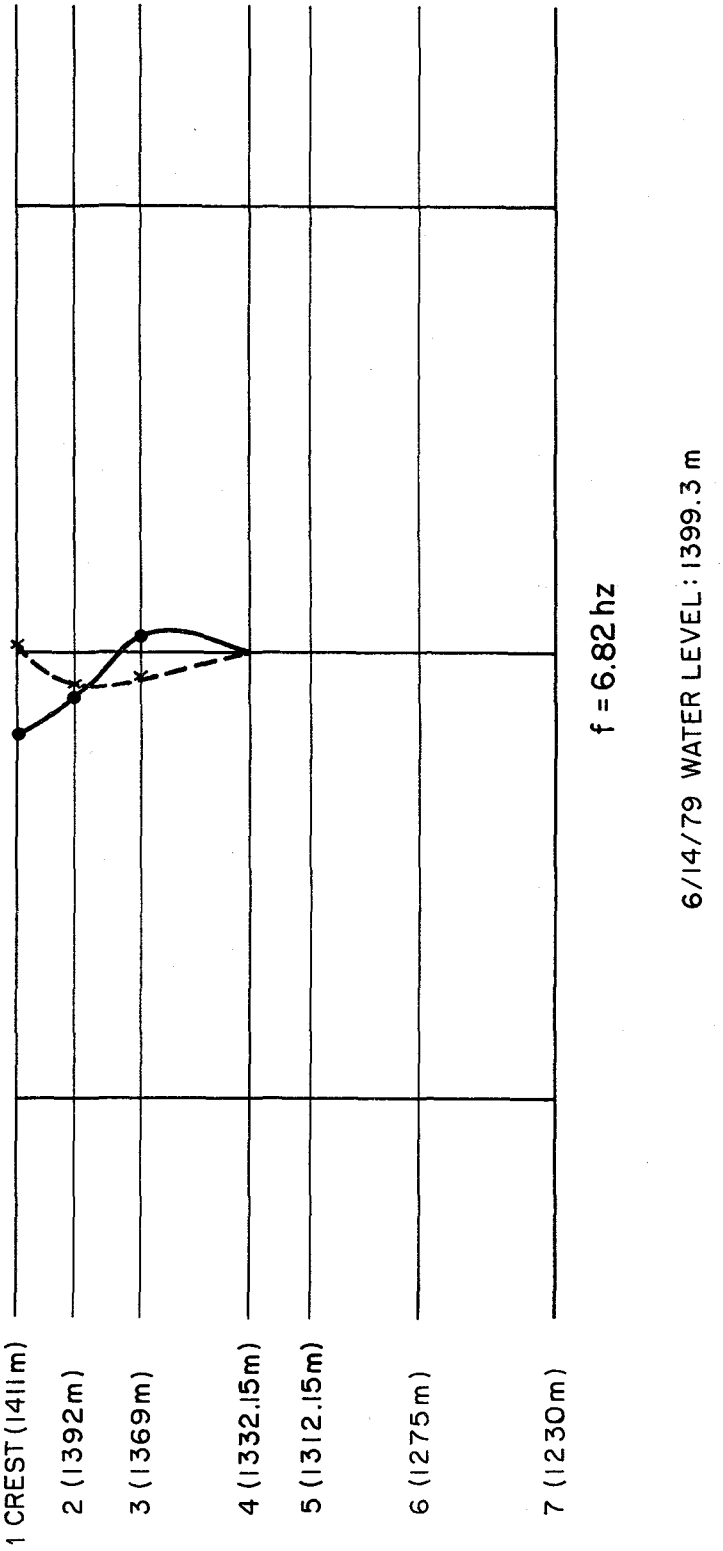

FIG. 26 ANTI-SYMMETRIC EXCITATION - MODE SHAPES ON SECTION II

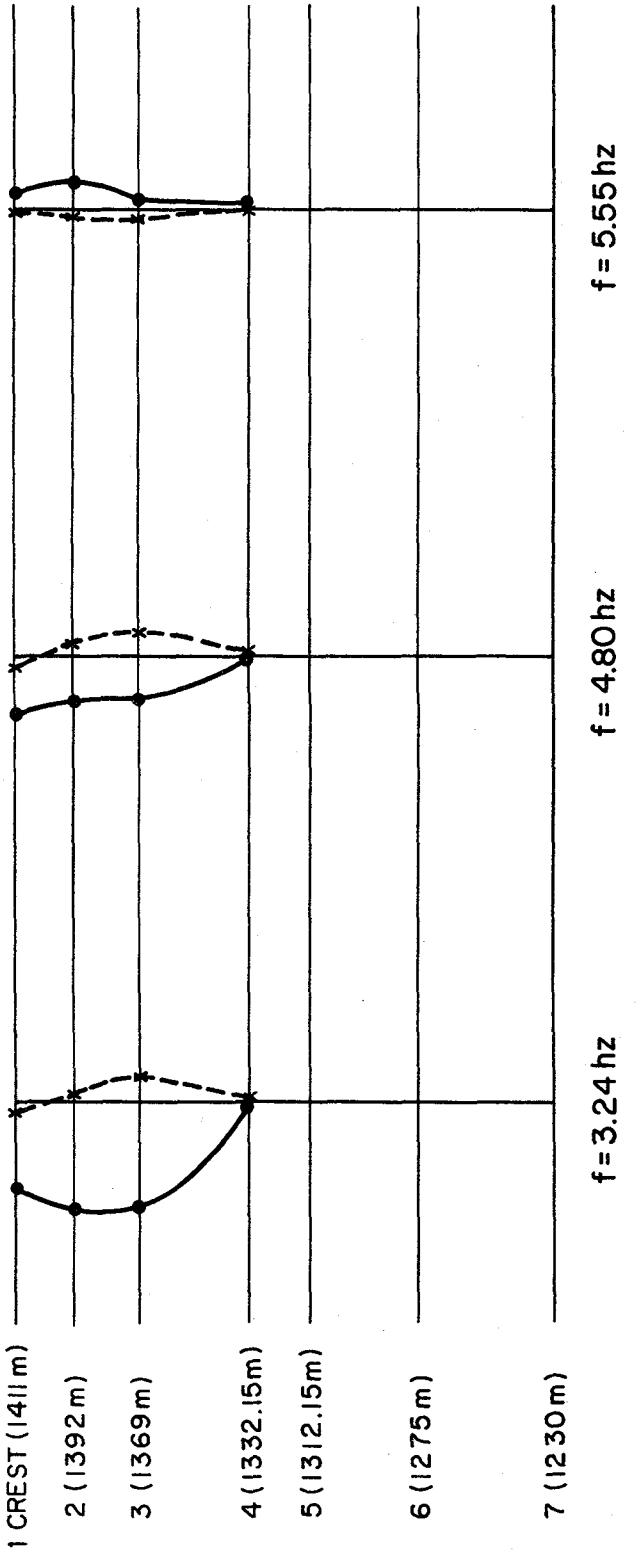

FIG. 27 SYMMETRIC EXCITATION - MODE SHAPES ON SECTION 4

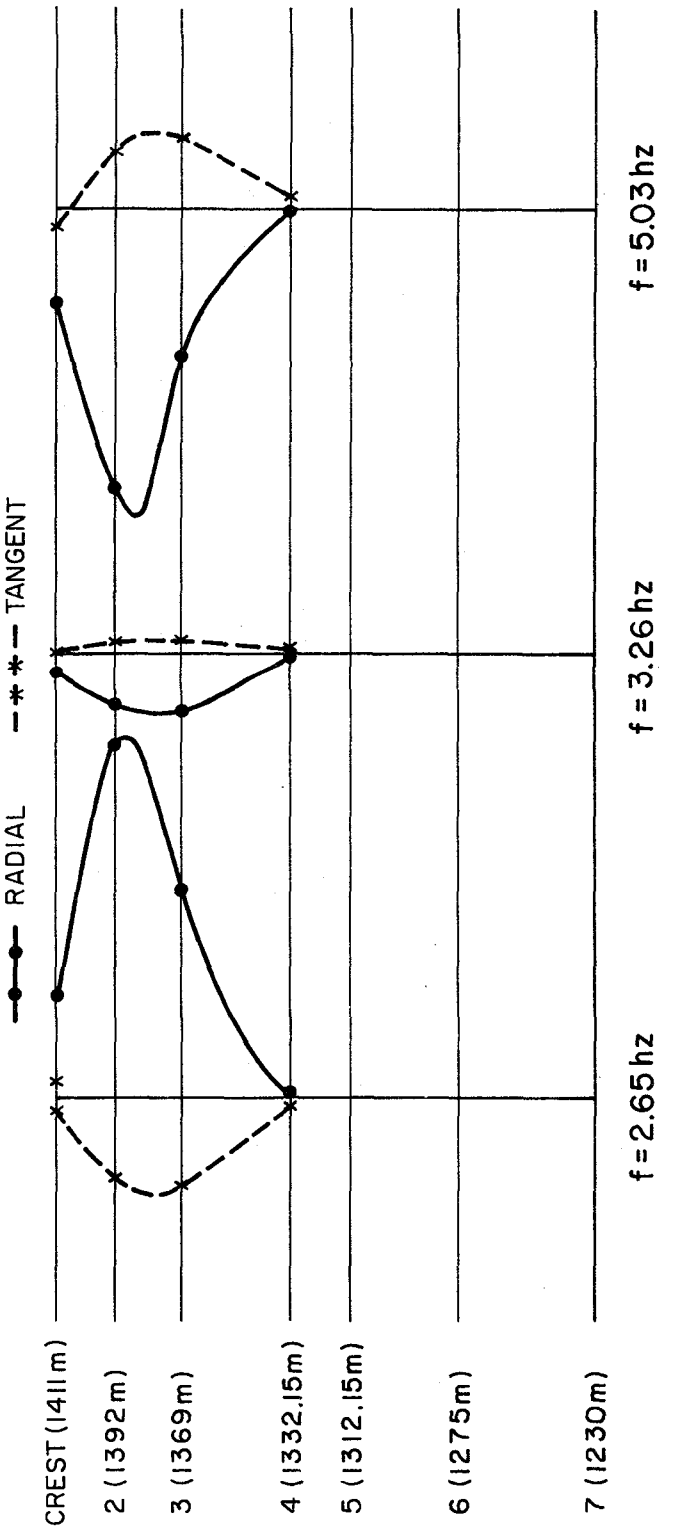

FIG.28 ANTI-SYMMETRIC EXCITATION - MODE SHAPES ON SECTION 4

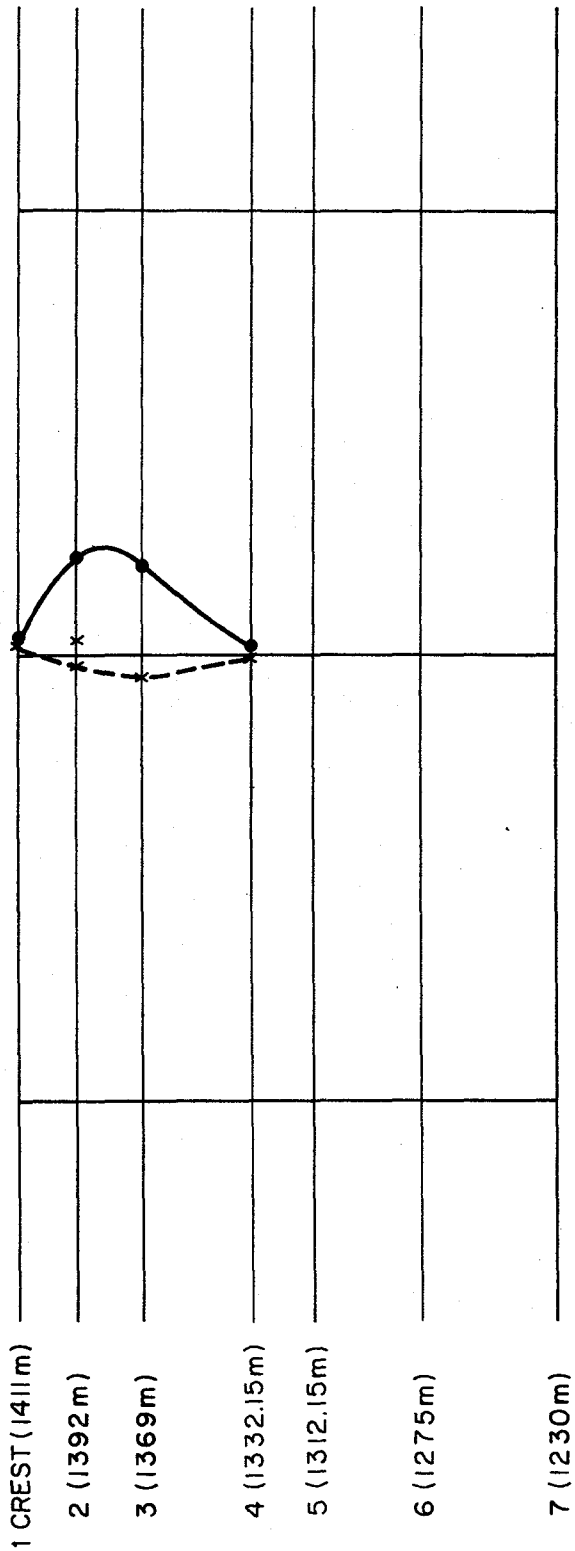

FIG.29 ANTI-SYMMETRIC EXCITATION - MODE SHAPES ON SECTION 4

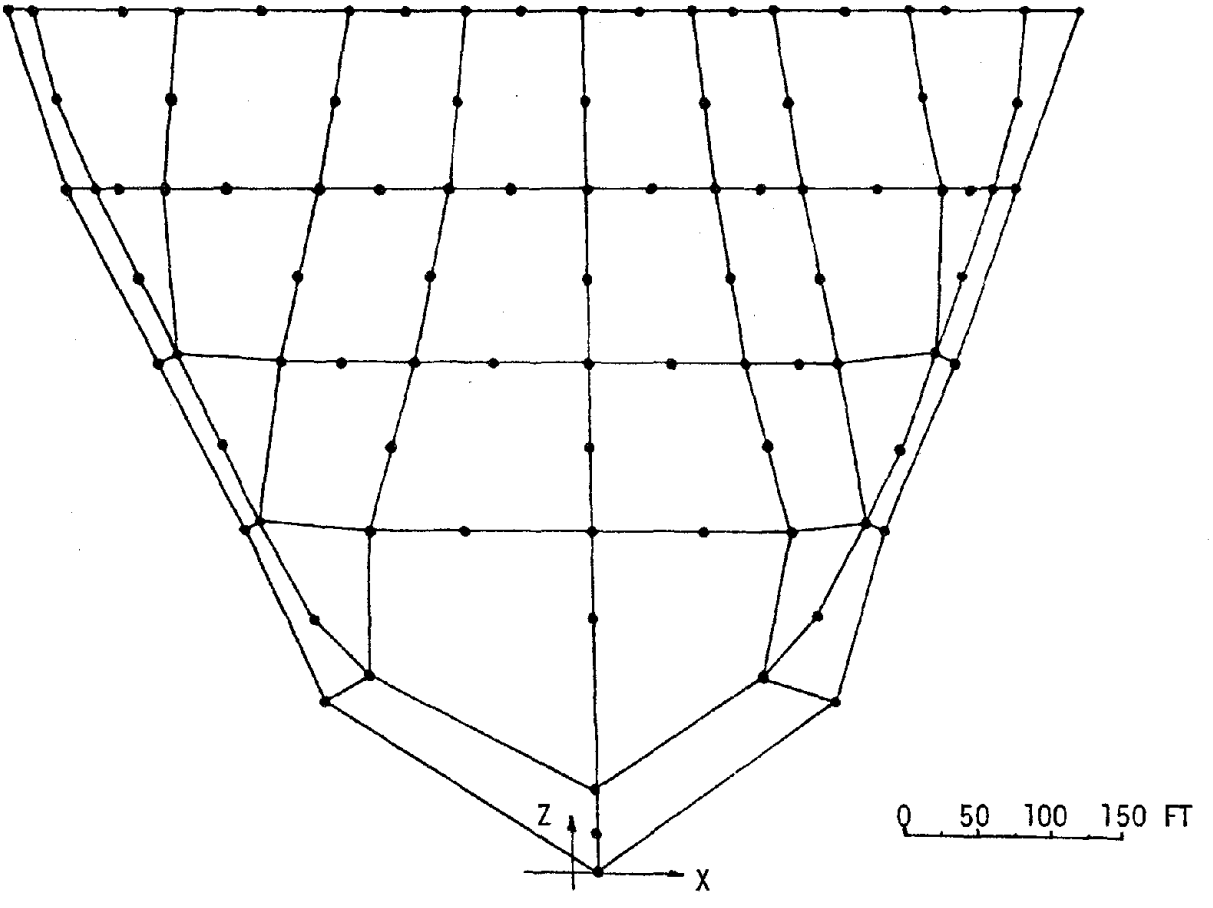

FIG. 30 FINITE ELEMENT MESH OF TECHI DAM

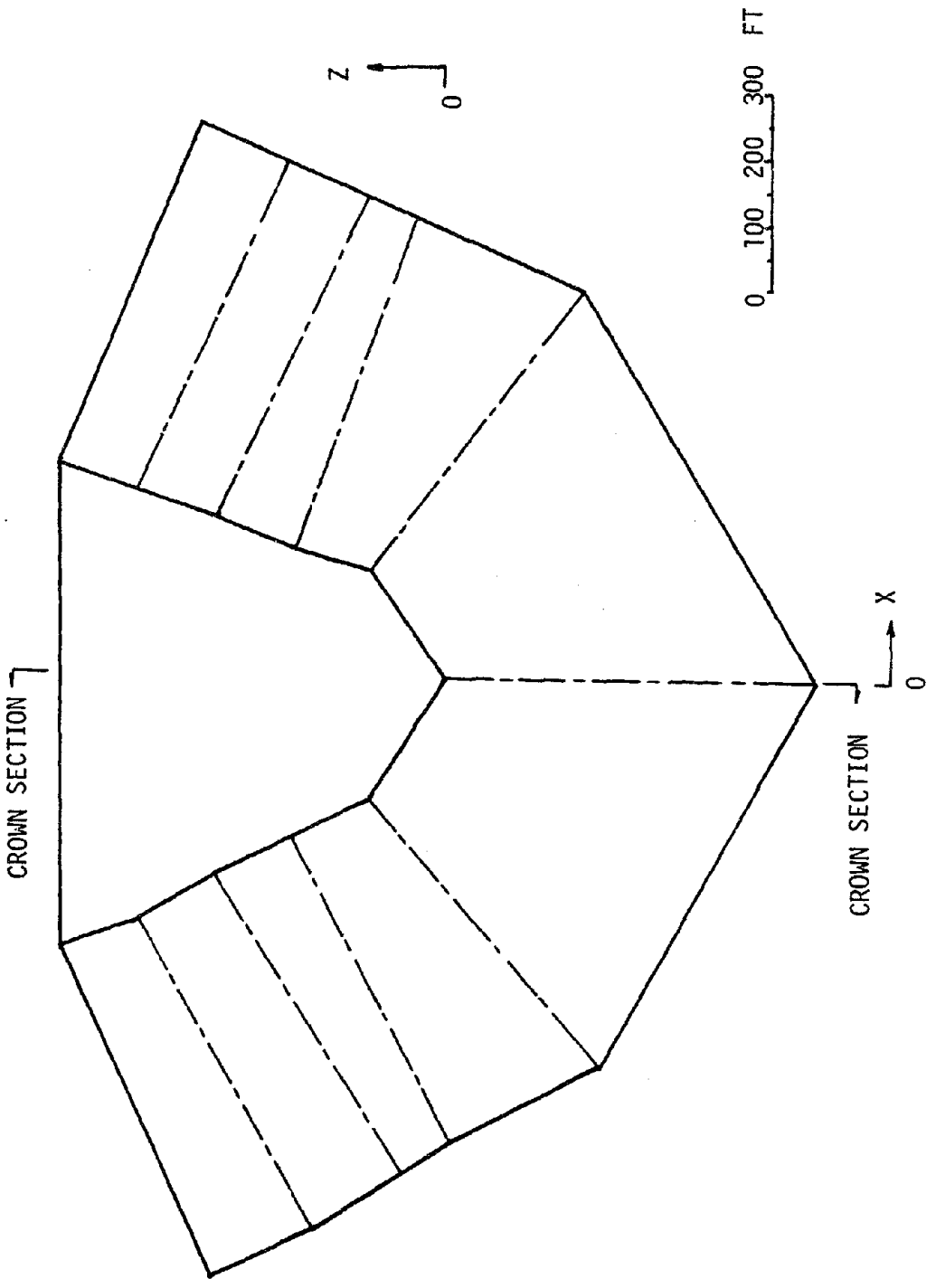

FIG. 31 SECTION OF FOUNDATION BLOCK AT X-Z PLANE
(SHOWING TRACES OF ELEMENT SECTION LINES)

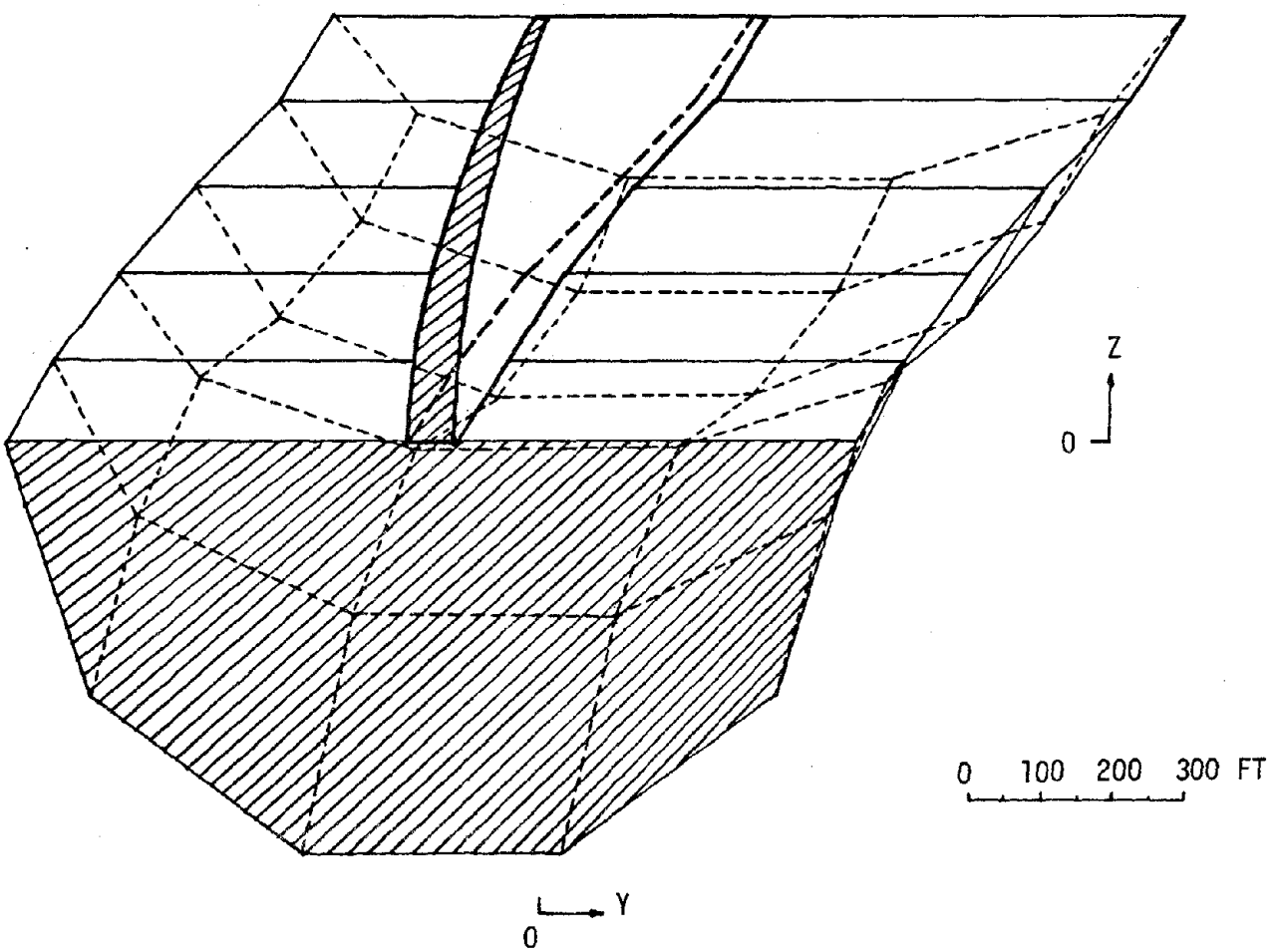

FIG. 32 SECTION OF FOUNDATION BLOCK AND DAM AT Y-Z PLANE
(SHOWING ELEMENT MESH AT THE BOUNDARY)

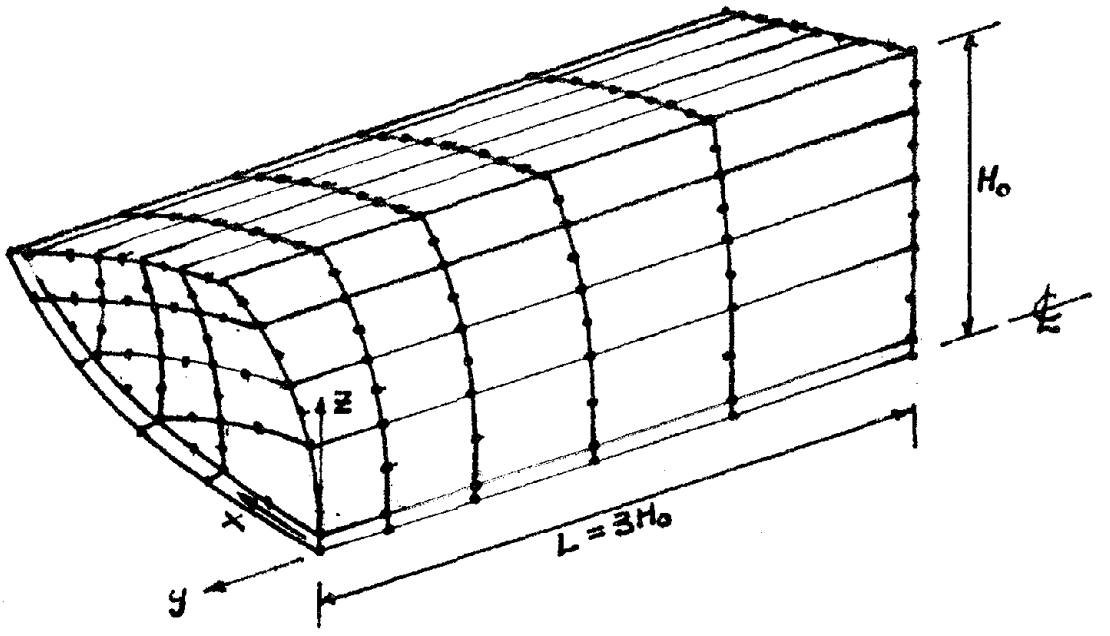

FIG. 33 PRISMATIC FINITE ELEMENT RESERVOIR MODEL

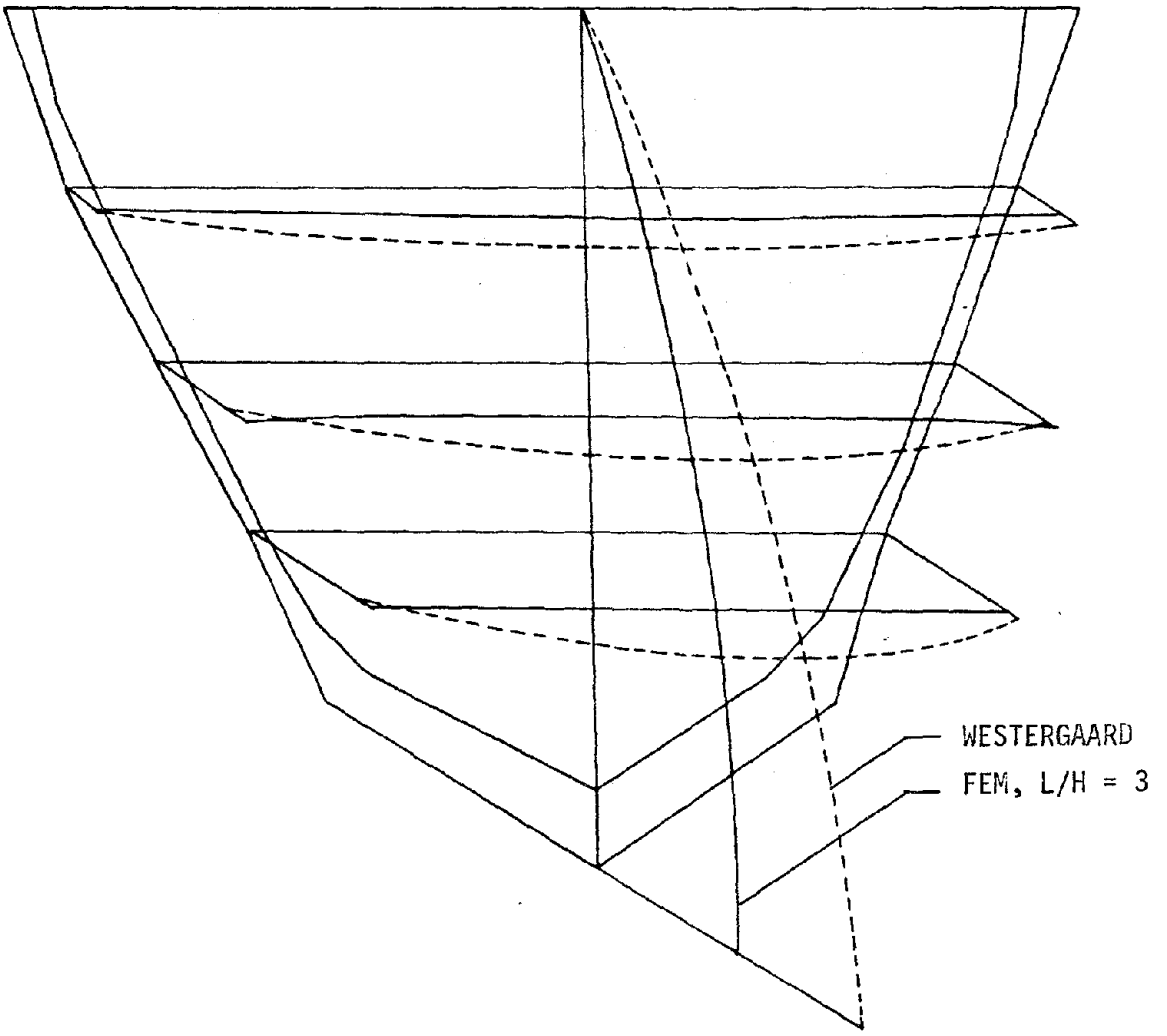

FIG. 34 PRESSURE DISTRIBUTION ON RIGID TECHI DAM FACE
(DUE TO 1 g ACCELERATION UPSTREAM)

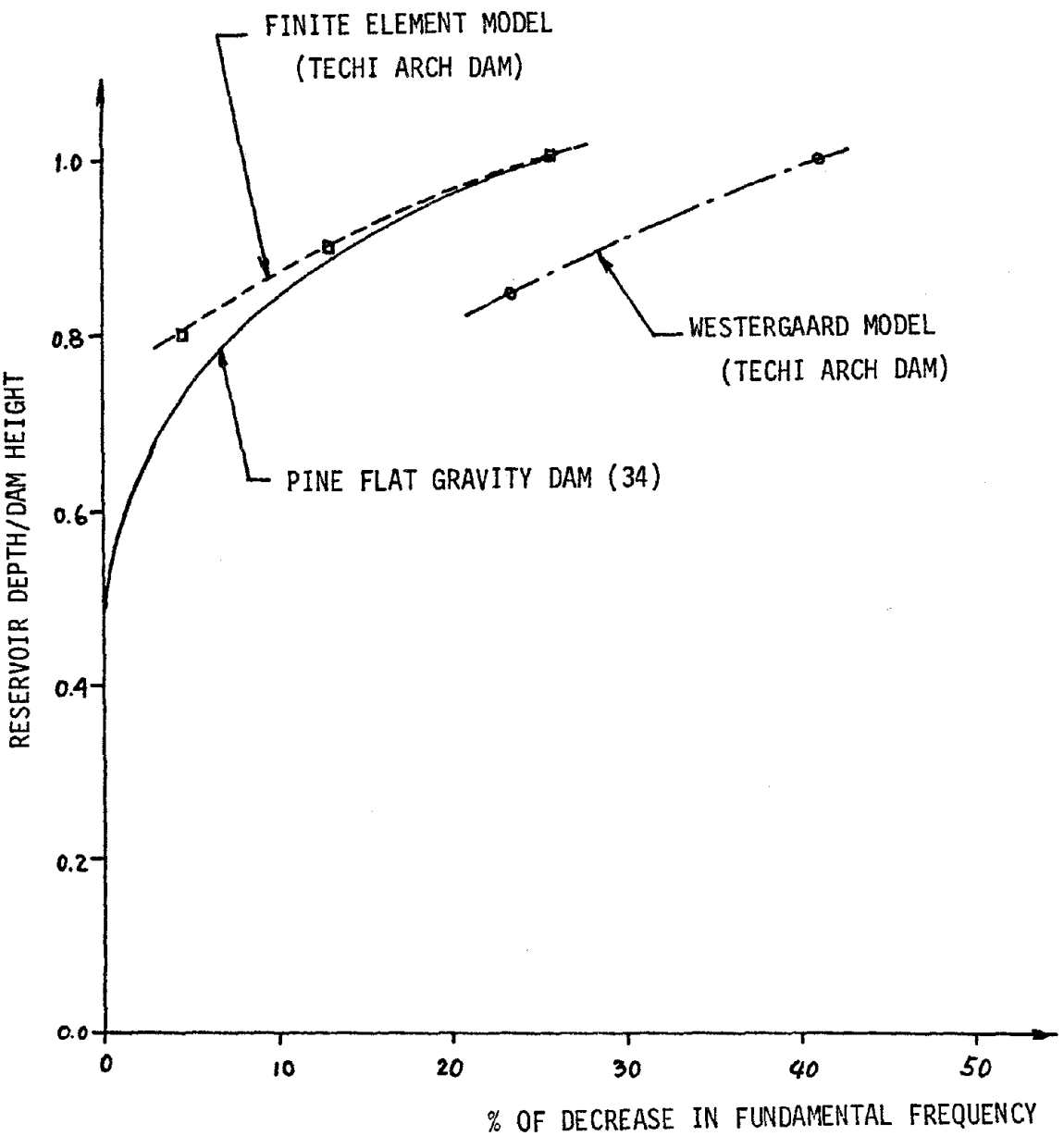

FIG. 35 DECREASE OF FIXED MODE FREQUENCY WITH RESERVOIR DEPTH

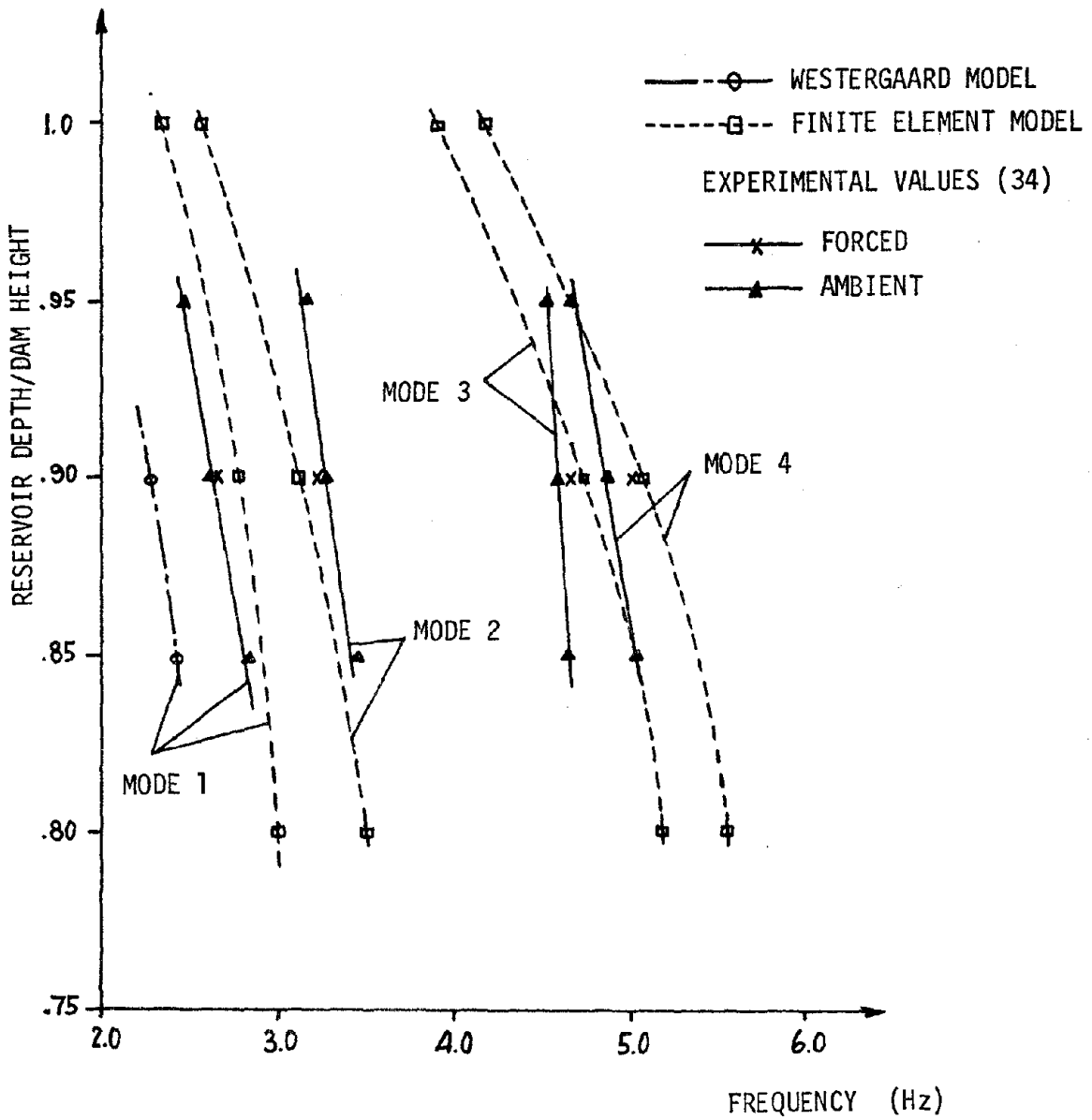

FIG. 36 VARIATION OF MODAL FREQUENCY WITH RESERVOIR DEPTH

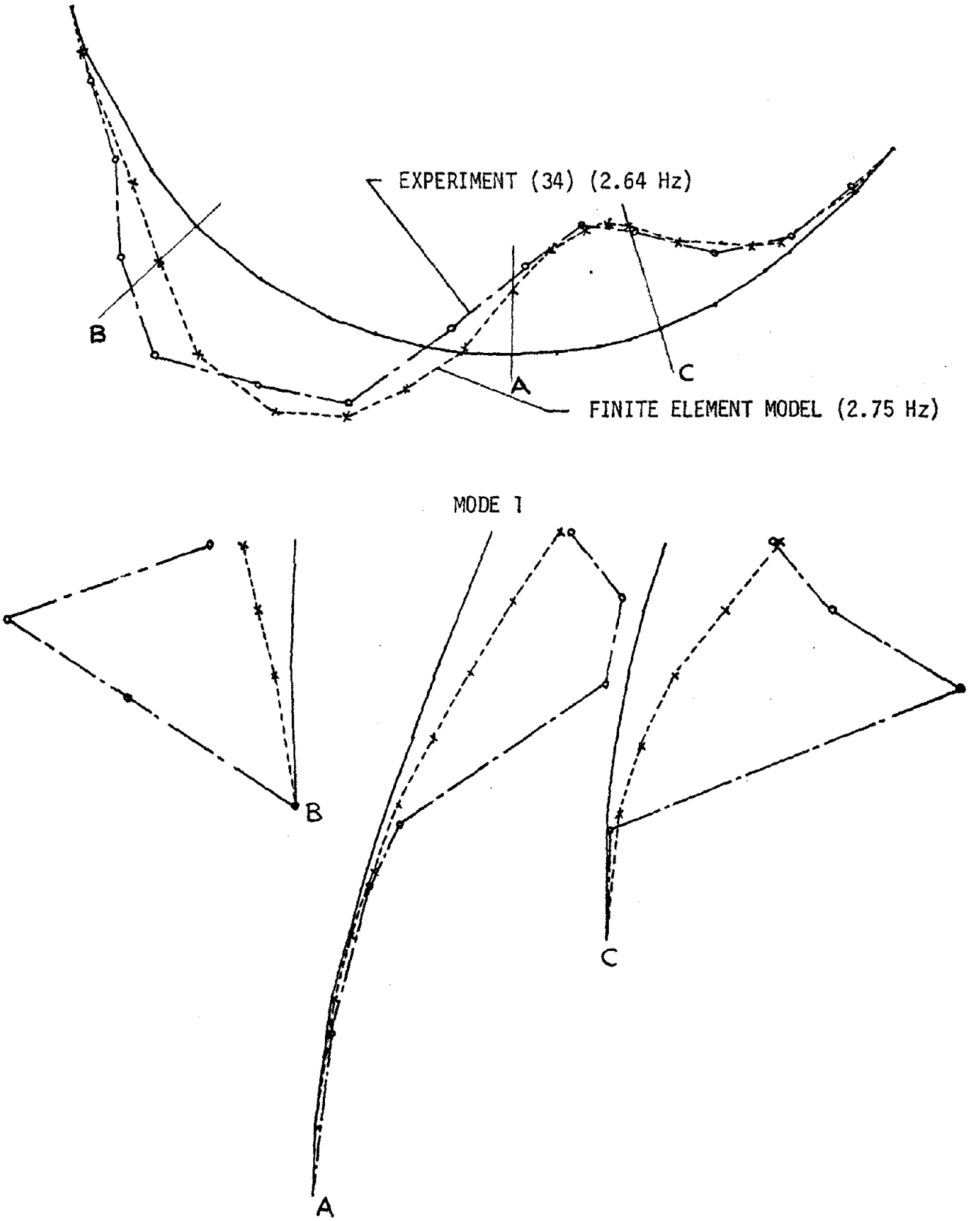

FIG. 37a FIRST VIBRATION MODE SHAPE CORRELATION

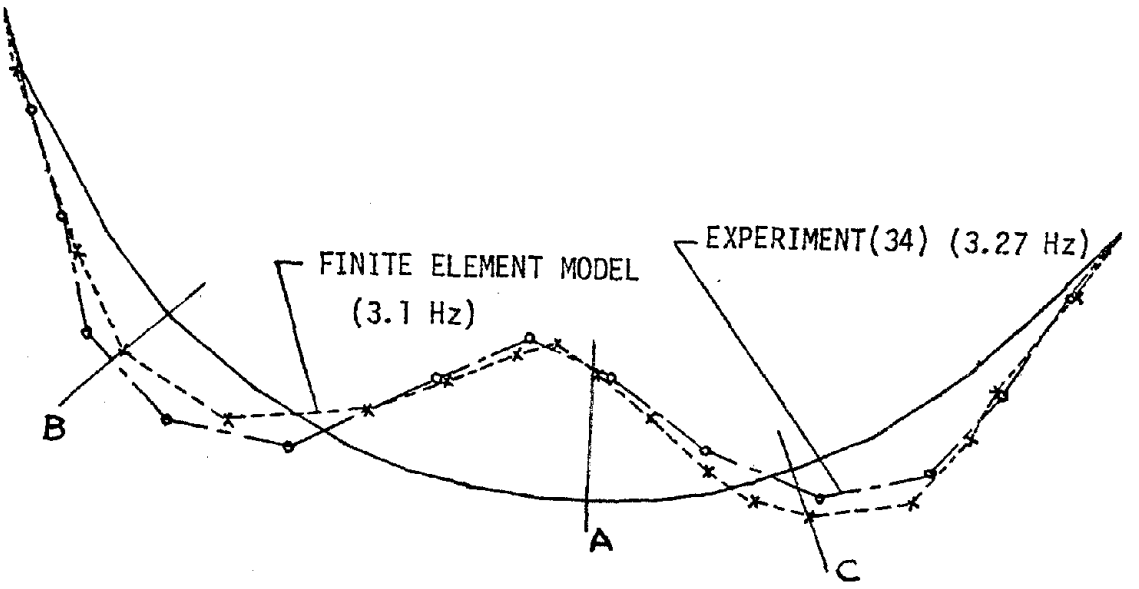

MODE 2

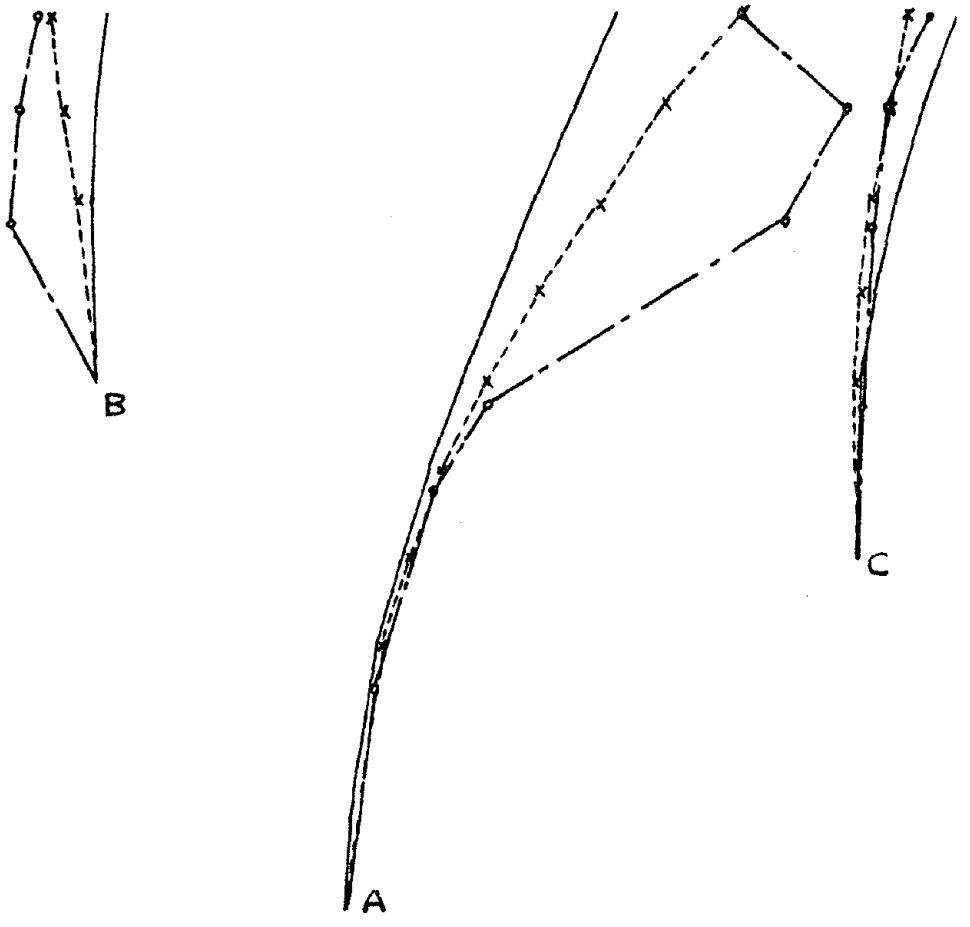

FIG. 37b SECOND VIBRATION MODE SHAPE CORRELATION

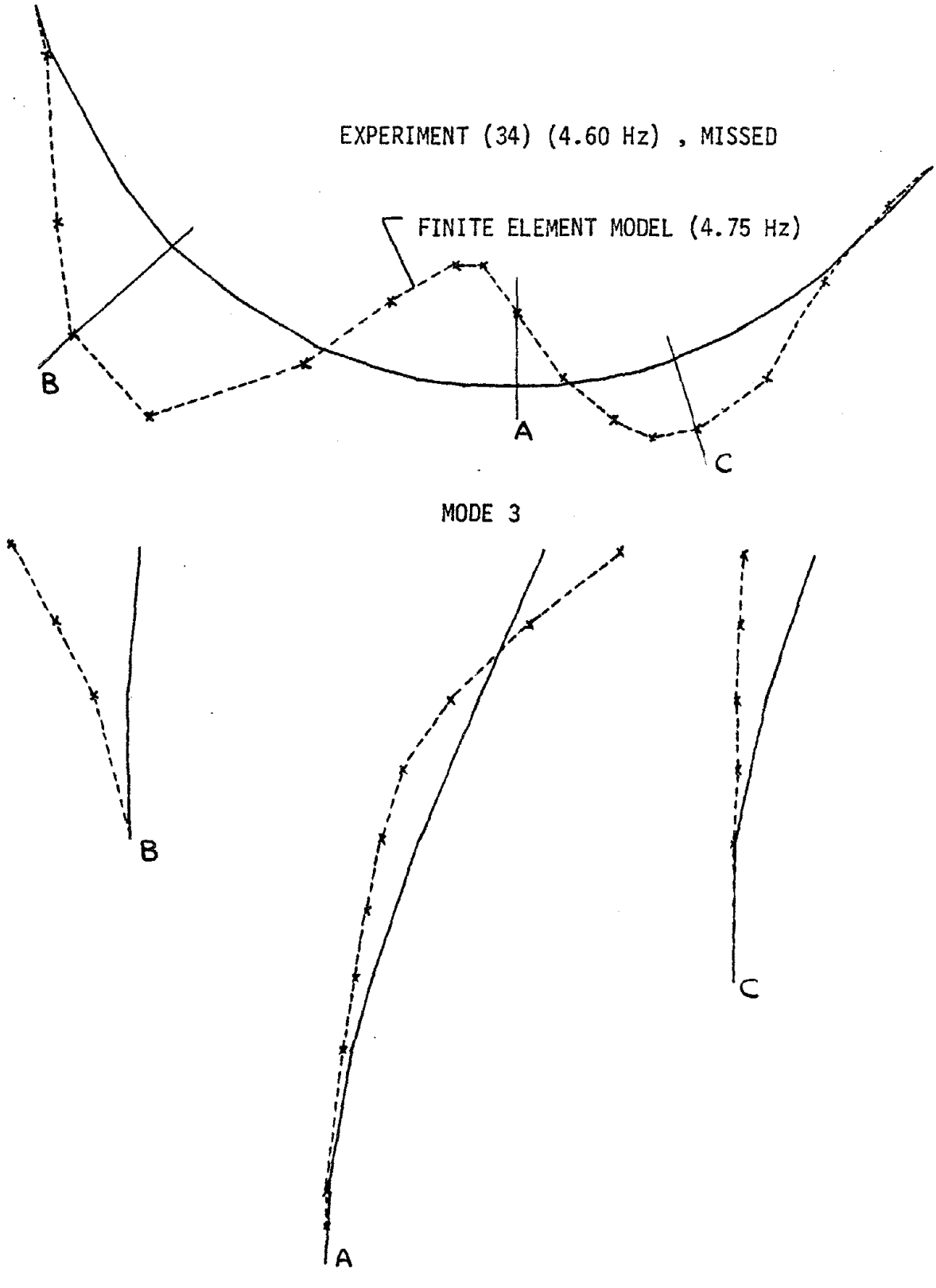

FIG. 37c THIRD VIBRATION MODE SHAPE CORRELATION

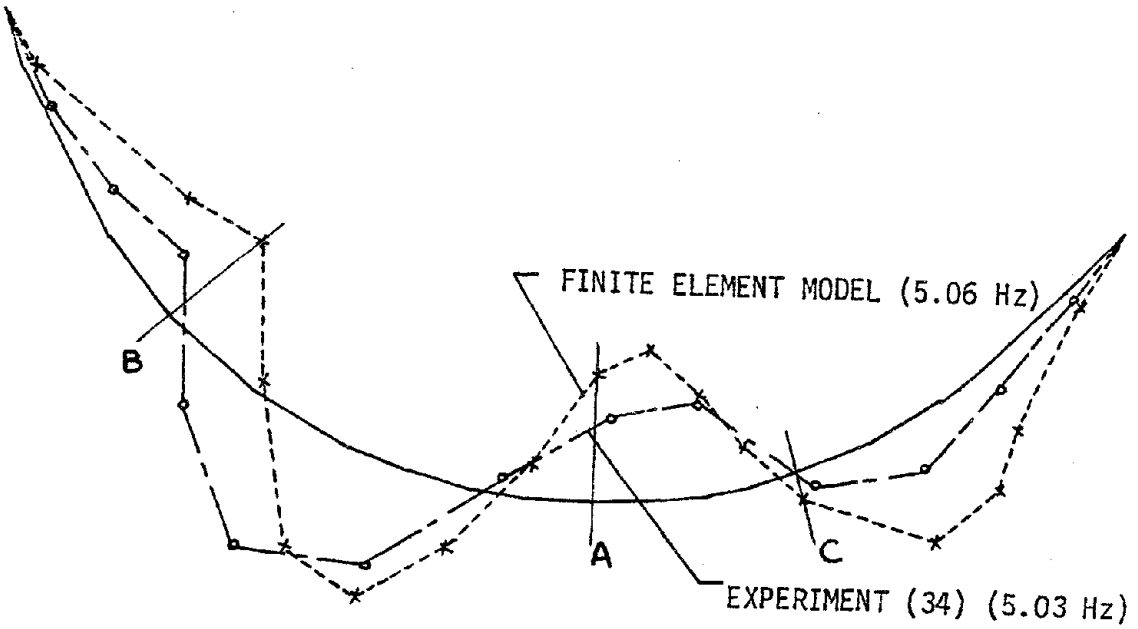

MODE 4

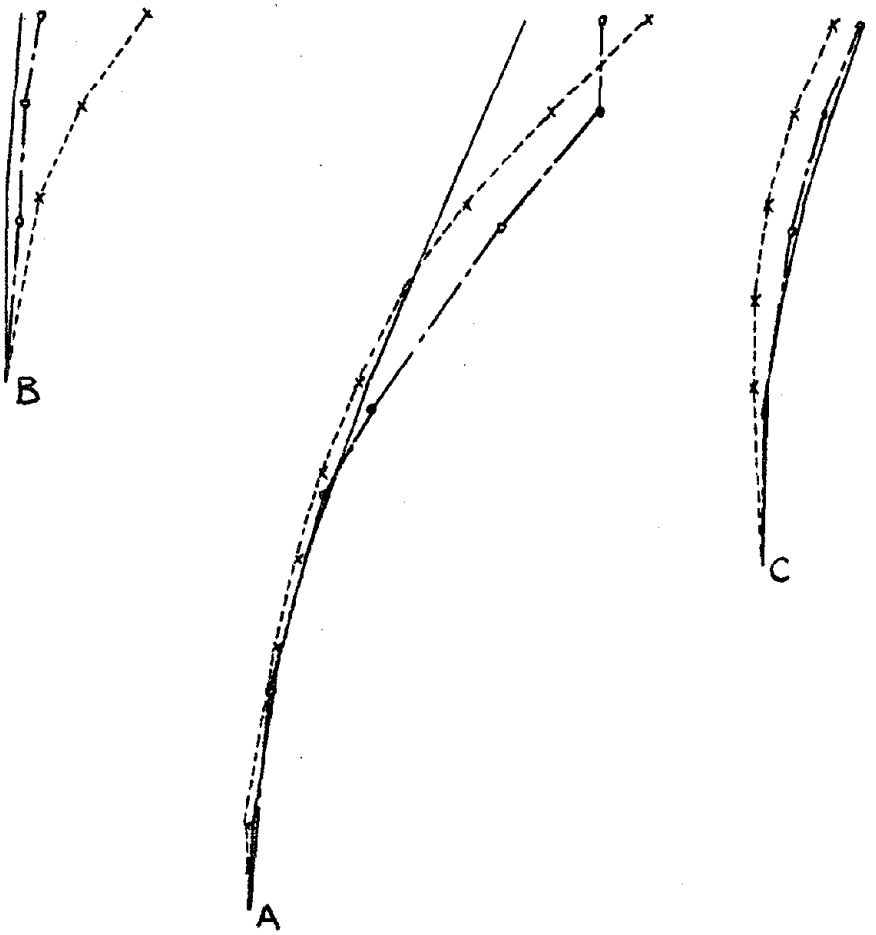

FIG. 37d FOURTH VIBRATION MODE SHAPE CORRELATION

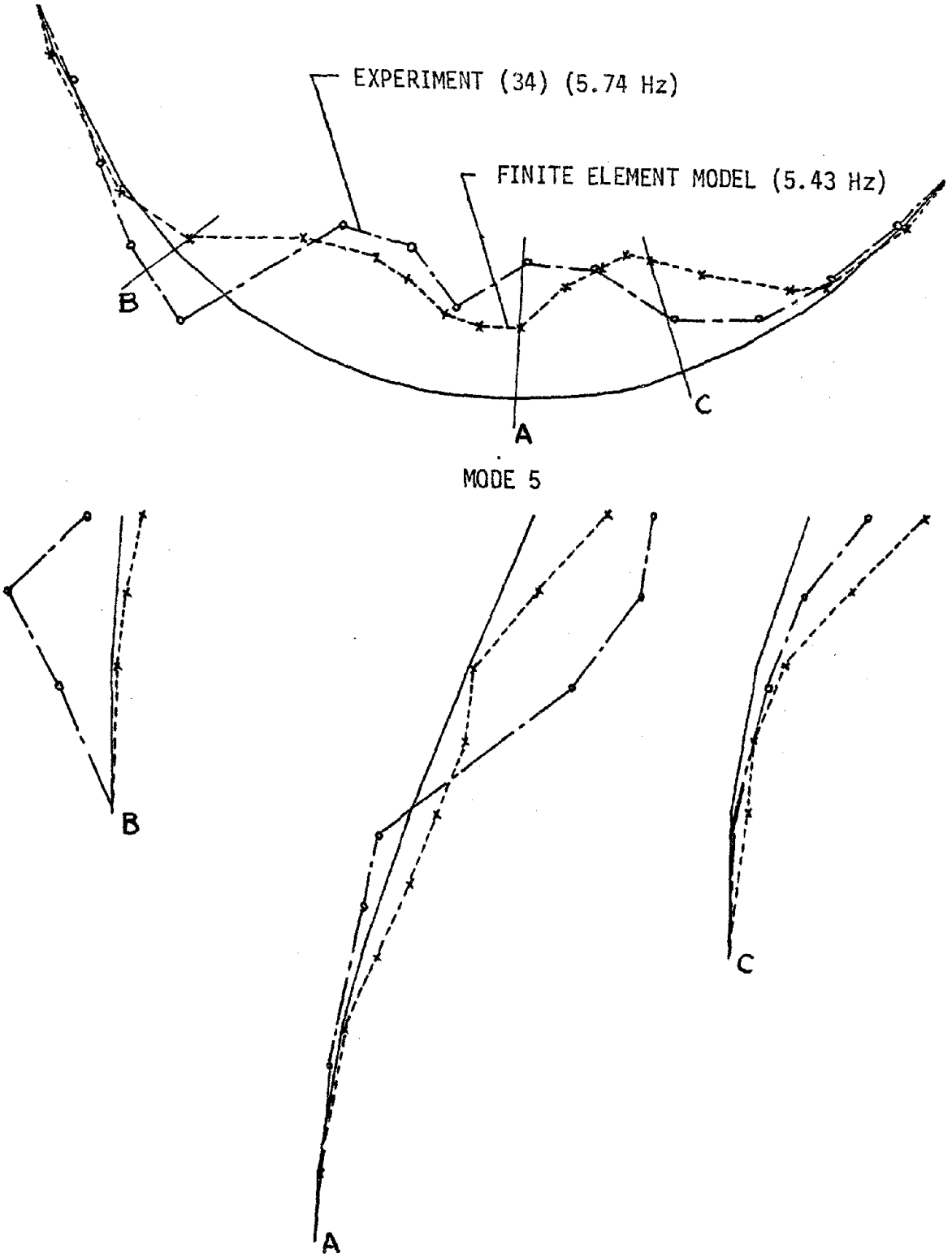

FIG. 37e FIFTH VIBRATION MODE SHAPE CORRELATION

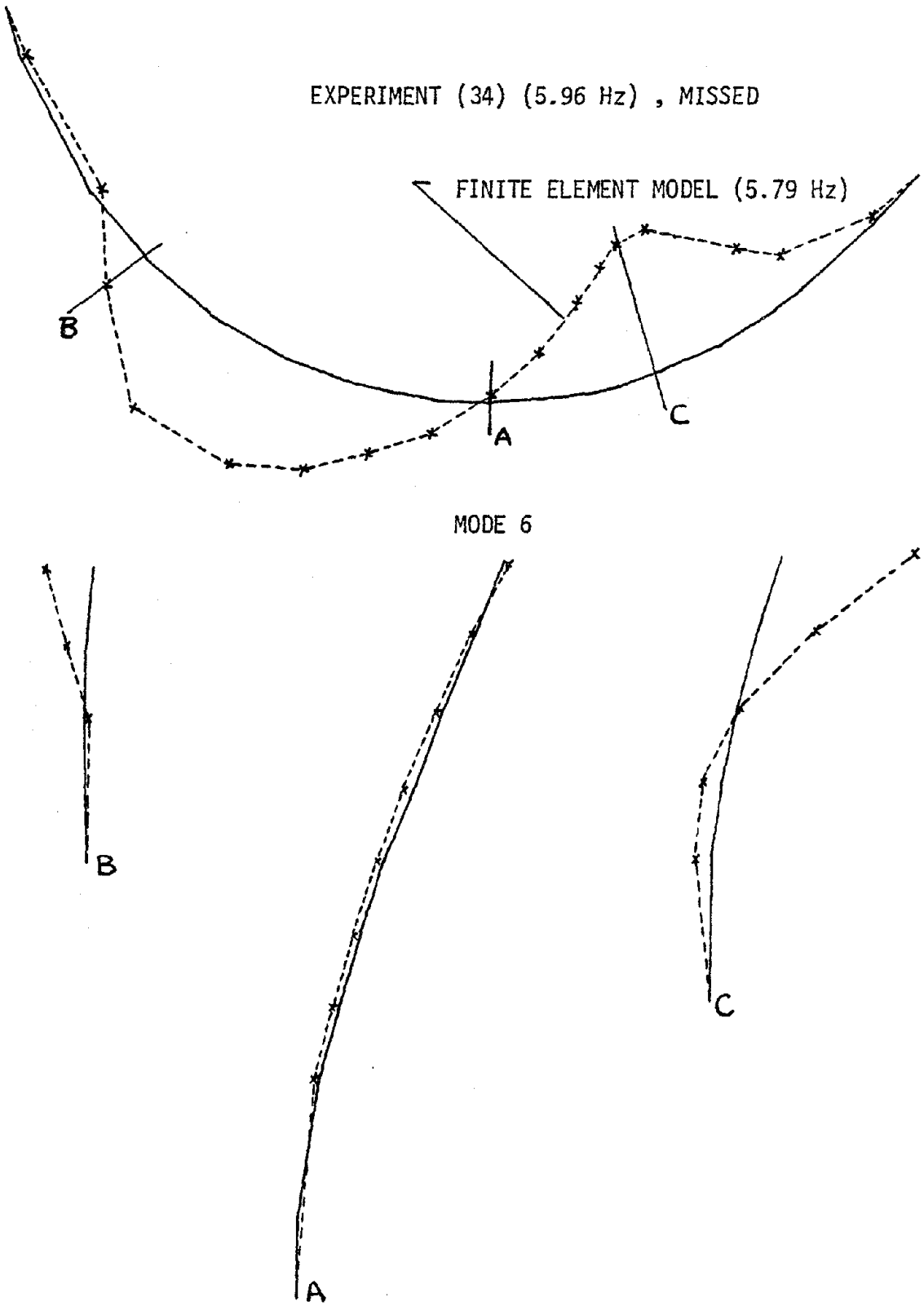

FIG. 37f SIXTH VIBRATION MODE SHAPE CORRELATION

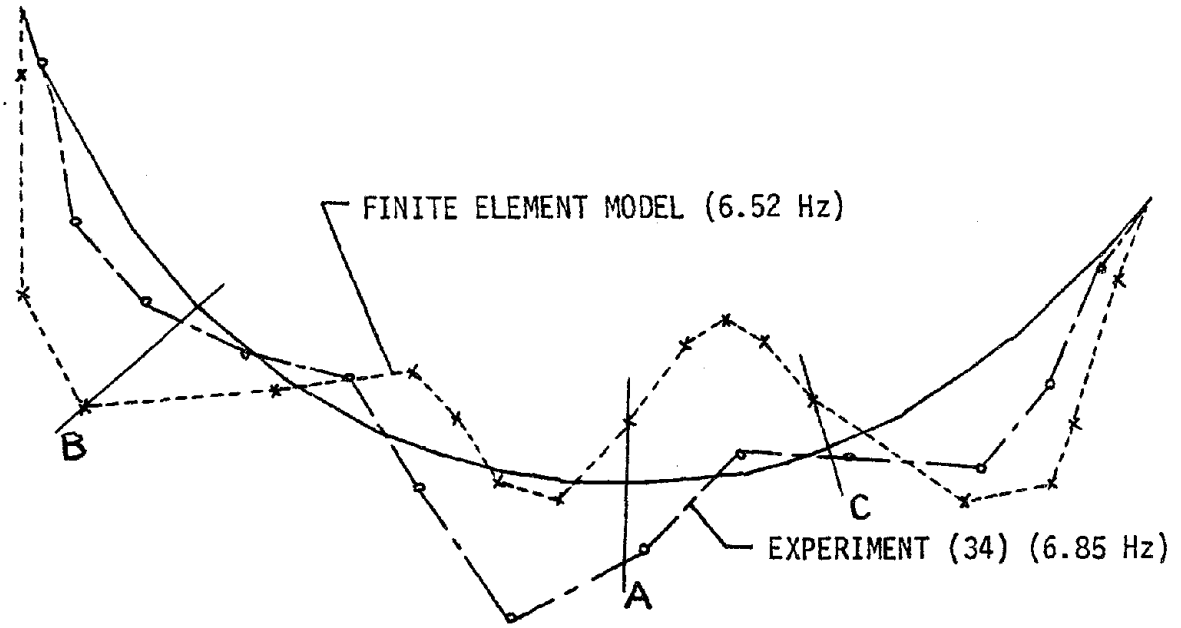

MODE 7

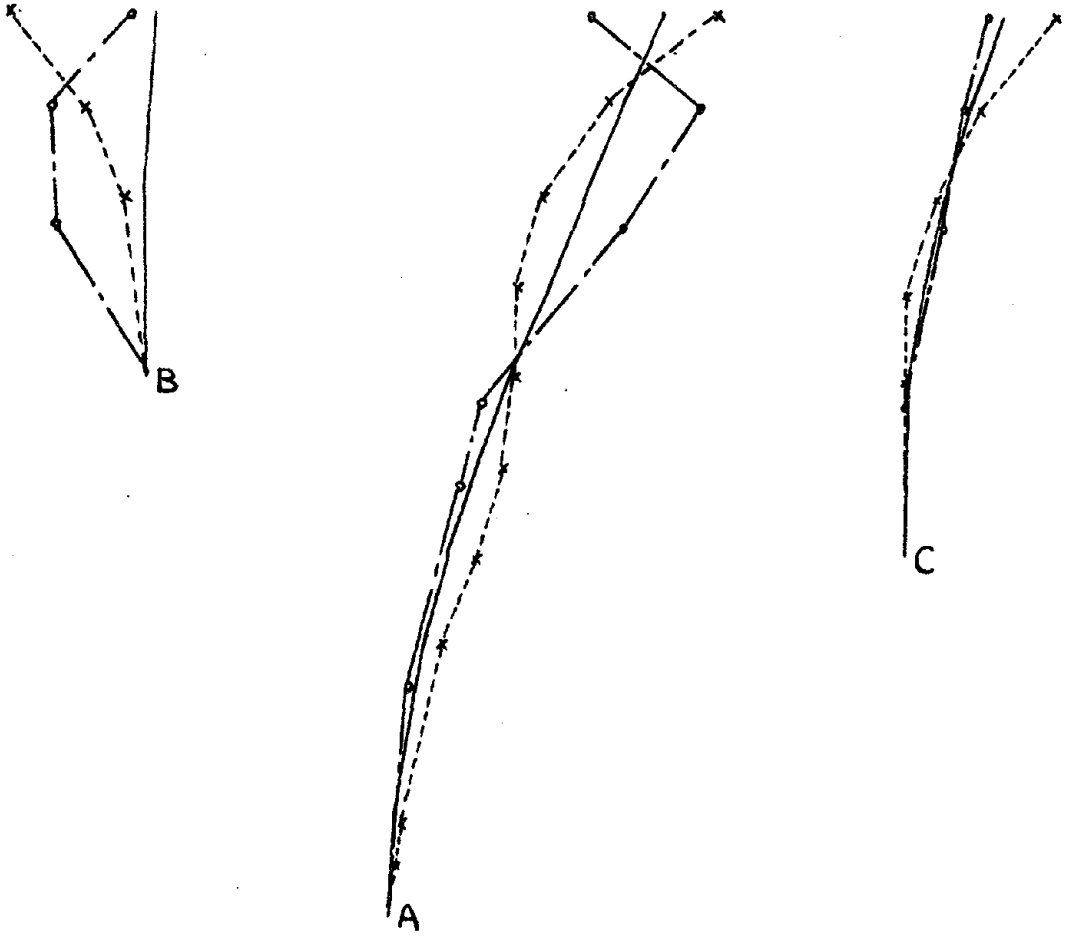

FIG. 37g SEVENTH VIBRATION MODE SHAPE CORRELATION

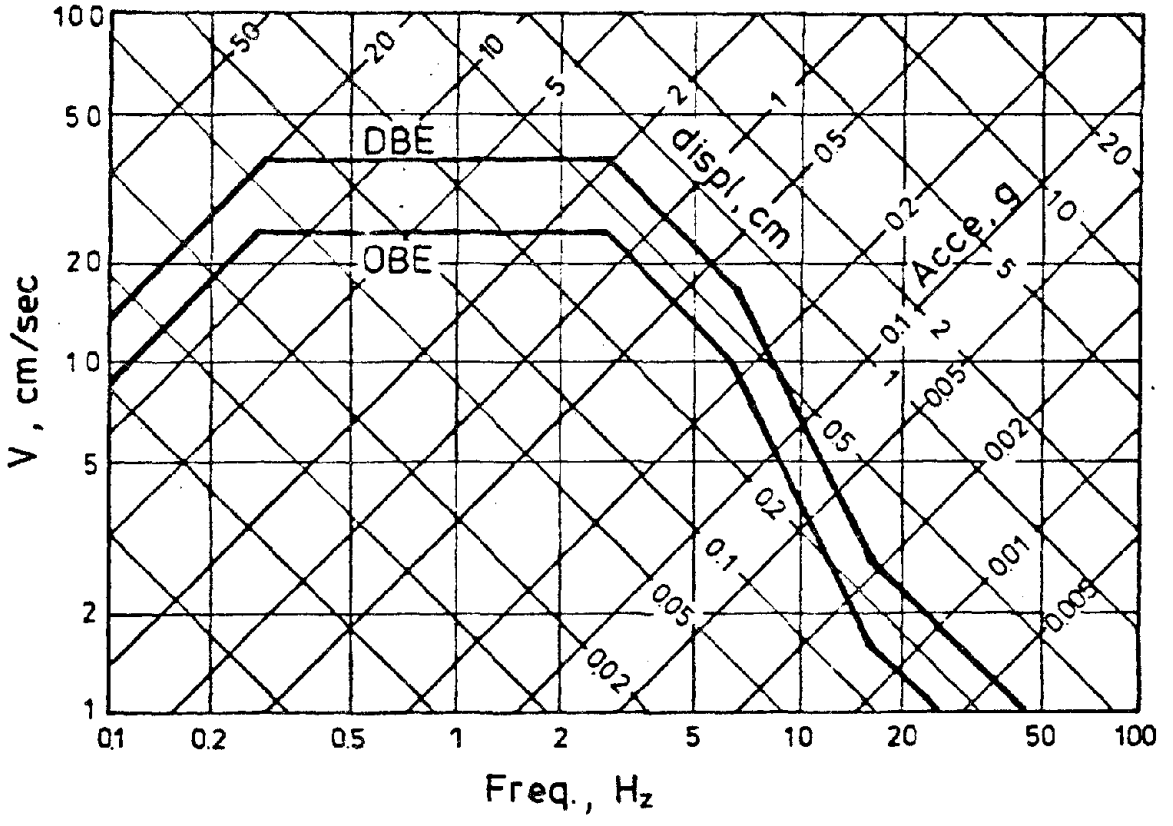

FIG. 38 RESPONSE SPECTRA FOR OPERATIONAL BASIS EARTHQUAKE AND DESIGN BASIS EARTHQUAKE -- 5% DAMPING (REFERENCE 2)

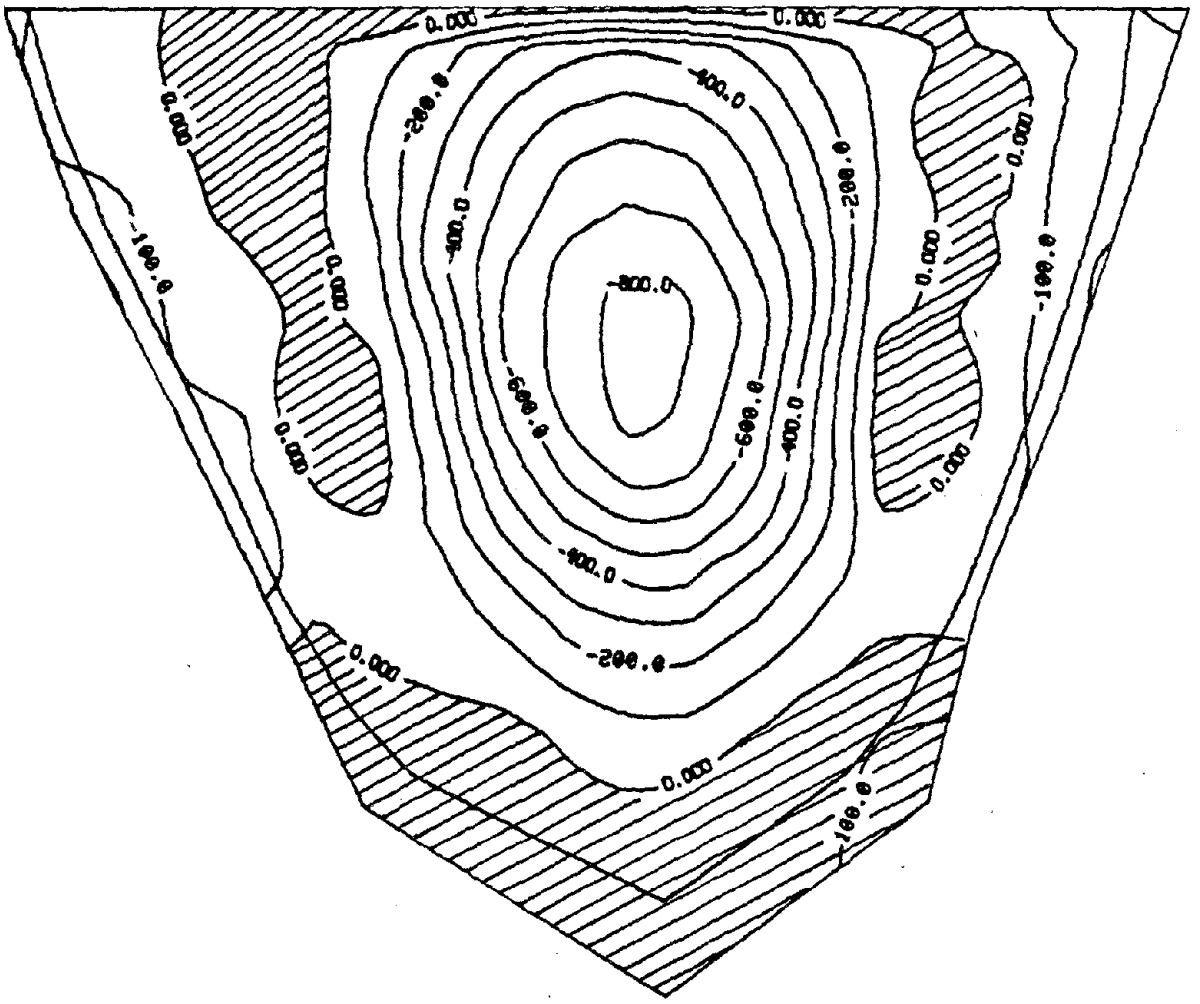

UPSTREAM FACE

SIG-XX

UNIT : PSI

CONTOUR INTERVAL= 100.0

HYDROSTATIC + GRAVITY LOADS ONLY

(a)

FIG. 39 STATIC STRESS DISTRIBUTION, TECHI DAM

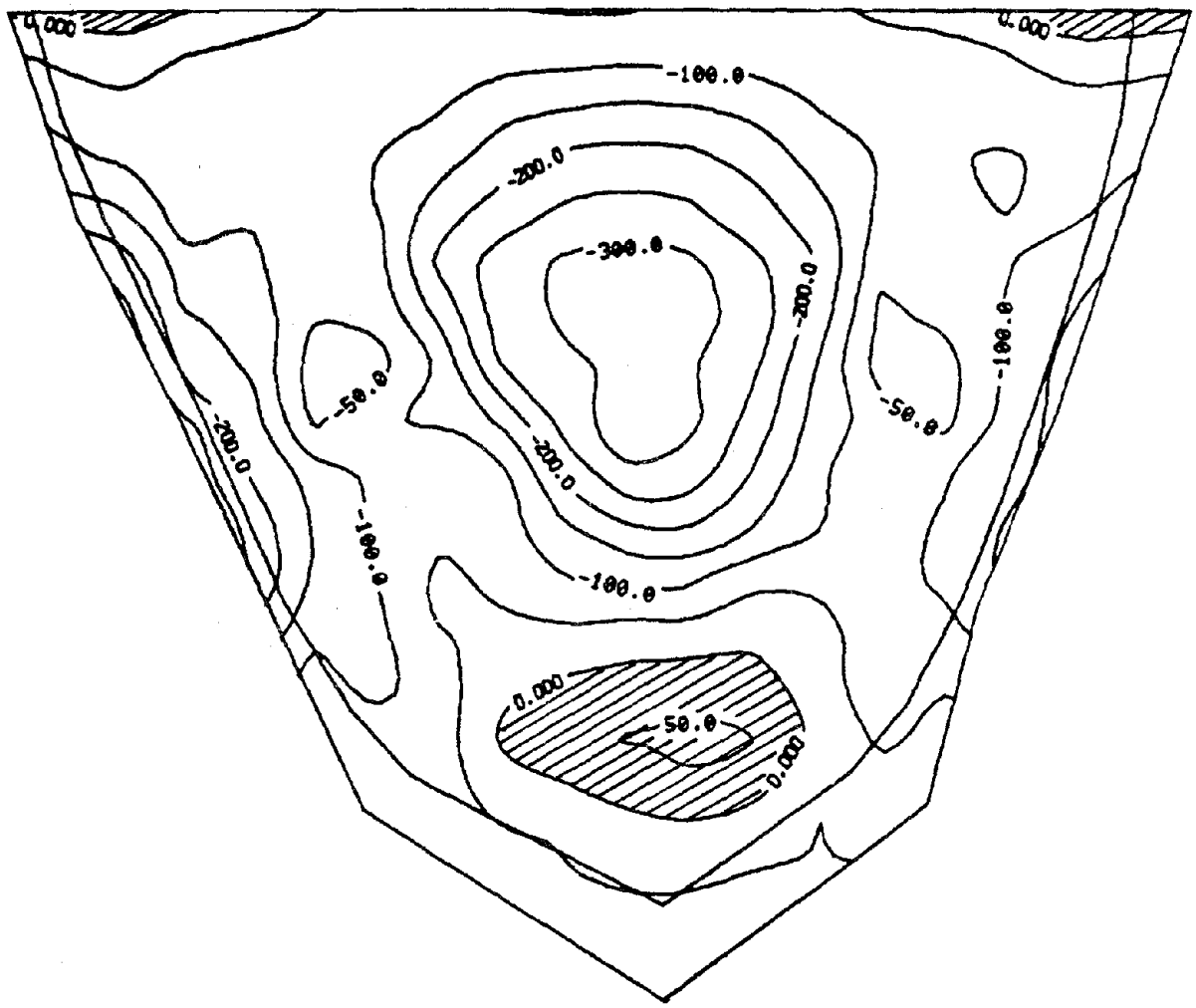

UPSTREAM FACE

SIG-YY

UNIT : PSI

CONTOUR INTERVAL= 50.0

HYDROSTATIC + GRAVITY LOADS ONLY

(b)

FIG. 39 (Cont.)

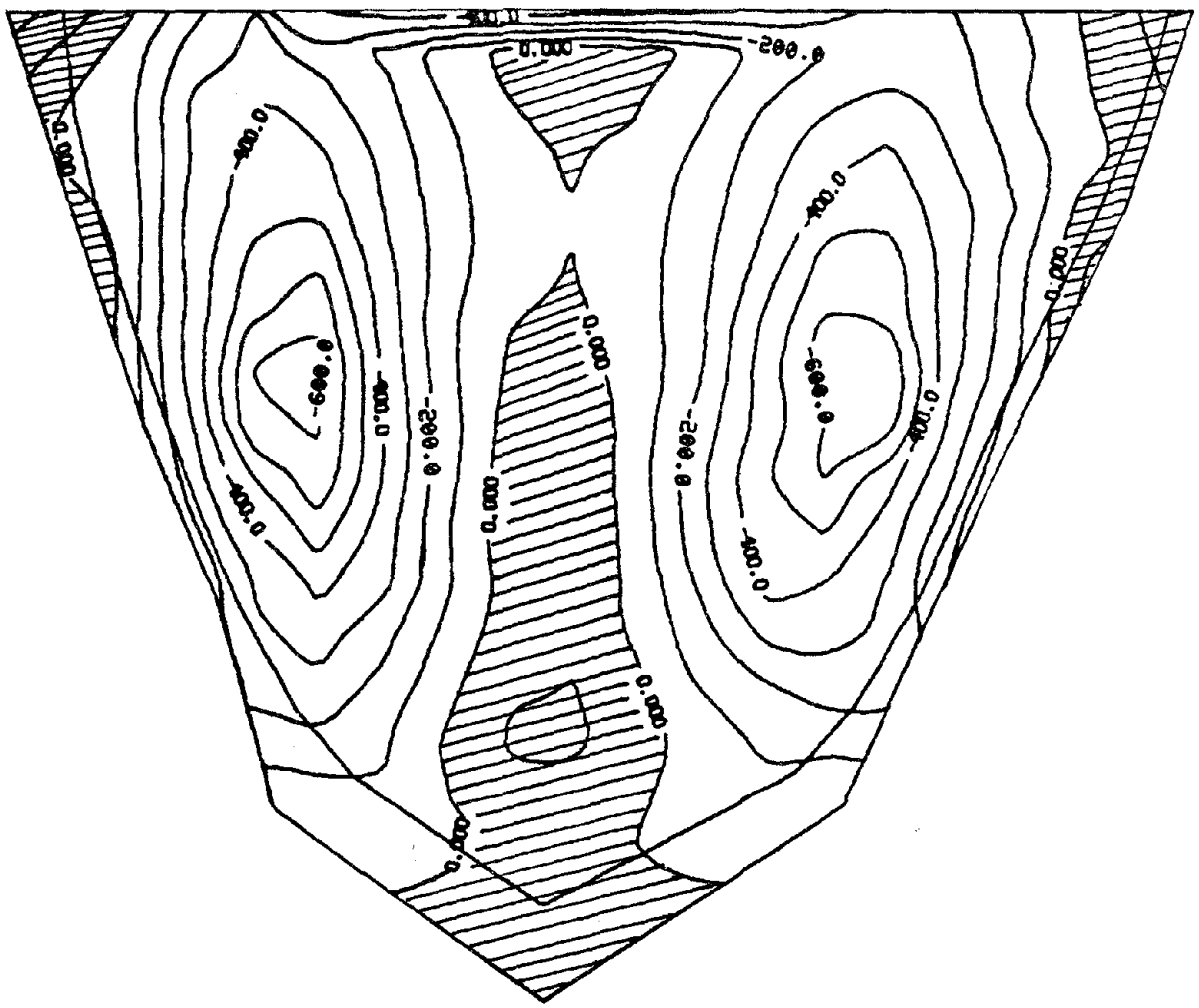

DOWNSTREAM FACE

SIG-XX

UNIT : PSI

CONTOUR INTERVAL= 100.0

HYDROSTATIC + GRAVITY LOADS ONLY

(c)

FIG. 39 (Cont.)

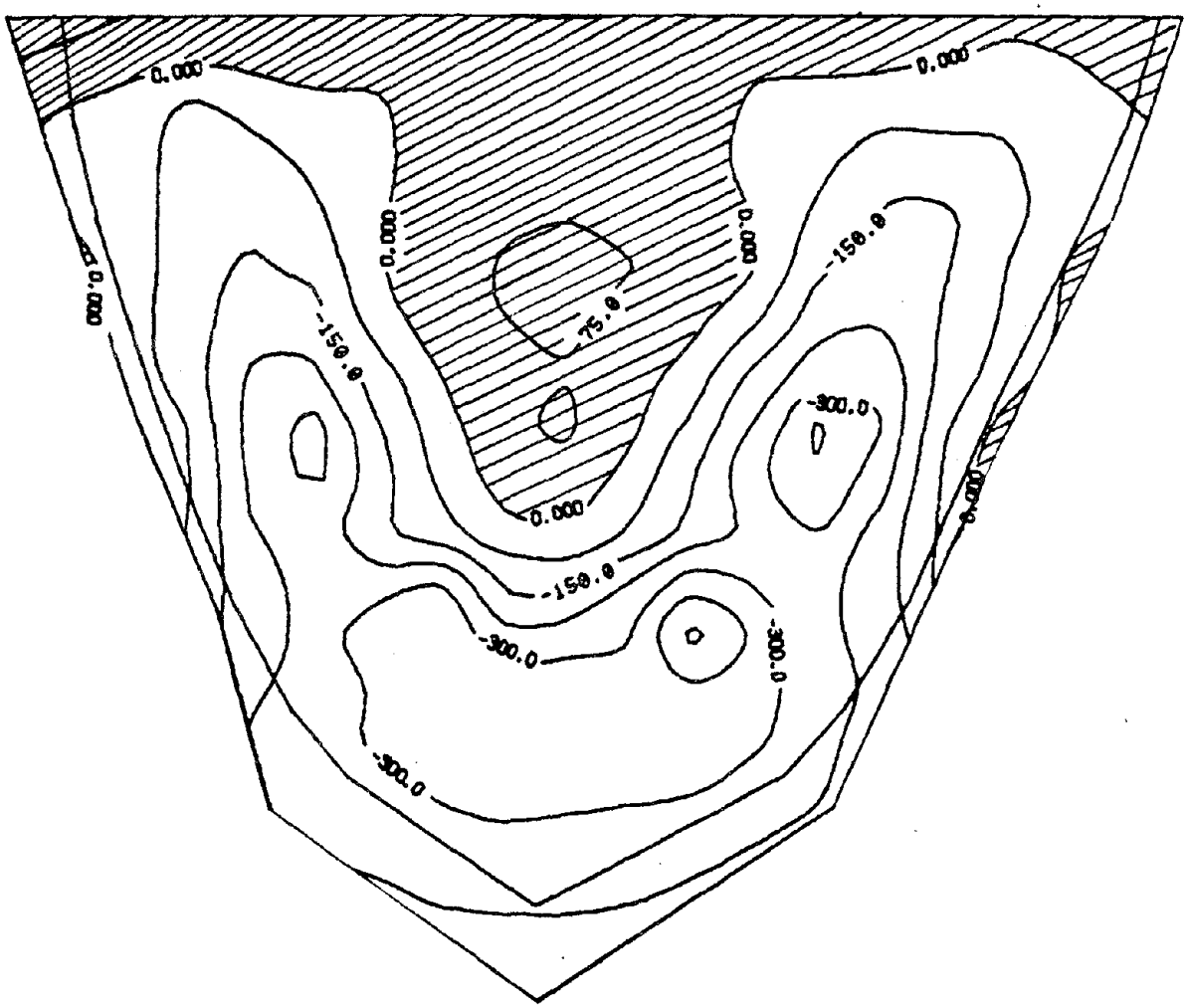

DOWNSTREAM FACE

SIG-YY

UNIT : PSI

CONTOUR INTERVAL= 75.0

HYDROSTATIC + GRAVITY LOADS ONLY

(d)

FIG. 39 (Cont.)

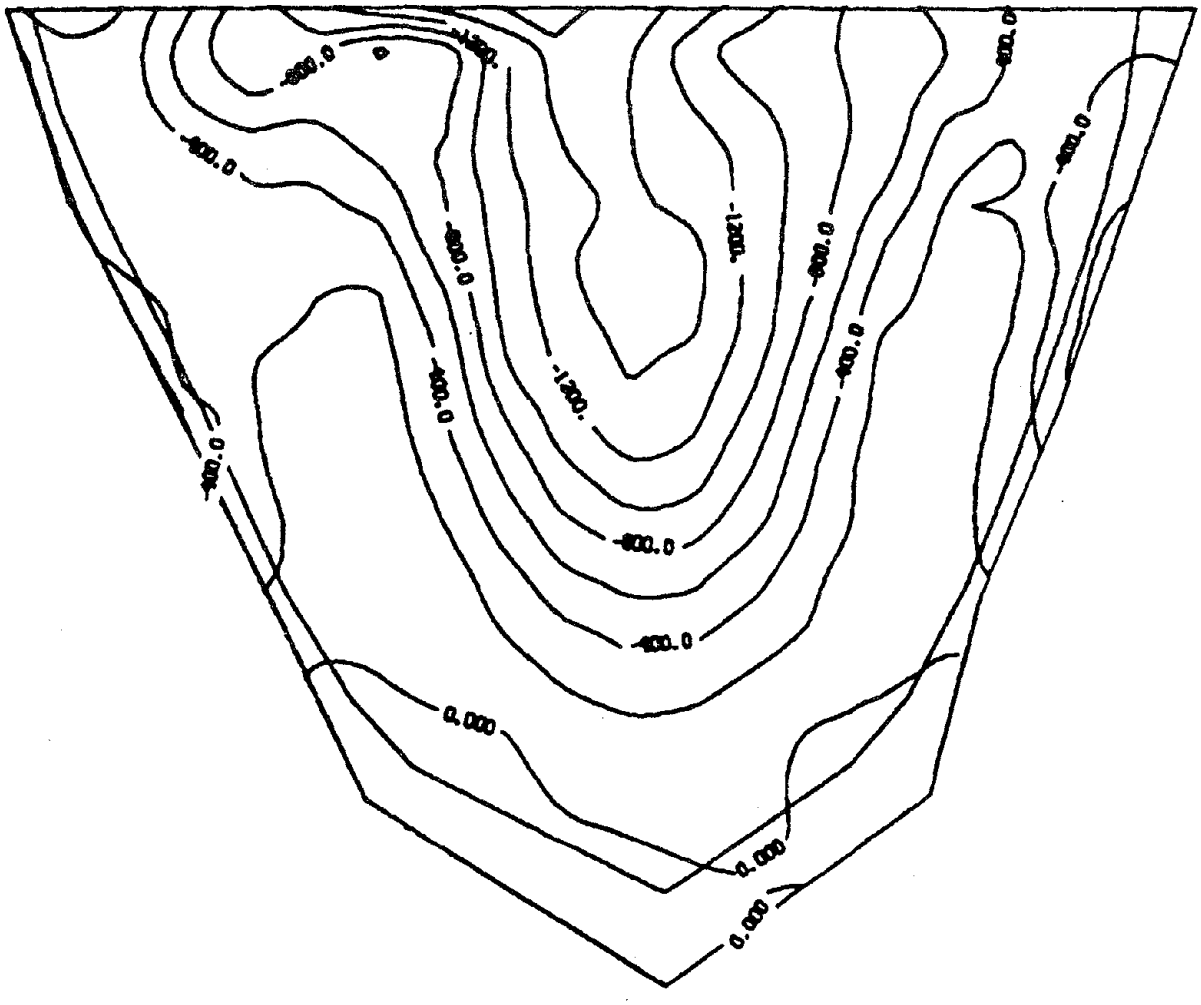

UPSTREAM FACE

MINIMUM SIG-XX

UNIT : PSI

CONTOUR INTERVAL= 200.0

UPSTREAM-DOWNSTREAM EXCITATIONS

AND HYDROSTATIC + GRAVITY LOADS

(a)

FIG. 40 MAXIMUM COMPRESSIVE STRESSES: STATIC PLUS U-D EARTHQUAKE

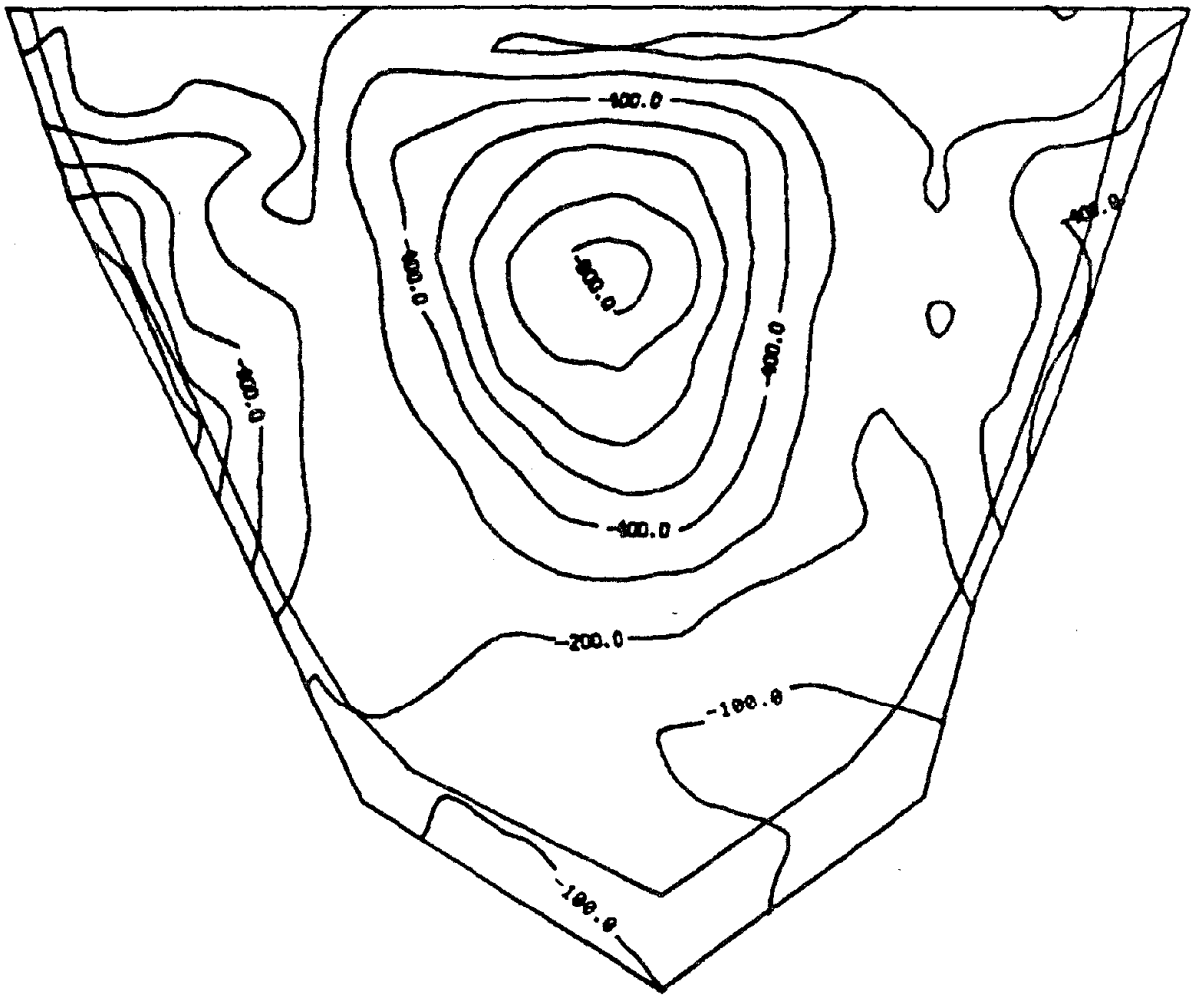

UPSTREAM FACE

MINIMUM SIG-YY

UNIT : PSI

CONTOUR INTERVAL= 100.0

UPSTREAM-DOWNSTREAM EXCITATIONS

AND HYDROSTATIC + GRAVITY LOADS

(b)

FIG. 40 (Cont.)

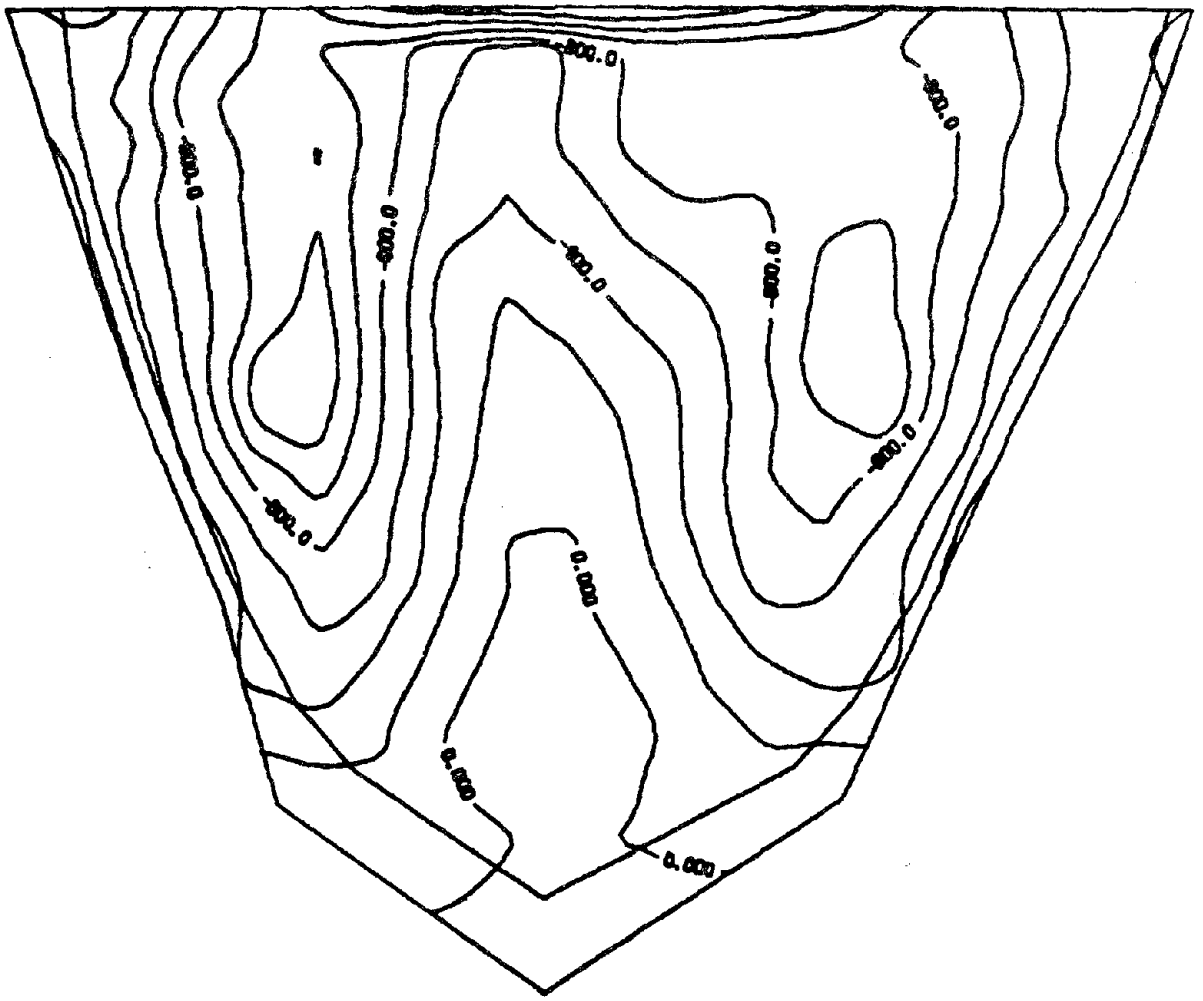

DOWNSTREAM FACE

MINIMUM SIG-XX

UNIT : PSI

CONTOUR INTERVAL= 200.0

UPSTREAM-DOWNSTREAM EXCITATIONS

AND HYDROSTATIC + GRAVITY LOADS

(c)

FIG. 40 (Cont.)

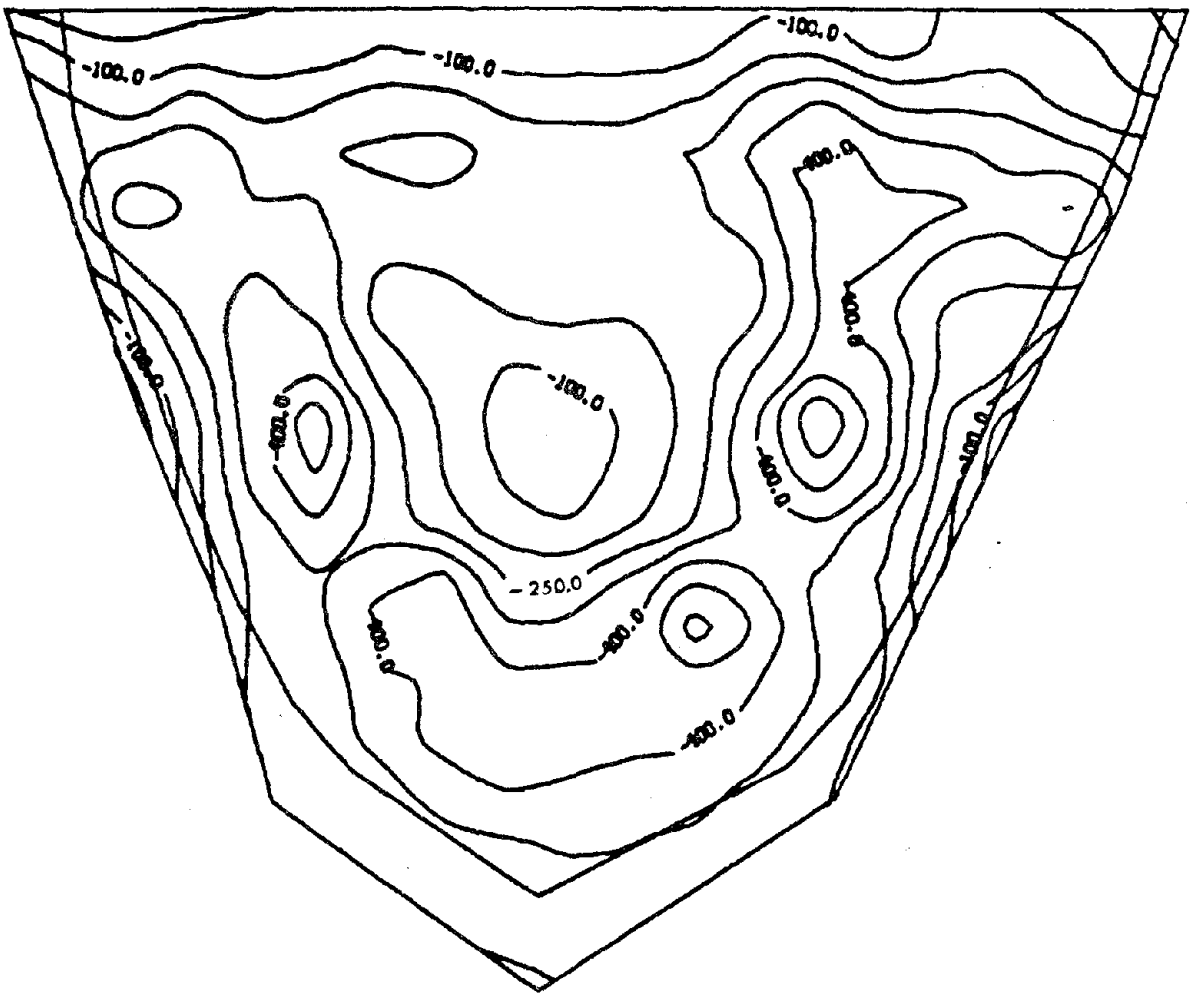

DOWNSTREAM FACE

MINIMUM SIG-YY

UNIT : PSI

CONTOUR INTERVAL= 75.0

UPSTREAM-DOWNSTREAM EXCITATIONS

AND HYDROSTATIC + GRAVITY LOADS

(d)

FIG. 40 (Cont.)

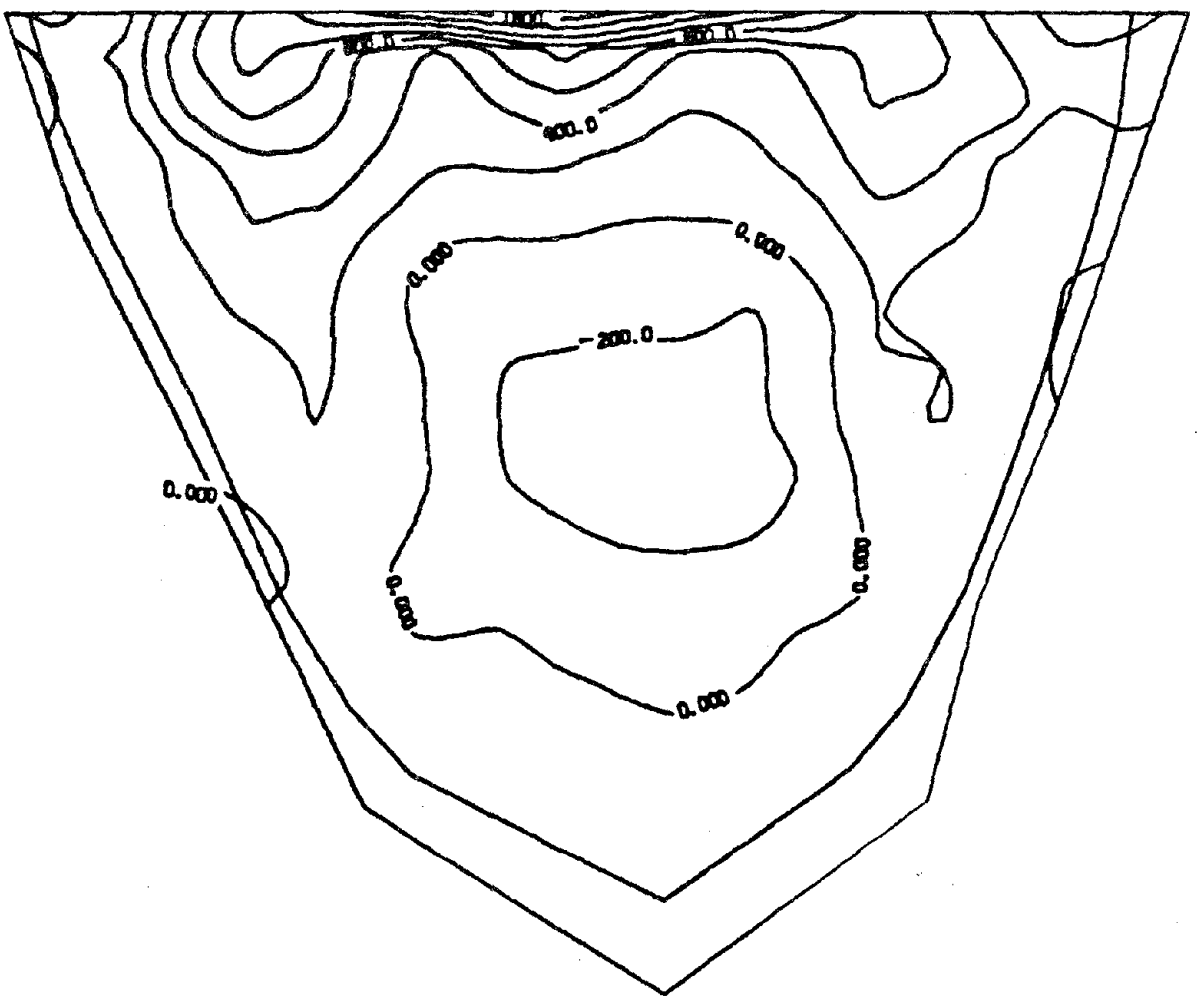

UPSTREAM FACE

MAXIMUM SIG-XX

UNIT : PSI

CONTOUR INTERVAL= 200.0

UPSTREAM-DOWNSTREAM EXCITATIONS

AND HYDROSTATIC + GRAVITY LOADS

(a)

FIG. 41 MAXIMUM TENSILE STRESSES: STATIC PLUS U-D EARTHQUAKE

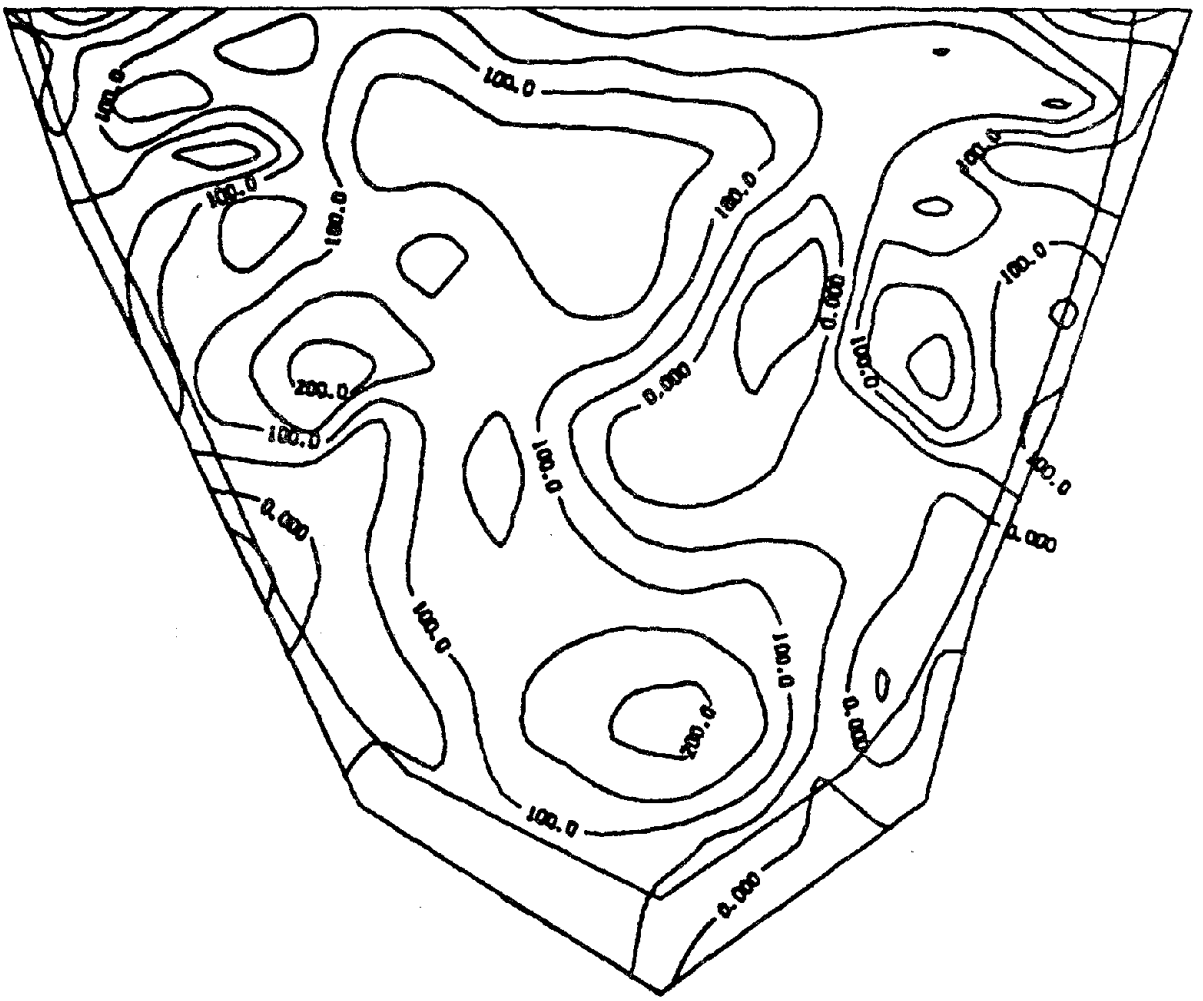

UPSTREAM FACE

MAXIMUM SIG-YY

UNIT : PSI

CONTOUR INTERVAL= 50.0

UPSTREAM-DOWNSTREAM EXCITATIONS

AND HYDROSTATIC + GRAVITY LOADS

(b)

FIG. 41 (Cont.)

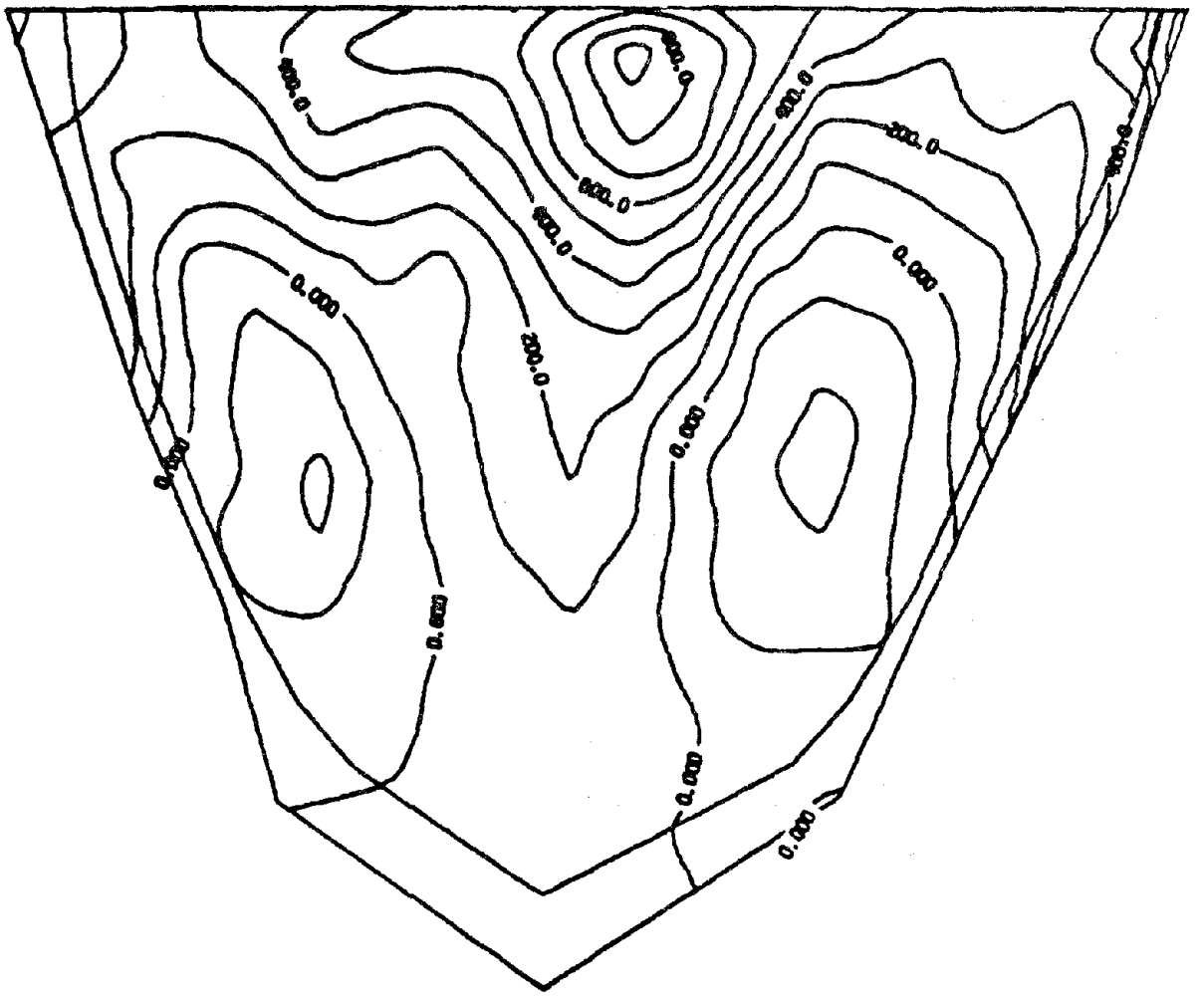
DOWNSTREAM FACE
MAXIMUM SIG-XX
UNIT : PSI
CONTOUR INTERVAL= 100.0
UPSTREAM-DOWNSTREAM EXCITATIONS
AND HYDROSTATIC + GRAVITY LOADS

(c)

FIG. 41 (Cont.)

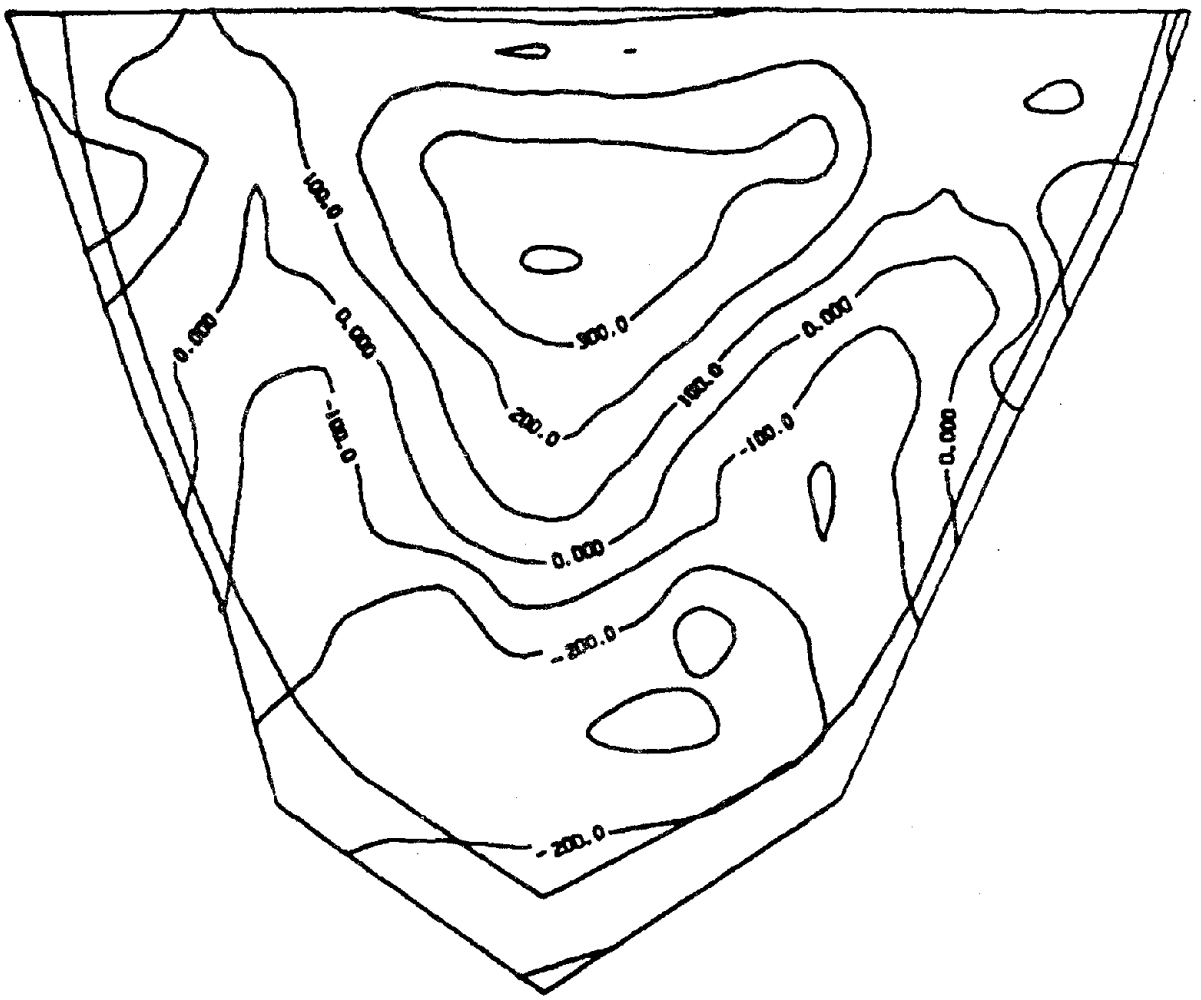

DOWNSTREAM FACE

MAXIMUM SIG-YY

UNIT : PSI

CONTOUR INTERVAL= 100.0

UPSTREAM-DOWNSTREAM EXCITATIONS

AND HYDROSTATIC + GRAVITY LOADS

(d)

FIG. 41 (Cont.)

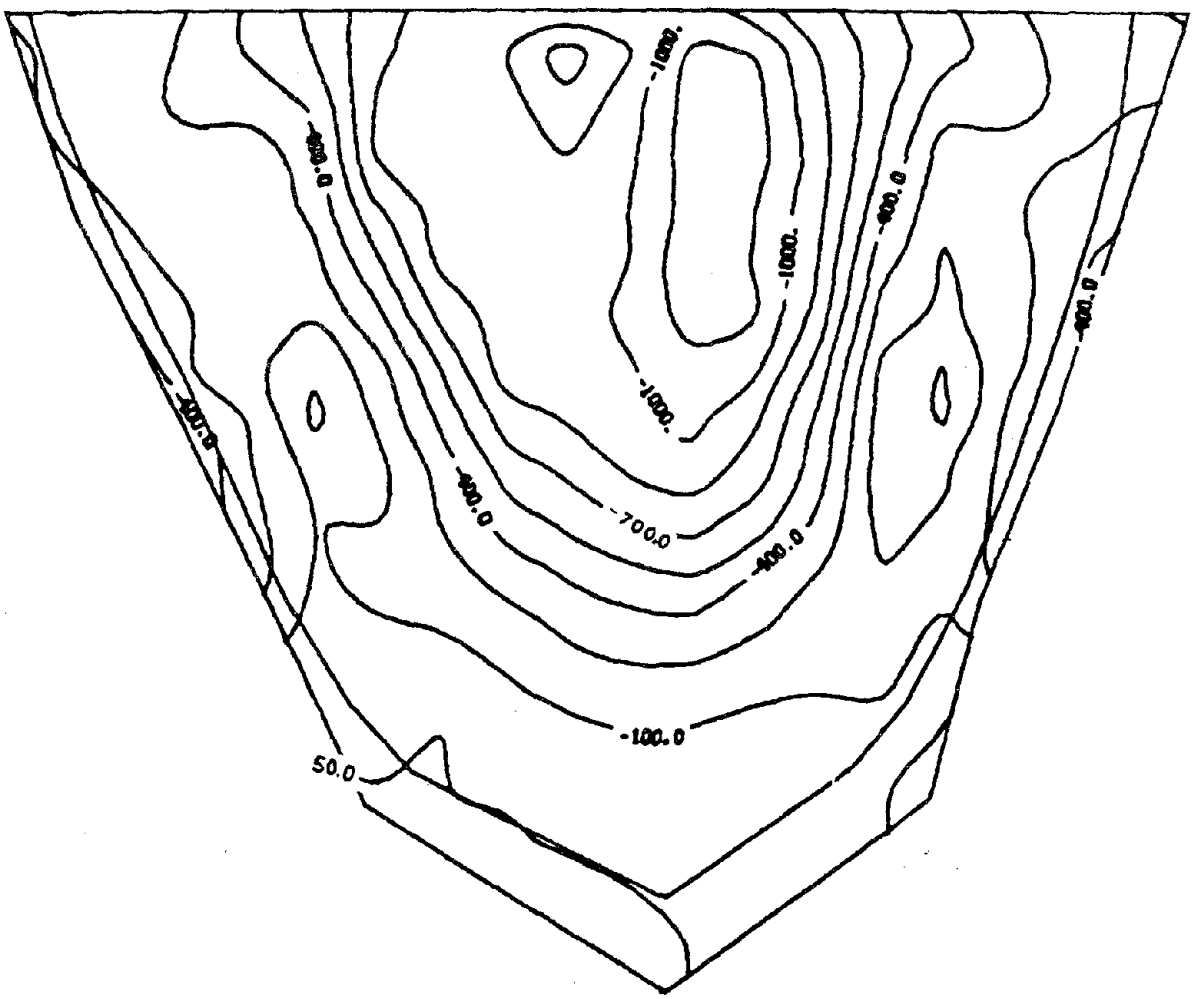

UPSTREAM FACE

MINIMUM SIG-XX

UNIT : PSI

CONTOUR INTERVAL= 150.0

CROSS-CANYON EXCITATIONS

AND HYDROSTATIC + GRAVITY LOADS

(a)

FIG. 42 MAXIMUM COMPRESSIVE STRESSES: STATIC PLUS C-C EARTHQUAKE

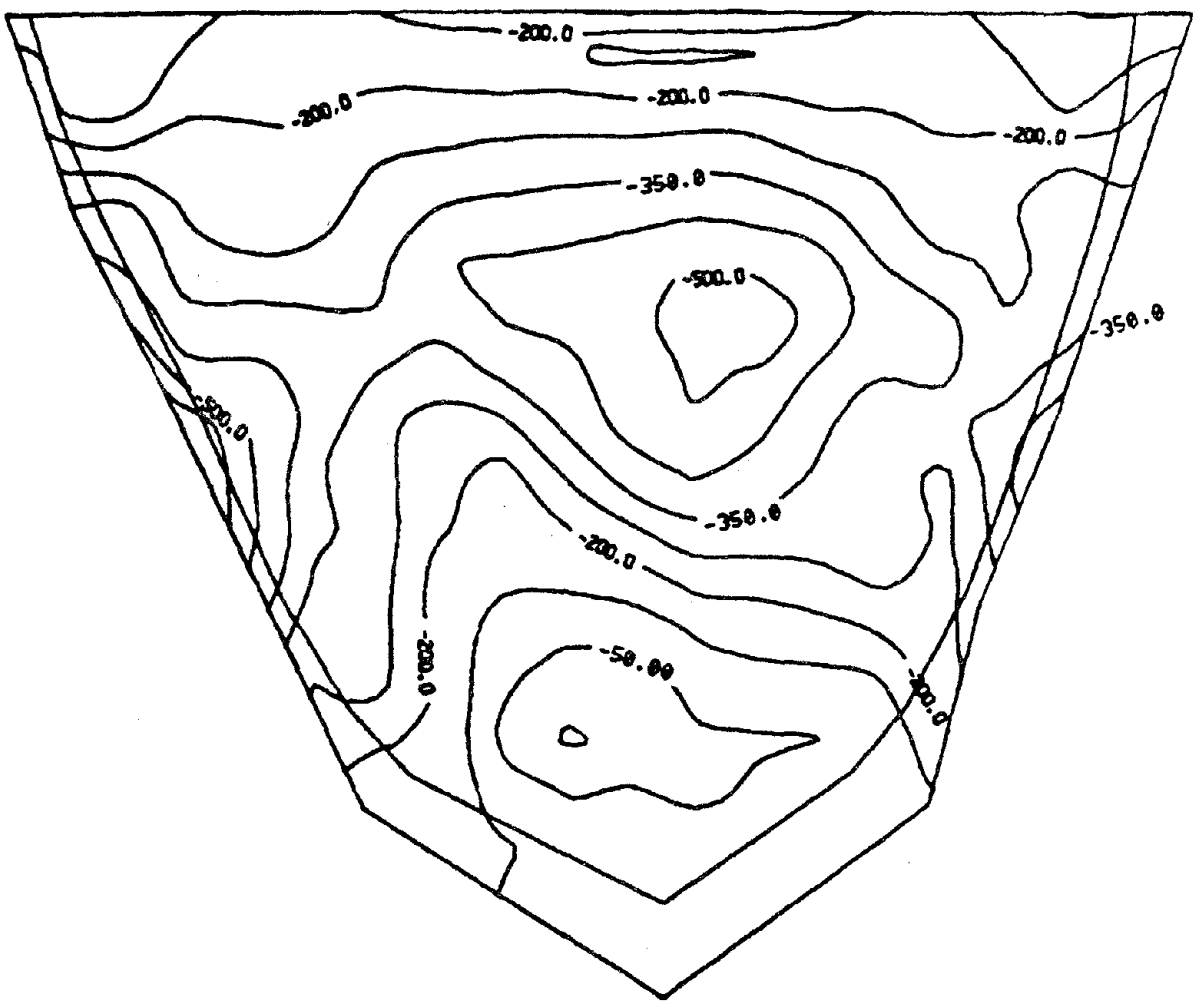

UPSTREAM FACE

MINIMUM SIG-YY

UNIT : PSI

CONTOUR INTERVAL= 75.0

CROSS-CANYON EXCITATIONS

AND HYDROSTATIC + GRAVITY LOADS

(b)

FIG. 42 (Cont.)

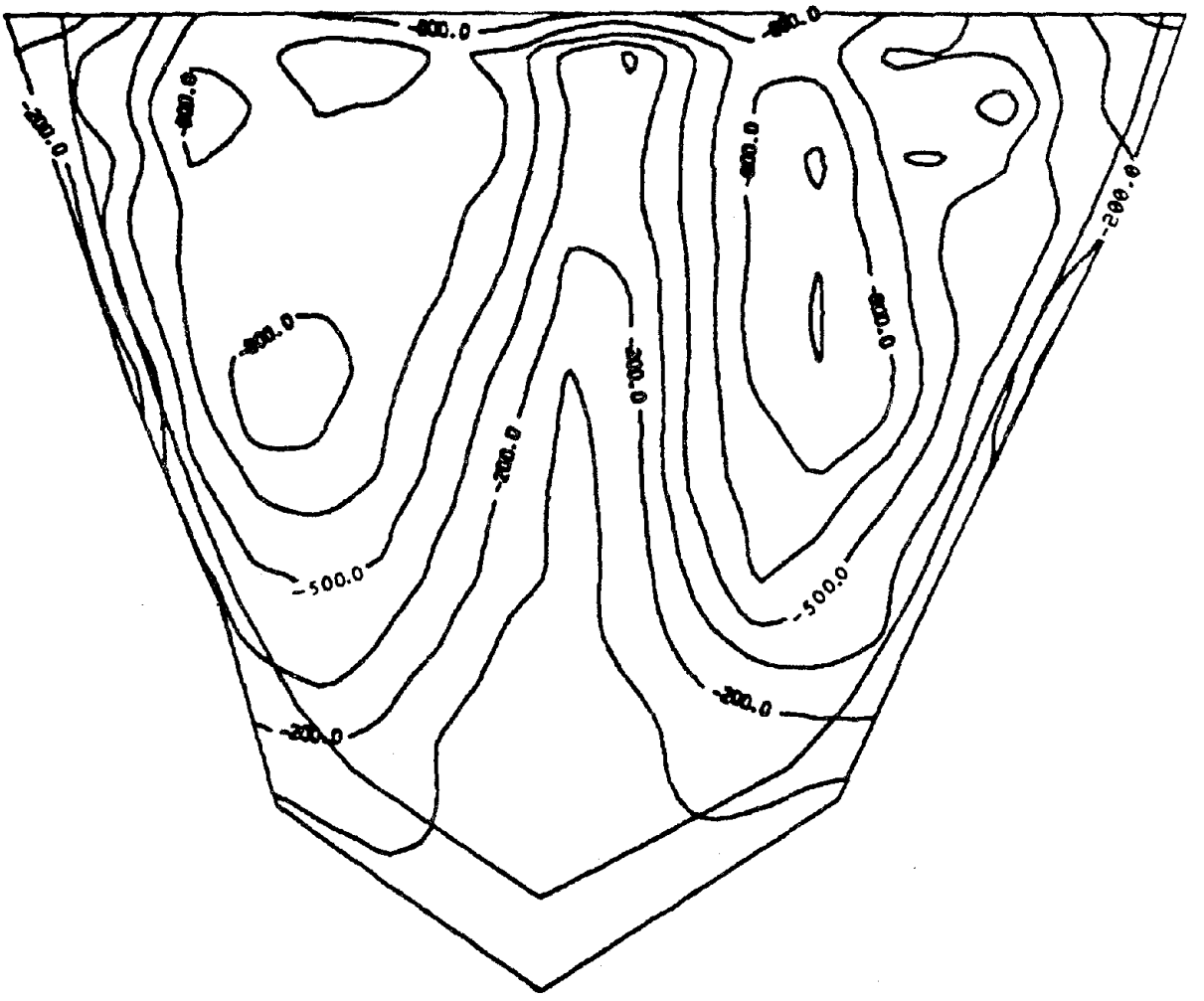

DOWNSTREAM FACE

MINIMUM SIG-XX

UNIT : PSI

CONTOUR INTERVAL= 150.0

CROSS-CANYON EXCITATIONS

AND HYDROSTATIC + GRAVITY LOADS

(c)

FIG. 42 (Cont.)

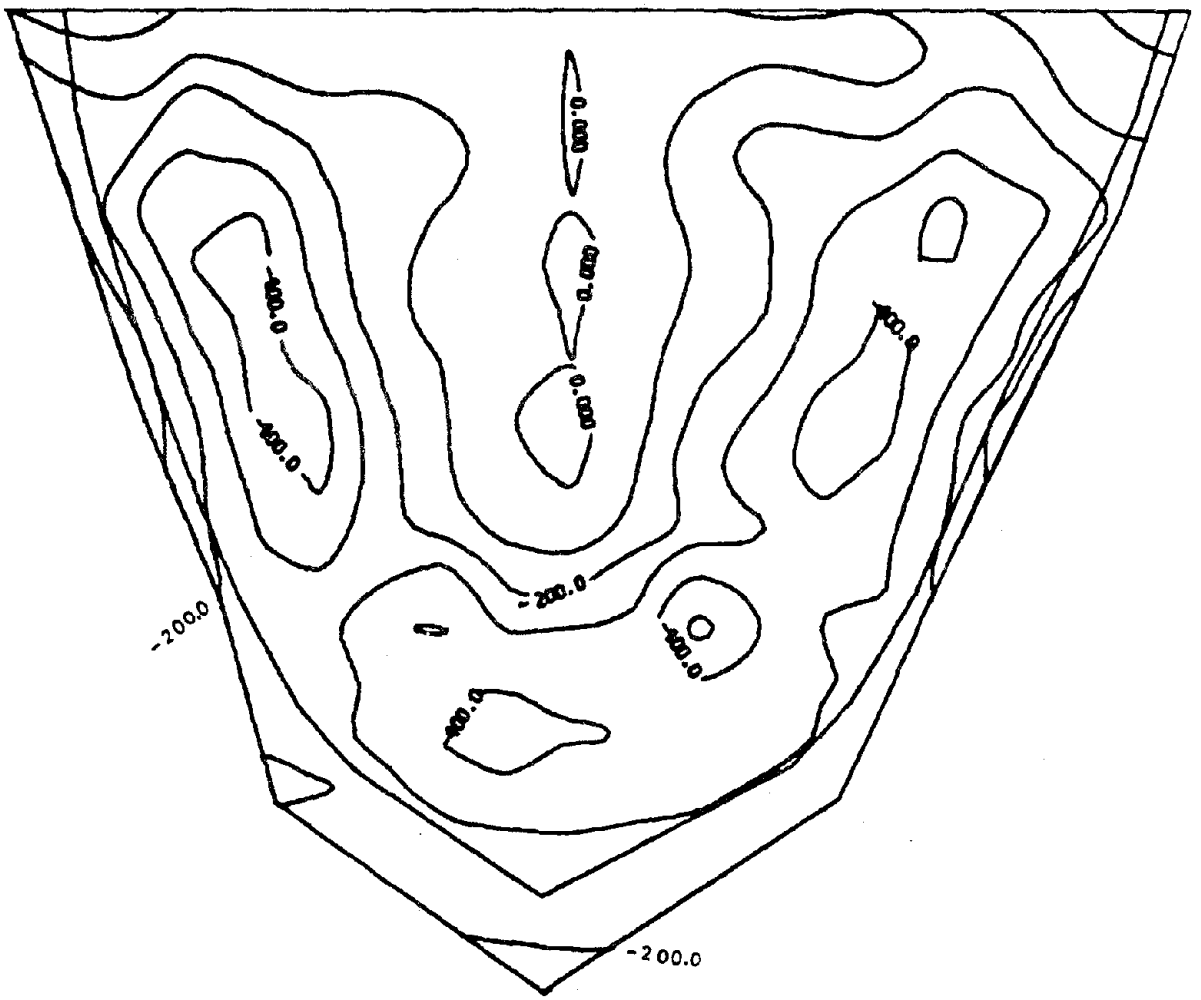

DOWNSTREAM FACE

MINIMUM SIG-YY

UNIT : PSI

CONTOUR INTERVAL= 100.0

CROSS-CANYON EXCITATIONS

AND HYDROSTATIC + GRAVITY LOADS

(d)

FIG. 42 (Cont.)

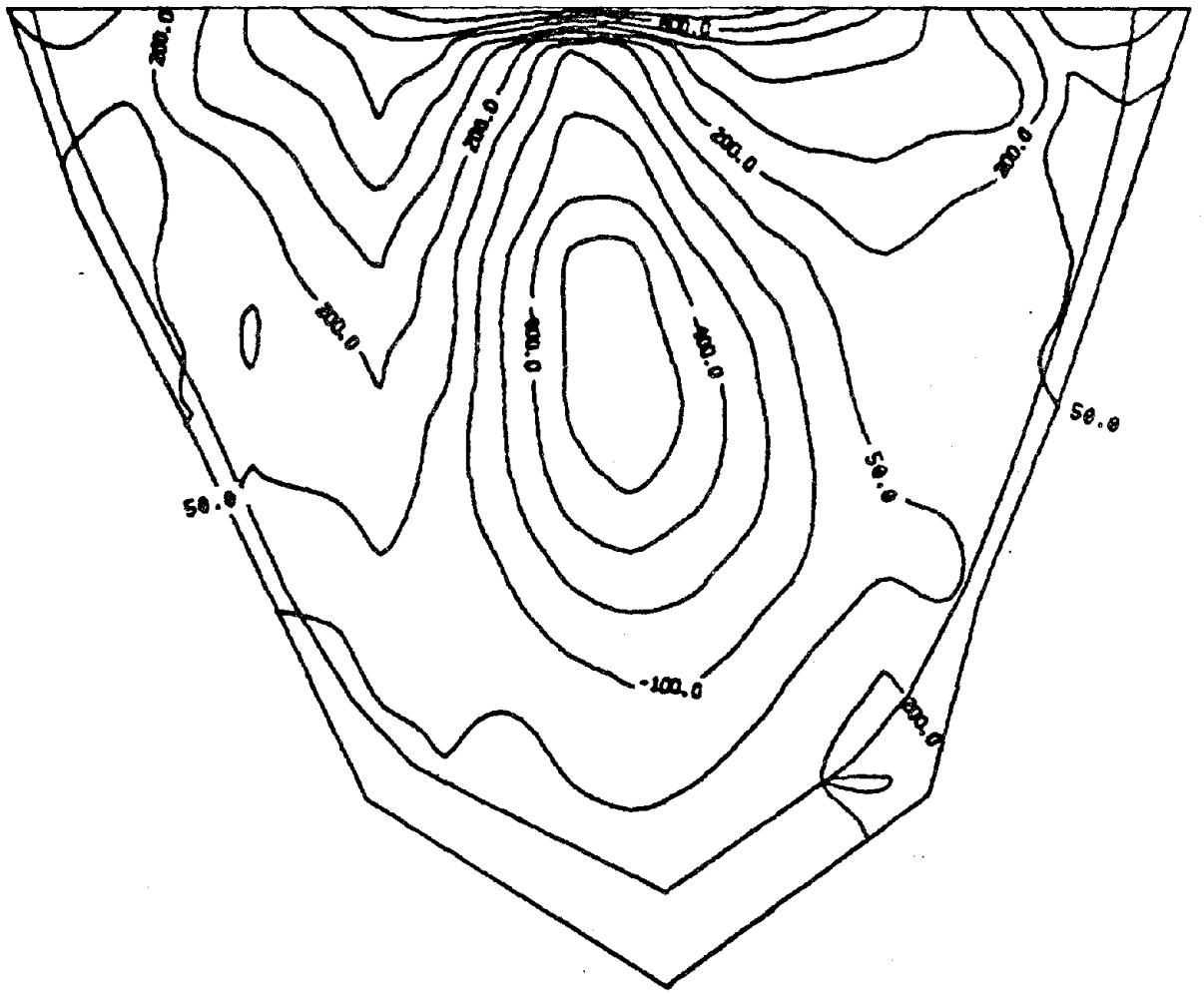

UPSTREAM FACE

MAXIMUM SIG-XX

UNIT : PSI

CONTOUR INTERVAL= 150.0

CROSS-CANYON EXCITATIONS

AND HYDROSTATIC + GRAVITY LOADS

(a)

FIG. 43 MAXIMUM TENSILE STRESSES: STATIC PLUS C-C EARTHQUAKE

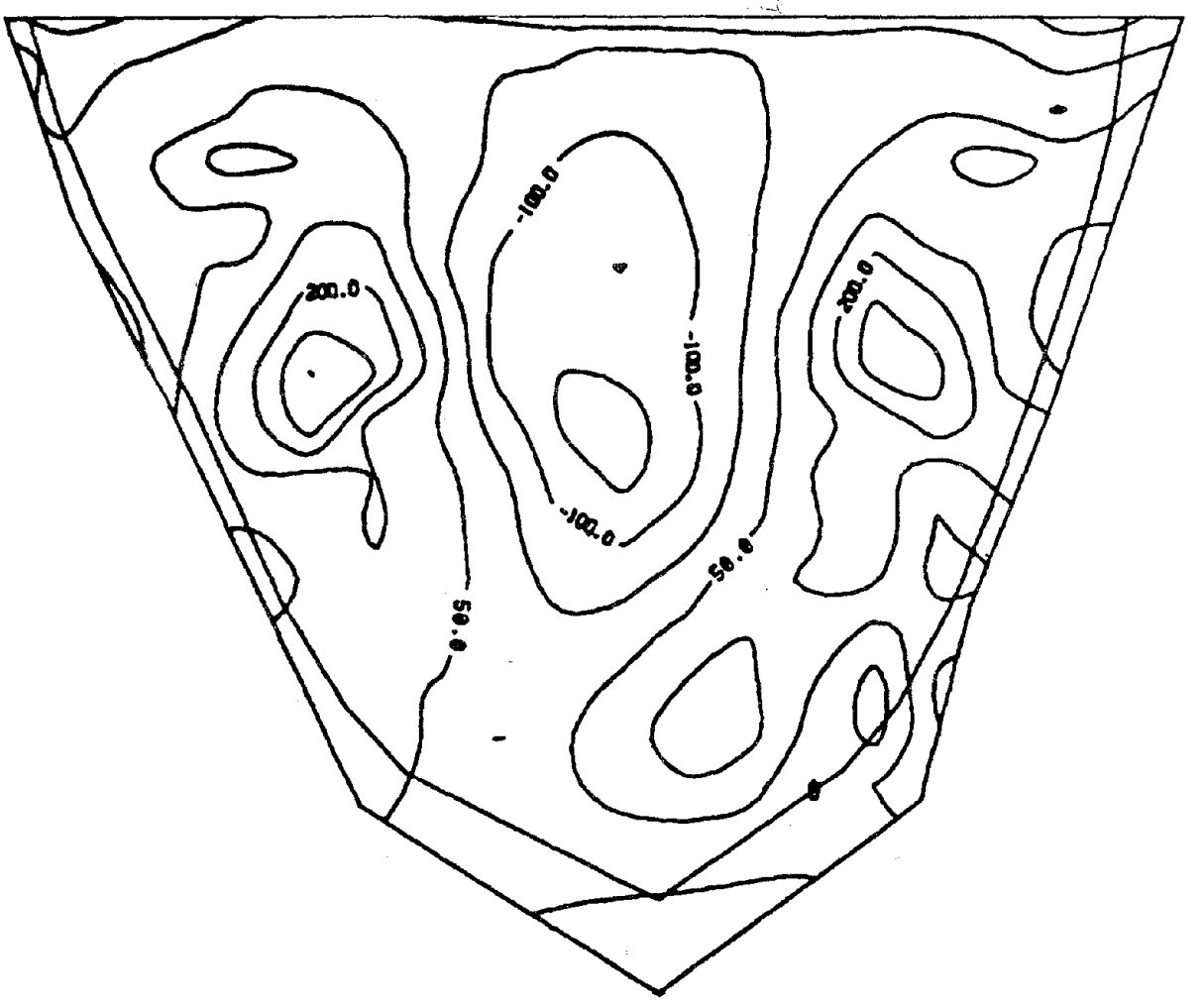

UPSTREAM FACE

MAXIMUM SIG-YY

UNIT : PSI

CONTOUR INTERVAL= 75.0

CROSS-CANYON EXCITATIONS

AND HYDROSTATIC + GRAVITY LOADS

(b)

FIG. 43 (Cont.)

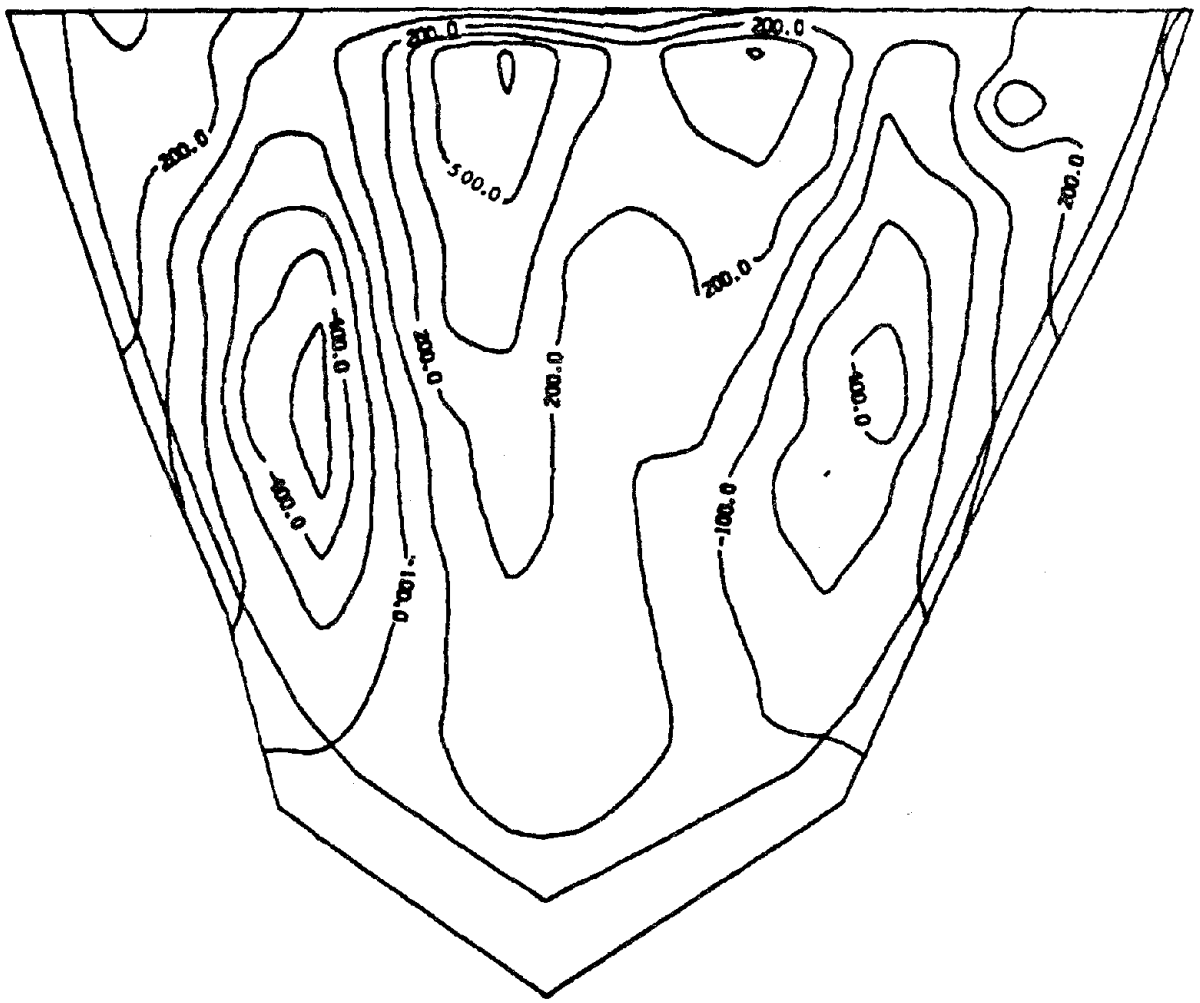

DOWNSTREAM FACE

MAXIMUM SIG-XX

UNIT : PSI

CONTOUR INTERVAL= 150.0

CROSS-CANYON EXCITATIONS

AND HYDROSTATIC + GRAVITY LOADS

(c)

FIG. 43 (Cont.)

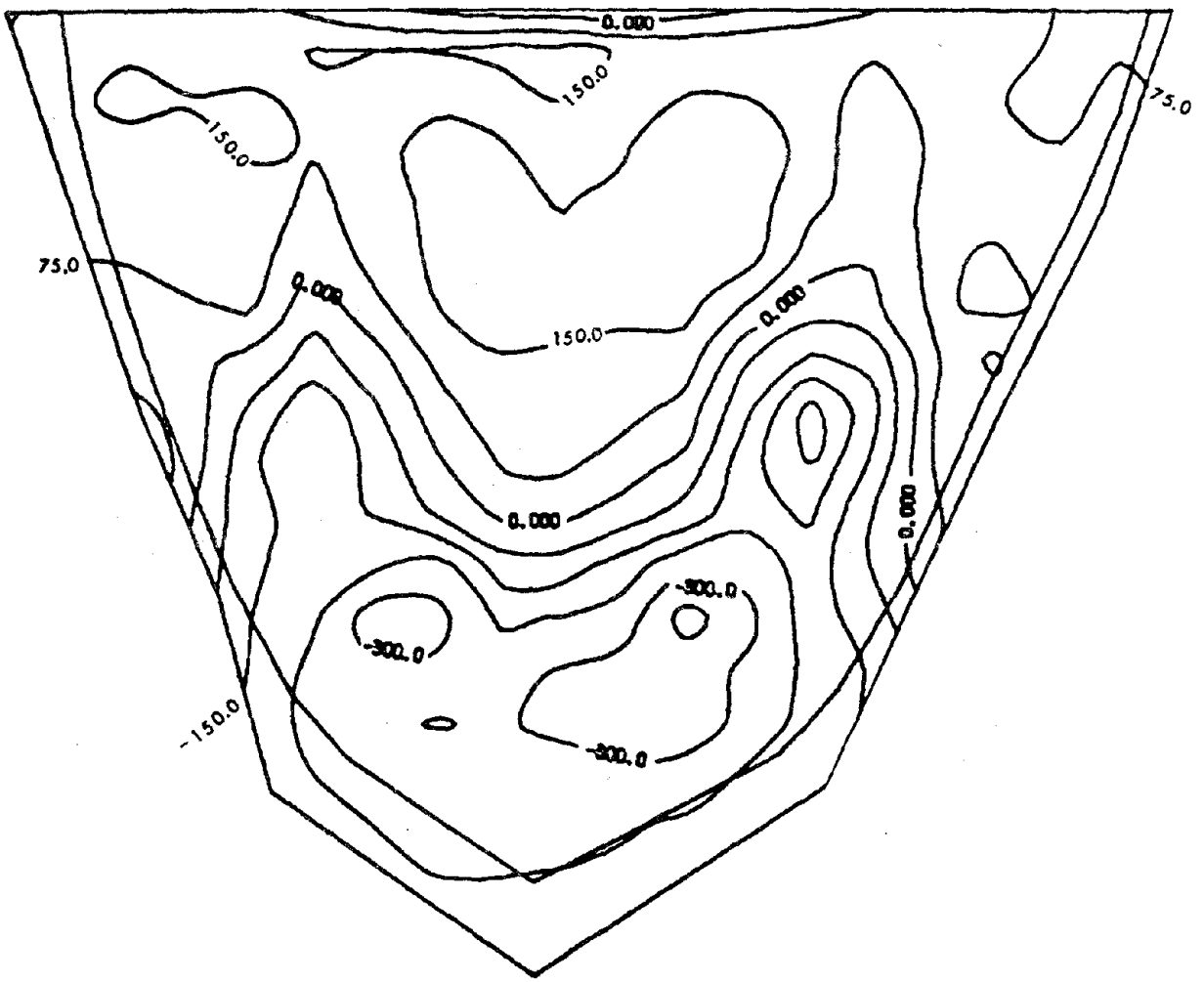

DOWNSTREAM FACE

MAXIMUM SIG-YY

UNIT : PSI

CONTOUR INTERVAL= 75.0

CROSS-CANYON EXCITATIONS

AND HYDROSTATIC + GRAVITY LOADS

(d)

FIG. 43 (Cont.)

EARTHQUAKE ENGINEERING RESEARCH CENTER REPORTS

NOTE: Numbers in parentheses are Accession Numbers assigned by the National Technical Information Service; these are followed by a price code. Copies of the reports may be ordered from the National Technical Information Service, 5285 Port Royal Road, Springfield, Virginia, 22161. Accession Numbers should be quoted on orders for reports (PB --- ---) and remittance must accompany each order. Reports without this information were not available at time of printing. The complete list of EERC reports (from EERC 67-1) is available upon request from the Earthquake Engineering Research Center, University of California, Berkeley, 47th Street and Hoffman Boulevard, Richmond, California 94804.

UCB/EERC-77/01 "PLUSH - A Computer Program for Probabilistic Finite Element Analysis of Seismic Soil-Structure Interaction," by M.P. Romo Organista, J. Lysmer and H.B. Seed - 1977 (PB81 177 651)A05

UCB/EERC-77/02 "Soil-Structure Interaction Effects at the Humboldt Bay Power Plant in the Ferndale Earthquake of June 7, 1975," by J.E. Valera, H.B. Seed, C.F. Tsai and J. Lysmer - 1977 (PB 265 795)A04

UCB/EERC-77/03 "Influence of Sample Disturbance on Sand Response to Cyclic Loading," by K. Mori, H.B. Seed and C.K. Chan - 1977 (PB 267 352)A04

UCB/EERC-77/04 "Seismological Studies of Strong Motion Records," by J. Shoja-Taheri - 1977 (PB 269 655)A10

UCB/EERC-77/05 Unassigned

UCB/EERC-77/06 "Developing Methodologies for Evaluating the Earthquake Safety of Existing Buildings," by No. 1 - B. Bresler; No. 2 - B. Bresler, T. Okada and D. Zisling; No. 3 - T. Okada and B. Bresler; No. 4 - V.V. Bertero and B. Bresler - 1977 (PB 267 354)A08

UCB/EERC-77/07 "A Literature Survey - Transverse Strength of Masonry Walls," by Y. Omote, R.L. Mayes, S.W. Chen and R.W. Clough - 1977 (PB 277 933)A07

UCB/EERC-77/08 "DRAIN-TABS: A Computer Program for Inelastic Earthquake Response of Three Dimensional Buildings," by R. Guendelman-Israel and G.H. Powell - 1977 (PB 270 693)A07

UCB/EERC-77/09 "SUBWALL: A Special Purpose Finite Element Computer Program for Practical Elastic Analysis and Design of Structural Walls with Substructure Option," by D.Q. Le, H. Peterson and E.P. Popov - 1977 (PB 270 567)A05

UCB/EERC-77/10 "Experimental Evaluation of Seismic Design Methods for Broad Cylindrical Tanks," by D.P. Clough (PB 272 280)A13

UCB/EERC-77/11 "Earthquake Engineering Research at Berkeley - 1976," - 1977 (PB 273 507)A09

UCB/EERC-77/12 "Automated Design of Earthquake Resistant Multistory Steel Building Frames," by N.D. Walker, Jr. - 1977 (PB 276 526)A09

UCB/EERC-77/13 "Concrete Confined by Rectangular Hoops Subjected to Axial Loads," by J. Vallenas, V.V. Bertero and E.P. Popov - 1977 (PB 275 165)A06

UCB/EERC-77/14 "Seismic Strain Induced in the Ground During Earthquakes," by Y. Sugimura - 1977 (PB 284 201)A04

UCB/EERC-77/15 Unassigned

UCB/EERC-77/16 "Computer Aided Optimum Design of Ductile Reinforced Concrete Moment Resisting Frames," by S.W. Zagajeski and V.V. Bertero - 1977 (PB 280 137)A07

UCB/EERC-77/17 "Earthquake Simulation Testing of a Stepping Frame with Energy-Absorbing Devices," by J.M. Kelly and D.F. Tsztoo - 1977 (PB 273 506)A04

UCB/EERC-77/18 "Inelastic Behavior of Eccentrically Braced Steel Frames under Cyclic Loadings," by C.W. Roeder and E.P. Popov - 1977 (PB 275 526)A15

UCB/EERC-77/19 "A Simplified Procedure for Estimating Earthquake-Induced Deformations in Dams and Embankments," by F.I. Makdisi and H.B. Seed - 1977 (PB 276 820)A04

UCB/EERC-77/20 "The Performance of Earth Dams during Earthquakes," by H.B. Seed, F.I. Makdisi and P. de Alba - 1977 (PB 276 821)A04

UCB/EERC-77/21 "Dynamic Plastic Analysis Using Stress Resultant Finite Element Formulation," by P. Lukkunapvasit and J.M. Kelly - 1977 (PB 275 453)A04

UCB/EERC-77/22 "Preliminary Experimental Study of Seismic Uplift of a Steel Frame," by R.W. Clough and A.A. Huckelbridge 1977 (PB 278 769)A08

UCB/EERC-77/23 "Earthquake Simulator Tests of a Nine-Story Steel Frame with Columns Allowed to Uplift," by A.A. Huckelbridge - 1977 (PB 277 944)A09

UCB/EERC-77/24 "Nonlinear Soil-Structure Interaction of Skew Highway Bridges," by M.-C. Chen and J. Penzien - 1977 (PB 276 176)A07

UCB/EERC-77/25 "Seismic Analysis of an Offshore Structure Supported on Pile Foundations," by D.D.-N. Liou and J. Penzien 1977 (PB 283 180)A06

UCB/EERC-77/26 "Dynamic Stiffness Matrices for Homogeneous Viscoelastic Half-Planes," by G. Dasgupta and A.K. Chopra - 1977 (PB 279 654)A06

UCB/EERC-77/27 "A Practical Soft Story Earthquake Isolation System," by J.M. Kelly, J.M. Eidinger and C.J. Derham - 1977 (PB 276 814)A07

UCB/EERC-77/28 "Seismic Safety of Existing Buildings and Incentives for Hazard Mitigation in San Francisco: An Exploratory Study," by A.J. Meltsner - 1977 (PB 281 970)A05

UCB/EERC-77/29 "Dynamic Analysis of Electrohydraulic Shaking Tables," by D. Rea, S. Abedi-Hayati and Y. Takahashi 1977 (PB 282 569)A04

UCB/EERC-77/30 "An Approach for Improving Seismic - Resistant Behavior of Reinforced Concrete Interior Joints," by B. Galunic, V.V. Bertero and E.P. Popov - 1977 (PB 290 870)A06

UCB/EERC-78/01 "The Development of Energy-Absorbing Devices for Aseismic Base Isolation Systems," by J.M. Kelly and D.F. Tsztoo - 1978 (PB 284 978)A04

UCB/EERC-78/02 "Effect of Tensile Prestrain on the Cyclic Response of Structural Steel Connections, by J.G. Bouwkamp and A. Mukhopadhyay - 1978

UCB/EERC-78/03 "Experimental Results of an Earthquake Isolation System using Natural Rubber Bearings," by J.M. Eidinger and J.M. Kelly - 1978 (PB 281 686)A04

UCB/EERC-78/04 "Seismic Behavior of Tall Liquid Storage Tanks," by A. Niwa - 1978 (PB 284 017)A14

UCB/EERC-78/05 "Hysteretic Behavior of Reinforced Concrete Columns Subjected to High Axial and Cyclic Shear Forces," by S.W. Zagajeski, V.V. Bertero and J.G. Bouwkamp - 1978 (PB 283 858)A13

UCB/EERC-78/06 "Three Dimensional Inelastic Frame Elements for the ANSR-I Program," by A. Riahi, D.G. Row and G.H. Powell - 1978 (PB 295 755)A04

UCB/EERC-78/07 "Studies of Structural Response to Earthquake Ground Motion," by O.A. Lopez and A.K. Chopra - 1978 (PB 282 790)A05

UCB/EERC-78/08 "A Laboratory Study of the Fluid-Structure Interaction of Submerged Tanks and Caissons in Earthquakes," by R.C. Byrd - 1978 (PB 284 957)A08

UCB/EERC-78/09 Unassigned

UCB/EERC-78/10 "Seismic Performance of Nonstructural and Secondary Structural Elements," by I. Sakamoto - 1978 (PB81 154 593)A05

UCB/EERC-78/11 "Mathematical Modelling of Hysteresis Loops for Reinforced Concrete Columns," by S. Nakata, T. Sproul and J. Penzien - 1978 (PB 298 274)A05

UCB/EERC-78/12 "Damageability in Existing Buildings," by T. Blejwas and B. Bresler - 1978 (PB 80 166 978)A05

UCB/EERC-78/13 "Dynamic Behavior of a Pedestal Base Multistory Building," by R.M. Stephen, E.L. Wilson, J.G. Bouwkamp and M. Button - 1978 (PB 286 650)A08

UCB/EERC-78/14 "Seismic Response of Bridges - Case Studies," by R.A. Imbsen, V. Nutt and J. Penzien - 1978 (PB 286 503)A10

UCB/EERC-78/15 "A Substructure Technique for Nonlinear Static and Dynamic Analysis," by D.G. Row and G.H. Powell - 1978 (PB 288 077)A10

UCB/EERC-78/16 "Seismic Risk Studies for San Francisco and for the Greater San Francisco Bay Area," by C.S. Oliveira - 1978 (PB 81 120 115)A07

UCB/EERC-78/17 "Strength of Timber Roof Connections Subjected to Cyclic Loads," by P. Gülkan, R.L. Mayes and R.W. Clough - 1978 (HUD-000 1491)A07

UCB/EERC-78/18 "Response of K-Braced Steel Frame Models to Lateral Loads," by J.G. Bouwkamp, R.M. Stephen and E.P. Popov - 1978

UCB/EERC-78/19 "Rational Design Methods for Light Equipment in Structures Subjected to Ground Motion," by J.L. Sackman and J.M. Kelly - 1978 (PB 292 357)A04

UCB/EERC-78/20 "Testing of a Wind Restraint for Aseismic Base Isolation," by J.M. Kelly and D.E. Chitty - 1978 (PB 292 833)A03

UCB/EERC-78/21 "APOLLO - A Computer Program for the Analysis of Pore Pressure Generation and Dissipation in Horizontal Sand Layers During Cyclic or Earthquake Loading," by P.P. Martin and H.B. Seed - 1978 (PB 292 835)A04

UCB/EERC-78/22 "Optimal Design of an Earthquake Isolation System," by M.A. Bhatti, K.S. Pister and E. Polak - 1978 (PB 294 735)A06

UCB/EERC-78/23 "MASH - A Computer Program for the Non-Linear Analysis of Vertically Propagating Shear Waves in Horizontally Layered Deposits," by P.P. Martin and H.B. Seed - 1978 (PB 293 101)A05

UCB/EERC-78/24 "Investigation of the Elastic Characteristics of a Three Story Steel Frame Using System Identification," by I. Kaya and H.D. McNiven - 1978 (PB 296 225)A06

UCB/EERC-78/25 "Investigation of the Nonlinear Characteristics of a Three-Story Steel Frame Using System Identification," by I. Kaya and H.D. McNiven - 1978 (PB 301 363)A05

UCB/EERC-78/26 "Studies of Strong Ground Motion in Taiwan," by Y.M. Hsiung, B.A. Bolt and J. Penzien - 1978 (PB 298 436)A06

UCB/EERC-78/27 "Cyclic Loading Tests of Masonry Single Piers: Volume 1 - Height to Width Ratio of 2," by P.A. Hidalgo, R.L. Mayes, H.D. McNiven and R.W. Clough - 1978 (PB 296 211)A07

UCB/EERC-78/28 "Cyclic Loading Tests of Masonry Single Piers: Volume 2 - Height to Width Ratio of 1," by S.-W.J. Chen, P.A. Hidalgo, R.L. Mayes, R.W. Clough and H.D. McNiven - 1978 (PB 296 212)A09

UCB/EERC-78/29 "Analytical Procedures in Soil Dynamics," by J. Lysmer - 1978 (PB 298 445)A06

UCB/EERC-79/01 "Hysteretic Behavior of Lightweight Reinforced Concrete Beam-Column Subassemblages," by B. Forzani, E.P. Popov and V.V. Bertero - April 1979(PB 298 267)A06

UCB/EERC-79/02 "The Development of a Mathematical Model to Predict the Flexural Response of Reinforced Concrete Beams to Cyclic Loads, Using System Identification," by J. Stanton & H. McNiven - Jan. 1979(PB 295 875)A10

UCB/EERC-79/03 "Linear and Nonlinear Earthquake Response of Simple Torsionally Coupled Systems," by C.L. Kan and A.K. Chopra - Feb. 1979(PB 298 262)A06

UCB/EERC-79/04 "A Mathematical Model of Masonry for Predicting its Linear Seismic Response Characteristics," by Y. Mengi and H.D. McNiven - Feb. 1979(PB 298 266)A06

UCB/EERC-79/05 "Mechanical Behavior of Lightweight Concrete Confined by Different Types of Lateral Reinforcement," by M.A. Manrique, V.V. Bertero and E.P. Popov - May 1979(PB 301 114)A06

UCB/EERC-79/06 "Static Tilt Tests of a Tall Cylindrical Liquid Storage Tank," by R.W. Clough and A. Niwa - Feb. 1979 (PB 301 167)A06

UCB/EERC-79/07 "The Design of Steel Energy Absorbing Restrainers and Their Incorporation into Nuclear Power Plants for Enhanced Safety: Volume 1 - Summary Report," by P.N. Spencer, V.F. Zackay, and E.R. Parker - Feb. 1979(UCB/EERC-79/07)A09

UCB/EERC-79/08 "The Design of Steel Energy Absorbing Restrainers and Their Incorporation into Nuclear Power Plants for Enhanced Safety: Volume 2 - The Development of Analyses for Reactor System Piping,""Simple Systems" by M.C. Lee, J. Penzien, A.K. Chopra and K, Suzuki "Complex Systems" by G.H. Powell, E.L. Wilson, R.W. Clough and D.G. Row - Feb. 1979(UCB/EERC-79/08)A10

UCB/EERC-79/09 "The Design of Steel Energy Absorbing Restrainers and Their Incorporation into Nuclear Power Plants for Enhanced Safety: Volume 3 - Evaluation of Commercial Steels," by W.S. Owen, R.M.N. Pelloux, R.O. Ritchie, M. Faral, T. Ohhashi, J. Toplosky, S.J. Hartman, V.F. Zackay and E.R. Parker - Feb. 1979(UCB/EERC-79/09)A04

UCB/EERC-79/10 "The Design of Steel Energy Absorbing Restrainers and Their Incorporation into Nuclear Power Plants for Enhanced Safety: Volume 4 - A Review of Energy-Absorbing Devices," by J.M. Kelly and M.S. Skinner - Feb. 1979(UCB/EERC-79/10)A04

UCB/EERC-79/11 "Conservatism In Summation Rules for Closely Spaced Modes," by J.M. Kelly and J.L. Sackman - May 1979(PB 301 328)A03

UCB/EERC-79/12 "Cyclic Loading Tests of Masonry Single Piers; Volume 3 - Height to Width Ratio of 0.5," by P.A. Hidalgo, R.L. Mayes, H.D. McNiven and R.W. Clough - May 1979(PB 301 321)A08

UCB/EERC-79/13 "Cyclic Behavior of Dense Course-Grained Materials in Relation to the Seismic Stability of Dams," by N.G. Banerjee, H.B. Seed and C.K. Chan - June 1979(PB 301 373)A13

UCB/EERC-79/14 "Seismic Behavior of Reinforced Concrete Interior Beam-Column Subassemblages," by S. Viwathanatepa, E.P. Popov and V.V. Bertero - June 1979(PB 301 326)A10

UCB/EERC-79/15 "Optimal Design of Localized Nonlinear Systems with Dual Performance Criteria Under Earthquake Excitations," by M.A. Bhatti - July 1979(PB 80 167 109)A06

UCB/EERC-79/16 "OPTDYN - A General Purpose Optimization Program for Problems with or without Dynamic Constraints," by M.A. Bhatti, E. Polak and K.S. Pister - July 1979(PB 80 167 091)A05

UCB/EERC-79/17 "ANSR-II, Analysis of Nonlinear Structural Response, Users Manual," by D.P. Mondkar and G.H. Powell July 1979(PB 80 113 301)A05

UCB/EERC-79/18 "Soil Structure Interaction in Different Seismic Environments," A. Gomez-Masso, J. Lysmer, J.-C. Chen and H.B. Seed - August 1979(PB 80 101 520)A04

UCB/EERC-79/19 "ARMA Models for Earthquake Ground Motions," by M.K. Chang, J.W. Kwiatkowski, R.F. Nau, R.M. Oliver and K.S. Pister - July 1979(PB 301 166)A05

UCB/EERC-79/20 "Hysteretic Behavior of Reinforced Concrete Structural Walls," by J.M. Vallenas, V.V. Bertero and E.P. Popov - August 1979(PB 80 165 905)A12

UCB/EERC-79/21 "Studies on High-Frequency Vibrations of Buildings - 1: The Column Effect," by J. Lubliner - August 1979 (PB 80 158 553)A03

UCB/EERC-79/22 "Effects of Generalized Loadings on Bond Reinforcing Bars Embedded in Confined Concrete Blocks," by S. Viwathanatepa, E.P. Popov and V.V. Bertero - August 1979(PB 81 124 018)A14

UCB/EERC-79/23 "Shaking Table Study of Single-Story Masonry Houses, Volume 1: Test Structures 1 and 2," by P. Gülkan, R.L. Mayes and R.W. Clough - Sept. 1979 (HUD-000 1763)A12

UCB/EERC-79/24 "Shaking Table Study of Single-Story Masonry Houses, Volume 2: Test Structures 3 and 4," by P. Gülkan, R.L. Mayes and R.W. Clough - Sept. 1979 (HUD-000 1836)A12

UCB/EERC-79/25 "Shaking Table Study of Single-Story Masonry Houses, Volume 3: Summary, Conclusions and Recommendations," by R.W. Clough, R.L. Mayes and P. Gülkan - Sept. 1979 (HUD-000 1837)A06

UCB/EERC-79/26 "Recommendations for a U.S.-Japan Cooperative Research Program Utilizing Large-Scale Testing Facilities," by U.S.-Japan Planning Group - Sept. 1979(PB 301 407)A06

UCB/EERC-79/27 "Earthquake-Induced Liquefaction Near Lake Amatitlan, Guatemala," by H.B. Seed, I. Arango, C.K. Chan, A. Gomez-Masso and R. Grant de Ascoli - Sept. 1979(NUREG-CR1341)A03

UCB/EERC-79/28 "Infill Panels: Their Influence on Seismic Response of Buildings," by J.W. Axley and V.V. Bertero Sept. 1979(PB 80 163 371)A10

UCB/EERC-79/29 "3D Truss Bar Element (Type 1) for the ANSR-II Program," by D.P. Mondkar and G.H. Powell - Nov. 1979 (PB 80 169 709)A02

UCB/EERC-79/30 "2D Beam-Column Element (Type 5 - Parallel Element Theory) for the ANSR-II Program," by D.G. Row, G.H. Powell and D.P. Mondkar - Dec. 1979(PB 80 167 224)A03

UCB/EERC-79/31 "3D Beam-Column Element (Type 2 - Parallel Element Theory) for the ANSR-II Program," by A. Riahi, G.H. Powell and D.P. Mondkar - Dec. 1979(PB 80 167 216)A03

UCB/EERC-79/32 "On Response of Structures to Stationary Excitation," by A. Der Kiureghian - Dec. 1979(PB 80166 929)A03

UCB/EERC-79/33 "Undisturbed Sampling and Cyclic Load Testing of Sands," by S. Singh, H.B. Seed and C.K. Chan Dec. 1979(ADA 087 298)A07

UCB/EERC-79/34 "Interaction Effects of Simultaneous Torsional and Compressional Cyclic Loading of Sand," by P.M. Griffin and W.N. Houston - Dec. 1979(ADA 092 352)A15

UCB/EERC-80/01 "Earthquake Response of Concrete Gravity Dams Including Hydrodynamic and Foundation Interaction Effects," by A.K. Chopra, P. Chakrabarti and S. Gupta - Jan. 1980(AD-A087297)A10

UCB/EERC-80/02 "Rocking Response of Rigid Blocks to Earthquakes," by C.S. Yim, A.K. Chopra and J. Penzien - Jan. 1980 (PB80 166 002)A04

UCB/EERC-80/03 "Optimum Inelastic Design of Seismic-Resistant Reinforced Concrete Frame Structures," by S.W. Zagajeski and V.V. Bertero - Jan. 1980(PB80 164 635)A06

UCB/EERC-80/04 "Effects of Amount and Arrangement of Wall-Panel Reinforcement on Hysteretic Behavior of Reinforced Concrete Walls," by R. Iliya and V.V. Bertero - Feb. 1980(PB81 122 525)A09

UCB/EERC-80/05 "Shaking Table Research on Concrete Dam Models," by A. Niwa and R.W. Clough - Sept. 1980(PB81 122 368)A06

UCB/EERC-80/06 "The Design of Steel Energy-Absorbing Restrainers and their Incorporation into Nuclear Power Plants for Enhanced Safety (Vol 1A): Piping with Energy Absorbing Restrainers: Parameter Study on Small Systems," by G.H. Powell, C. Oughourlian and J. Simons - June 1980

UCB/EERC-80/07 "Inelastic Torsional Response of Structures Subjected to Earthquake Ground Motions," by Y. Yamazaki April 1980(PB81 122 327)A08

UCB/EERC-80/08 "Study of X-Braced Steel Frame Structures Under Earthquake Simulation," by Y. Ghanaat - April 1980 (PB81 122 335)A11

UCB/EERC-80/09 "Hybrid Modelling of Soil-Structure Interaction," by S. Gupta, T.W. Lin, J. Penzien and C.S. Yeh May 1980(PB81 122 319)A07

UCB/EERC-80/10 "General Applicability of a Nonlinear Model of a One Story Steel Frame," by B.I. Sveinsson and H.D. McNiven - May 1980(PB81 124 877)A06

UCB/EERC-80/11 "A Green-Function Method for Wave Interaction with a Submerged Body," by W. Kioka - April 1980 (PB81 122 269)A07

UCB/EERC-80/12 "Hydrodynamic Pressure and Added Mass for Axisymmetric Bodies," by F. Nilrat - May 1980(PB81 122 343)A08

UCB/EERC-80/13 "Treatment of Non-Linear Drag Forces Acting on Offshore Platforms," by B.V. Dao and J. Penzien May 1980(PB81 153 413)A07

UCB/EERC-80/14 "2D Plane/Axisymmetric Solid Element (Type 3 - Elastic or Elastic-Perfectly Plastic) for the ANSR-II Program," by D.P. Mondkar and G.H. Powell - July 1980(PB81 122 350)A03

UCB/EERC-80/15 "A Response Spectrum Method for Random Vibrations," by A. Der Kiureghian - June 1980(PB81 122 301)A03

UCB/EERC-80/16 "Cyclic Inelastic Buckling of Tubular Steel Braces," by V.A. Zayas, E.P. Popov and S.A. Mahin June 1980(PB81 124 885)A10

UCB/EERC-80/17 "Dynamic Response of Simple Arch Dams Including Hydrodynamic Interaction," by C.S. Porter and A.K. Chopra - July 1980(PB81 124 000)A13

UCB/EERC-80/18 "Experimental Testing of a Friction Damped Aseismic Base Isolation System with Fail-Safe Characteristics," by J.M. Kelly, K.E. Beucke and M.S. Skinner - July 1980(PB81 148 595)A04

UCB/EERC-80/19 "The Design of Steel Energy-Absorbing Restrainers and their Incorporation into Nuclear Power Plants for Enhanced Safety (Vol 1B): Stochastic Seismic Analyses of Nuclear Power Plant Structures and Piping Systems Subjected to Multiple Support Excitations," by M.C. Lee and J. Penzien - June 1980

UCB/EERC-80/20 "The Design of Steel Energy-Absorbing Restrainers and their Incorporation into Nuclear Power Plants for Enhanced Safety (Vol 1C): Numerical Method for Dynamic Substructure Analysis," by J.M. Dickens and E.L. Wilson - June 1980

UCB/EERC-80/21 "The Design of Steel Energy-Absorbing Restrainers and their Incorporation into Nuclear Power Plants for Enhanced Safety (Vol 2): Development and Testing of Restraints for Nuclear Piping Systems," by J.M. Kelly and M.S. Skinner - June 1980

UCB/EERC-80/22 "3D Solid Element (Type 4-Elastic or Elastic-Perfectly-Plastic) for the ANSR-II Program," by D.P. Mondkar and G.H. Powell - July 1980(PB81 123 242)A03

UCB/EERC-80/23 "Gap-Friction Element (Type 5) for the ANSR-II Program," by D.P. Mondkar and G.H. Powell - July 1980 (PB81 122 285)A03

UCB/EERC-80/24 "U-Bar Restraint Element (Type 11) for the ANSR-II Program," by C. Oughourlian and G.H. Powell July 1980(PB81 122 293)A03

UCB/EERC-80/25 "Testing of a Natural Rubber Base Isolation System by an Explosively Simulated Earthquake," by J.M. Kelly - August 1980(PB81 201 360)A04

UCB/EERC-80/26 "Input Identification from Structural Vibrational Response," by Y. Hu - August 1980(PB81 152 308)A05

UCB/EERC-80/27 "Cyclic Inelastic Behavior of Steel Offshore Structures," by V.A. Zayas, S.A. Mahin and E.P. Popov August 1980(PB81 196 180)A15

UCB/EERC-80/28 "Shaking Table Testing of a Reinforced Concrete Frame with Biaxial Response," by M.G. Oliva October 1980(PB81 154 304)A10

UCB/EERC-80/29 "Dynamic Properties of a Twelve-Story Prefabricated Panel Building," by J.G. Bouwkamp, J.P. Kollegger and R.M. Stephen - October 1980(PB82 117 128)A06

UCB/EERC-80/30 "Dynamic Properties of an Eight-Story Prefabricated Panel Building," by J.G. Bouwkamp, J.P. Kollegger and R.M. Stephen - October 1980(PB81 200 313)A05

UCB/EERC-80/31 "Predictive Dynamic Response of Panel Type Structures Under Earthquakes," by J.P. Kollegger and J.G. Bouwkamp - October 1980(PB81 152 316)A04

UCB/EERC-80/32 "The Design of Steel Energy-Absorbing Restrainers and their Incorporation into Nuclear Power Plants for Enhanced Safety (Vol 3): Testing of Commercial Steels in Low-Cycle Torsional Fatigue," by P. Spencer, E.R. Parker, E. Jongewaard and M. Drory

UCB/EERC-80/33 "The Design of Steel Energy-Absorbing Restrainers and their Incorporation into Nuclear Power Plants for Enhanced Safety (Vol 4): Shaking Table Tests of Piping Systems with Energy-Absorbing Restrainers," by S.F. Stiemer and W.G. Godden - Sept. 1980

UCB/EERC-80/34 "The Design of Steel Energy-Absorbing Restrainers and their Incorporation into Nuclear Power Plants for Enhanced Safety (Vol 5): Summary Report," by P. Spencer

UCB/EERC-80/35 "Experimental Testing of an Energy-Absorbing Base Isolation System," by J.M. Kelly, M.S. Skinner and K.E. Beucke - October 1980(PB81 154 072)A04

UCB/EERC-80/36 "Simulating and Analyzing Artificial Non-Stationary Earthquake Ground Motions," by R.F. Nau, R.M. Oliver and K.S. Pister - October 1980(PB81 153 397)A04

UCB/EERC-80/37 "Earthquake Engineering at Berkeley - 1980," - Sept. 1980(PB81 205 874)A09

UCB/EERC-80/38 "Inelastic Seismic Analysis of Large Panel Buildings," by V. Schricker and G.H. Powell - Sept. 1980 (PB81 154 338)A13

UCB/EERC-80/39 "Dynamic Response of Embankment, Concrete-Gravity and Arch Dams Including Hydrodynamic Interaction," by J.F. Hall and A.K. Chopra - October 1980(PB81 152 324)A11

UCB/EERC-80/40 "Inelastic Buckling of Steel Struts Under Cyclic Load Reversal," by R.G. Black, W.A. Wenger and E.P. Popov - October 1980(PB81 154 312)A08

UCB/EERC-80/41 "Influence of Site Characteristics on Building Damage During the October 3, 1974 Lima Earthquake," by P. Repetto, I. Arango and H.B. Seed - Sept. 1980(PB81 161 739)A05

UCB/EERC-80/42 "Evaluation of a Shaking Table Test Program on Response Behavior of a Two Story Reinforced Concrete Frame," by J.M. Blondet, R.W. Clough and S.A. Mahin

UCB/EERC-80/43 "Modelling of Soil-Structure Interaction by Finite and Infinite Elements," by F. Medina - December 1980(PB81 229 270)A04

UCB/EERC-81/01 "Control of Seismic Response of Piping Systems and Other Structures by Base Isolation," edited by J.M. Kelly - January 1981 (PB81 200 735)A05

UCB/EERC-81/02 "OPTNSR - An Interactive Software System for Optimal Design of Statically and Dynamically Loaded Structures with Nonlinear Response," by M.A. Bhatti, V. Ciampi and K.S. Pister - January 1981 (PB81 218 851)A09

UCB/EERC-81/03 "Analysis of Local Variations in Free Field Seismic Ground Motions," by J.-C. Chen, J. Lysmer and H.B. Seed - January 1981 (AD-A099508)A13

UCB/EERC-81/04 "Inelastic Structural Modeling of Braced Offshore Platforms for Seismic Loading," by V.A. Zayas, P.-S.B. Shing, S.A. Mahin and E.P. Popov - January 1981(PB82 138 777)A07

UCB/EERC-81/05 "Dynamic Response of Light Equipment in Structures," by A. Der Kiureghian, J.L. Sackman and B. Nour-Omid - April 1981 (PB81 218 497)A04

UCB/EERC-81/06 "Preliminary Experimental Investigation of a Broad Base Liquid Storage Tank," by J.G. Bouwkamp, J.P. Kollegger and R.M. Stephen - May 1981(PB82 140 385)A03

UCB/EERC-81/07 "The Seismic Resistant Design of Reinforced Concrete Coupled Structural Walls," by A.E. Aktan and V.V. Bertero - June 1981(PB82 113 358)A11

UCB/EERC-81/08 "The Undrained Shearing Resistance of Cohesive Soils at Large Deformations," by M.R. Pyles and H.B. Seed - August 1981

UCB/EERC-81/09 "Experimental Behavior of a Spatial Piping System with Steel Energy Absorbers Subjected to a Simulated Differential Seismic Input," by S.F. Stiemer, W.G. Godden and J.M. Kelly - July 1981

UCB/EERC-81/10 "Evaluation of Seismic Design Provisions for Masonry in the United States," by B.I. Sveinsson, R.L. Mayes and H.D. McNiven - August 1981

UCB/EERC-81/11 "Two-Dimensional Hybrid Modelling of Soil-Structure Interaction," by T.-J. Tzong, S. Gupta and J. Penzien - August 1981(PB82 142 118)A04

UCB/EERC-81/12 "Studies on Effects of Infills in Seismic Resistant R/C Construction," by S. Brokken and V.V. Bertero - September 1981

UCB/EERC-81/13 "Linear Models to Predict the Nonlinear Seismic Behavior of a One-Story Steel Frame," by H. Valdimarsson, A.H. Shah and H.D. McNiven - September 1981(PB82 138 793)A07

UCB/EERC-81/14 "TLUSH: A Computer Program for the Three-Dimensional Dynamic Analysis of Earth Dams," by T. Kagawa, L.H. Mejia, H.B. Seed and J. Lysmer - September 1981(PB82 139 940)A06

UCB/EERC-81/15 "Three Dimensional Dynamic Response Analysis of Earth Dams," by L.H. Mejia and H.B. Seed - September 1981 (PB82 137 274)A12

UCB/EERC-81/16 "Experimental Study of Lead and Elastomeric Dampers for Base Isolation Systems," by J.M. Kelly and S.B. Hodder - October 1981

UCB/EERC-81/17 "The Influence of Base Isolation on the Seismic Response of Light Secondary Equipment," by J.M. Kelly - April 1981

UCB/EERC-81/18 "Studies on Evaluation of Shaking Table Response Analysis Procedures," by J. Marcial Blondet - November 1981

UCB/EERC-81/19 "DELIGHT.STRUCT: A Computer-Aided Design Environment for Structural Engineering," by R.J. Balling, K.S. Pister and E. Polak - December 1981

UCB/EERC-81/20 "Optimal Design of Seismic-Resistant Planar Steel Frames," by R.J. Balling, V. Ciampi, K.S. Pister and E. Polak - December 1981

UCB/EERC-82/01 "Dynamic Behavior of Ground for Seismic Analysis of Lifeline Systems," by T. Sato and A. Der Kiureghian - January 1982 (PB82 218 926) A05

UCB/EERC-82/02 "Shaking Table Tests of a Tubular Steel Frame Model," by Y. Ghanaat and R. W. Clough - January 1982 (PB82 220 161) A07

UCB/EERC-82/03 "Experimental Behavior of a Spatial Piping System with Shock Arrestors and Energy Absorbers under Seismic Excitation," by S. Schneider, H.-M. Lee and G. W. Godden - May 1982

UCB/EERC-82/04 "New Approaches for the Dynamic Analysis of Large Structural Systems," by E. L. Wilson - June 1982

UCB/EERC-82/05 "Model Study of Effects on the Vibration Properties of Steel Offshore Platforms," by F. Shahrivar and J. G. Bouwkamp - June 1982

UCB/EERC-82/06 "States of the Art and Practice in the Optimum Seismic Design and Analytical Response Prediction of R/C Frame-Wall Structures," by A. E. Aktan and V. V. Bertero - July 1982.

UCB/EERC-82/07 "Further Study of the Earthquake Response of a Broad Cylindrical Liquid-Storage Tank Model," by G. C. Manos and R. W. Clough - July 1982

UCB/EERC-82/08 "An Evaluation of the Design and Analytical Seismic Response of a Seven Story Reinforced Concrete Frame - Wall Structure," by A. C. Finley and V. V. Bertero - July 1982

UCB/EERC-82/09 "Fluid-structure Interactions: Added Mass Computations for Incompressible Fluid," by J. S.-H. Kuo - August 1982

UCB/EERC-82/10 "Joint-Opening Nonlinear Mechanism: Interface Smeared Crack Model," by J. S.-H. Kuo - August 1982

UCB/EERC-82/11 "Dynamic Response Analysis of Techi Dam," by R. W. Clough, R. M. Stephen and J. S.-H. Kuo - August 1982